Study of solid-state transitions and its impact on solubility and stability of Repaglinide

A DISSERTATION

In Pharmaceutical Sciences

Presented to the Graduate faculty of the University of the Sciences in Philadelphia in

Partial Fulfillment of Requirements for the Degree of

DOCTOR OF PHILOSOPHY

Submitted By

Meet N. Desai

July 29, 2021

Study of solid-state transitions and its impact on solubility and stability of Repaglinide

Meet N. Desai, Doctor of Philosophy

University of the Sciences, 2021

Abstract

The aim of this research was to study the impact of melting and quenching approach on solid-state characteristics of amorphous dispersion and its impact on dissolution and solubility of Repaglinide, a BCS Class II drug. Solid dispersions of Repaglinide were prepared separately by quench cooling technique using Syloid® 244FP (porous silicon dioxide) and Microcrystalline Cellulose (MCC) PH 101 (Vivapur® 101) as carriers in 1:3, 1:1 and 3:1 ratio. A Repaglinide control sample was prepared using melting followed by rapid cooling. The control and solid dispersions prepared using both carriers were placed on stability at 40ºC/75% RH and 30ºC/60% RH conditions for 4 weeks to observe their physical state and solubility. Partial crystallinity in the samples was determined using differential scanning calorimetry (DSC). The DSC data showed that there was an increase of 31% crystallinity of drug in 4 weeks for amorphous samples that were stored at 40ºC/75%RH. The crystallinity of Repaglinide in solid dispersions with Syloid® 244FP (all three ratios) and MCC PH101 (1:3, 1:1 ratios) was less than 3% suggesting substantial stabilization in amorphous state. The amorphous dispersions were further characterized by Scanning Electron Microscope and Fourier Transform Infrared (FT-IR) which suggested that there was a hydrogen bond formation between Repaglinide and both carriers and was more prominent at higher carrier ratios of 1:3 and 1:1. Solubility of the Repaglinide and its dispersion were measured in presence of citrate-phosphate buffer at pH 5.0 using UV spectrophotometer. Repaglinide is a zwitter-ionic compound has less

solubility at pH 5. The saturation solubility of Repaglinide original sample was 4.9 µg/ml in pH 5.0 citro-phosphate buffer, which was improved in the solid dispersions prepared with Syloid® 244FP and MCC PH 101 as a carrier in the ratio of 1:3 and 1:1 (Repaglinide: Carrier). Repaglinide: Syloid® 244FP dispersion showed significantly higher solubility than Repaglinide: MCC PH 101. The porous silicon dioxide (Syloid® 244FP) incorporated into solid dispersion acted as a carrier with high surface area to disperse the Repaglinide in dissolution media and prevented precipitation to keep the drug in solution and hence, enhance solubility of the drug. This research indicates that colloidal surface solid dispersion is a unique approach of adsorbing an amorphous drug onto a colloidal carrier, that could be useful to enhance solubility of a poorly soluble drug.

UNIVERSITY OF THE SCIENCES

This is to certify that the thesis prepared by

Meet Desai

Titled

Study of solid-state transitions and its impact on solubility and stability of Repaglinide

Complies with the Policies of the Graduate Faculty of the University of the Sciences and is approved by the Advisory Committee as Fulfilling the Dissertation Requirements for the Degree of

DOCTOR OF PHILOSOPHY

_____

Sriramakamal Jonnalagadda, Ph.D.
Chair, Advisory Committee

_____

Pardeep Gupta, Ph.D.
Member, Advisory Committee

_____

Bela Peethambaran, Ph.D.
Member, Advisory Committee

_____

Sumeet Narang, M.Pharm.
Member, Advisory Committee

_____

Gautam Dalwadi, Ph.D.
External Reviewer

Dedication

I am dedicating this thesis to my parents, Nitin Desai and Sandhya Desai, who always encouraged me to pursue higher education and my loving wife, Herini Patel, who has been a great support through my journey of higher education and professional development.

Personal Background:

Meet Desai completed his Bachelor of Sciences in pharmacy from Sardar Patel University in 2006 and Master of Sciences in Pharmaceutical Manufacturing Engineering from Stevens Institute of Technology in 2008. He is currently working as Development Director, US R&D for GlaxoSmithKline (GSK). Prior to this, he served in various small, mid and large size pharmaceutical companies such as Purdue Pharma, Sun Pharmaceutical Industries, and CorePharma LLC in the area of formulation development. His experience includes preclinical/clinical development as well as end to end product development for generic, branded and consumer products.

Table of Contents

List of Figures

List of Tables

Chapter 1 Introduction

Primarily pharmaceutical solids could exist in two states: crystalline or amorphous. Most of the small molecular drugs typically exist in the crystalline form, which is thermodynamically stable and exhibits both short-range and long-range order[1]. In contrast to a crystalline solid, an amorphous solid has no long-range order of molecular arrangement, due to conformational flexibility within the molecular structures[1]. Amorphous forms of drugs have high free energy and do not present lattice energy barriers for dissolution. This results in higher solubility and faster dissolution rate for amorphous solids, especially when compared to their corresponding crystalline forms[2].

Given, more than 60% of new drug entities in the development pipeline are poorly soluble in water, amorphization has been a widely explored approach for solubility enhancement of poorly soluble drugs[3]. However, due to the high energy associated with the amorphous state, these solids tend to be thermodynamically unstable, and present poor physical stability upon storage. They also tend to re-crystallize on storage, resulting in physical forms with slower dissolution rates[2]. Therefore, preparation and stabilization of amorphous solids dispersion continues to be an area of great interest to the pharmaceutical industry. These approaches have the potential to improve bioavailability and improve efficacy, thereby improving overall therapeutic outcomes to the patient.

1.1 Biopharmaceutical Classification System

Amidon et. al. developed the biopharmaceutical classification system (BCS) in 1995. The BCS classification is based on solubility and gastrointestinal permeability of drug, which are the key factors controlling the rate and the amount of drug absorption.[4] The BCS has been used widely

to classify molecules and has been adopted by the pharmaceutical industry and regulatory agencies.[5] Based on BCS, drugs are categorized as below in Figure 1:

Figure 1 BCS classification in product development[5]

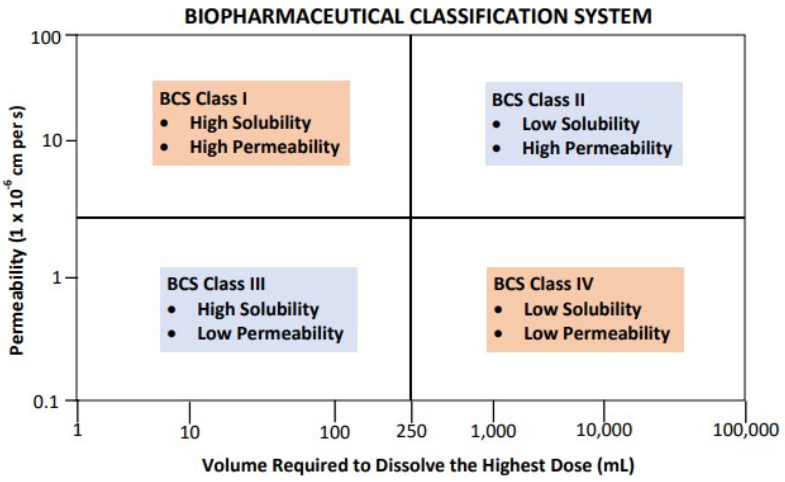

In the figure above, drug solubility and permeability are defined with respect to the dose required. If the highest dose strength completely dissolves in 250 ml volume of media at pH range of 1.2 to 7.4 (physiological pH range), it can be classified as a highly soluble drug.[4] Highly permeable drugs are defined as those in which more than 90% of the dose administered is absorbed.[4]

BCS class I drugs are easy to formulate as Immediate release and provide predictable absorption profile after administration. The high solubility makes it challenging to formulate delayed release dosage forms, unless mechanisms to retard drug release can be adopted in the formulation. In contrast, class II compounds have poor solubility, but acceptable permeability. If such poorly soluble drug (BCS class II drug) could be solubilized, the absorption profile could be improved, and expected to proceed in a manner similar to BCS class I drugs.[6] For BCS class II drugs wherein solubility is the limiting factor, a dissolution test in bio-relevant media may be

used to predict *in vivo* performance, suggesting the possibility for better *in vitro*/*in vivo* correlations (IVIVC) using dissolution data. For BCS class III with higher solubility and lower permeability, formulations typically tend to be immediate release, with pro-drug approaches adopted to improve permeability and overall efficacy[5]. Given permeability is an intrinsic property of the compound, it cannot be fixed by formulation approaches, unless excipients are altering permeability through specific or non-specific mechanism e.g p-glycoprotein (PgP) inhibition or disrupting tight junction. BCS Class IV drugs are the most difficult in terms of formulating, owing to challenges with both solubility and permeability. In early discovery development, it is difficult to realize if such compound's *in vivo* exposure is related to permeability or solubility, unless the compound's solubility is improved to an extent that allows to realize whether if permeability is a limiting factor. In such cases, solubility and dissolution enhancement remain a desirable approach.

1.2 Methods of solubility enhancement of Active Ingredients

1.2.1 Amorphization of solid drug compounds

Amorphous materials may be readily obtained by rapid cooling from a molten or liquid state, especially if rapid cooling does not allow enough time for recrystallization of molecules from the liquid to solid state. The formation of amorphous solids is a kinetic (rather than a thermodynamic) process, which means that a crystalline structure would be obtained if sufficient equilibration time is allowed for structural reorganization. The structure of an amorphous state tends to represent that of a liquid of higher viscosity; consequently, amorphous materials may also be referred to as a super cooled liquid, in a state of non-equilibrium. The temperature at

which the "jump" in specific heat occurs is called as glass transition temperature (T_g)[7]. The glass transition temperature is a glassy to rubbery phase transition at which the specific heat of the materials transforms from that of a solid material (glassy state) to a liquid material (rubbery state). The heat capacity of a super-cooled liquid is more than that of a crystalline phase, which is thermodynamically stable. The heat capacity of supercooled liquid increases with rate of supercooling. The metastable liquid loses entropy and enthalpy faster than the crystal with reduction in temperarute.[8] If there was no intervention called glass transition, the entropy of supercooled liquid would be equal to that of a crystal, at a temperature recognized as Kauzmann temperature.[9] At Kauzmann temperature (T_k), the entropy of super-cooled liquid will be equal to that of the crystal.[8] At lower temperatures below T_g the entropy and molecular mobility of the amorphous compound is low, hence, amorphous drugs tend to be more stable below T_g.

Figure 2 Variation of enthalpy with temperature[7]

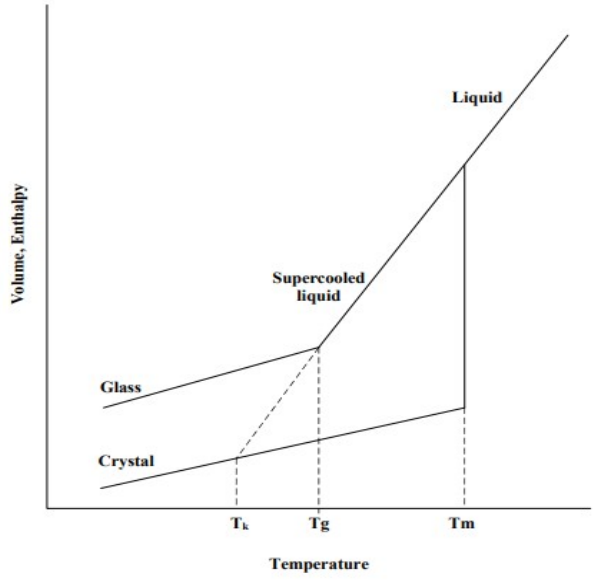

Amorphous compounds have short range order of molecular arrangement as compared crystalline compounds with long range order of molecular arrangement.[10] Amorphous solids also tend to have higher energy, due to which they have higher saturation solubility compared to crystalline solids.[11] The advantages associated with higher solubility are frequently offset by poor stability, as amorphous compounds tend to convert into more stable crystalline polymorphs, given sufficient time.[12]

Amorphous materials can be readily characterized by Differential Scanning Calorimetry (DSC), whereby, T_g is shown as a change in specific heat (ΔC_p). The extent of this change in specific heat shows difference between the enthalpies of the "glassy" and "rubbery" states of the amorphous materials and may be used as a measure of stability when amorphous materials are stored below the T_g. The use of plastizers that lower the T_g of amorphous material could impact the mobility hence rate of recrystallization; moisture is the most common plasticizer for pharmaceutical solids when stored under varying humidity.[13] The lowered T_g resulting from plasticization by water molecules is a critical parameter for maintaining physical stability of the amorphous state, especially when such material are stored closer to the T_g.[13]

Figure 3 Methods of amorphization[7]

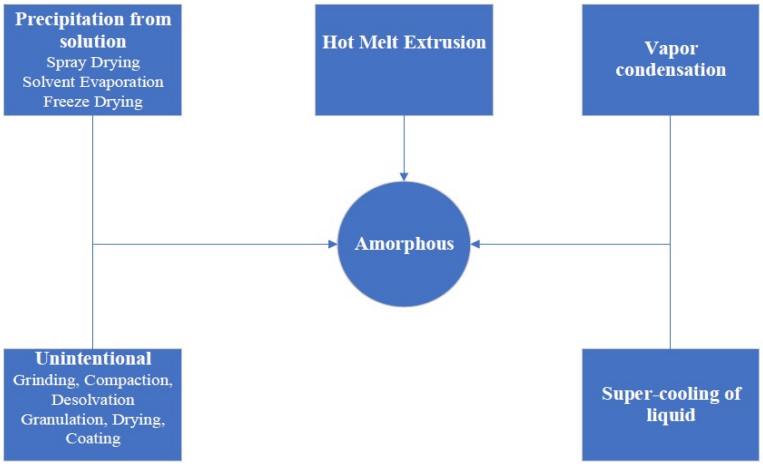

The solid dispersion is a preferred approach to stabilize drugs in amorphous state. This is generally achieved by homogeneously dissolved/molecularly dispersing drug in polymeric matrix or by absorbing on to inorganic carrier .[14] Common processes for amorphous solid dispersions (ASDs) include hot melt extrusion, quench cool, solvent evaporation and spray drying.[15]

1.2.2 Particle size reduction

Particle size reduction enhances solubility as well as dissolution of drug substances. Solubility enhancement is described by Kelvin and Ostwald-Freundlich, who showed that dissolution pressure (vapor pressure to surface curvature) of smaller particles (having smaller radius) is lower compared to larger particles, resulting in higher solubility for smaller particles.[16] Since the surface area of a sphere is radius squared, a small reduction in radius would result in large increase in surface area.[16] The Ostwald-Freundlich equation is a derivation from the Kelvin equation and it explains the co-relation between saturation solubility and particle size.

$$-\Delta(\Delta G) = RTln\frac{S}{S_0} = \frac{2\gamma V}{r} \quad \text{---------- (1)}$$

In the above equation, $\Delta(\Delta G)$ = the difference in the free energy of a solution of small and large particles; S = solubility of a spherical particle of radius r; S_0 = solubility of a surface without any curvature ($r = \infty$); V = molar volume of the solute; γ = solid–liquid interfacial tension; R = universal gas constant; T = absolute temperature; r = particle radius.[17]

Figure 4 Relative solubility with particle size based on the Ostwald–Freundlich equation for Cilostazol derived by Johnson et. al., at two interfacial tensions: 30 mN/m (solid line), 50 mN/m (long-dashed line)[18]

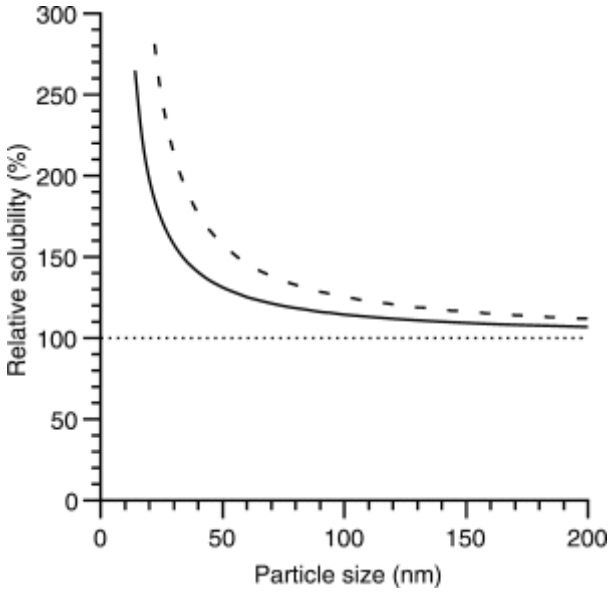

Figure 4 shows that the increase in solubility is prominently observed at lower particle size. Particle size reduction also enhances dissolution through the well-known Noyes-Whitney equation as shown below:

$$\frac{dC}{dt} = \frac{DA}{Vh}(C_S - C_x) \quad \text{---------- (2)}$$

where D is diffusion coefficient, dC/dt is rate of dissolution, V is the volume of the dissolution medium, A is surface area, Cs is saturation solubility, Cx is the concentration of drug in solution, and h is the thickness of hydrodynamic boundary layer.[18]

Reduction in particle size can be achieved by milling, grinding, nano-sizing, or through synthesis or precipitation from a solvent.[19] Milling is a common technique used to reduce particle size of drugs.[20, 21] Impact mills such as a hammer-mill and fluid energy mills such as a jet-mill are most commonly used for particle size reduction.[22] Hammer mill produces particles of mean diameters greater than 10 μm, while a fluid energy mill provides particles approximately

ten times smaller.[22] There are some limitations with these processes as they exert thermal and physical stress on drug compounds which may result in degradation. The key limitation of physical particle size reduction in dry state is aggregation due to triboelectrification and difficulties in redispersion of those aggregates in formulation. This often hampers dissolution enhancement. During size reduction, some polymorphic changes that may occur that may impact physicochemical characteristics of the finished product.[3] To reduce the degradation effect of thermal stress during particle size reduction, cryoprotectants such as Sucrose, Glucose, Mannitol, Polyethylene Glycols, etc., may be used.[23]

Recently, there is an increased attention to increasing surface area and drug dissolution by reducing particle size to the nanometer range using wet milling approach as compared to dry milling described above.[24] Nanoparticles have physical dimensions less than 1 micron.[25] Nanoparticles may be prepared by combining lipid excipients to enhance bio availability.[26]

Nanocrystals are produced by methods such as precipitation, milling and homogenization. Liversidge et. al. described nanocrystal technology which produces sub-micron sized particles using wet milling.[25, 27] There are three types of technologies well known for homogenization: (i) Microfluidizer technology which involves collision of two fluid streams under pressures as high as 1700 bar (commercially known as IDD-P™™ technology), (ii) Piston gap homogenization where drug dissolved in water is forced by a piston through a tiny homogenizer gap at pressures of up to 4000 bar at room temperature (known as Dissocubes® technology) and (iii) Nanopure® technology uses drug in water mixtures or in nonaqueous media with a low vapor pressure and homogenization at low temperatures which is ideal for temperature labile and water sensitive drugs.[28] Triglide® was developed using IDD-P™ technology by Sciele Pharma for hypercholesterolemia.[28] Since Nanocrystals are a formulation in

themselves, they can be used for multiple routes of administration, are more stable and have reduced in-vivo variability between fasted and fed state.[22] The ideal for Nanocrystal technology are low dose drugs such as Rapamune®, marketed by Wyeth. This formulation containing Rapamycin (an immunosuppressive drug) was the first product developed using this technology.[28] Some other examples of products developed and marketed using this technology are Emend® (antiemetic drug marketed by Merck), Tricor® (hypercholesterolemia drug marketed by Abbott) and Megace ES® (antianorexic drug marketed by Par Pharmaceuticals).[28] One of the disadvantages of nanoparticles is, they tend to aggregate to a less energetic state. The inter-particle interaction is described by Derjaguin et al. and later on refined by Verwey et al., commonly known as DLVO model which states, solid particles in a liquid medium are subject to van der Waals forces of attraction that would either aid the attractive or repulsive element, depending of the nature of the particle and the fluid.[25]

1.2.3 Screening of polymorphic form for solubility enhancement

Polymorphs of a compound have same chemical composition but vary in lattice structures and arrangement of molecules.[11] Many drugs exhibit multiple polymorphic crystalline forms. Polymorphs of same drug may have different physicochemical properties such as melting point, solubility, rheology and stability. Mukherjee et al. classified single entity polymorphism into synthon, conformation, packing and tautomeric polymorphism.[29]

Hydrates and solvates are considered as pseudo polymorphic forms where water or other solvents are combined into a crystal lattice structure.[30] Hydrate formation could be typically mediated via hydrogen bond formation.[31] In hydrates, the change in the intermolecular forces induced by the incorporation of water molecules impact solubility, dissolution, stability

and bioavailability of these compounds.[30] A cocrystal is a crystalline adduct of two or more chemical compounds. Aitipamula et. al. studied hydrates and cocrystal hydrates of Griseofulvin and its physicochemical properties.[32]

Polymorphs, solvates, and co-crystals are studied for solubility enhancement, improve compressibility, enhance chemical instability, reduce hygroscopicity, etc.[33, 34] It was observed that 50% of the pharmaceutical compounds screened had polymorphism and cocrystals, while a slightly lower percentage had solvates/hydrates.[35] Based on the review of impact of polymorphs on solubility, it was reported that the ratio of solubility of polymorphs of a same compound is usually less than 2, but higher ratios of up to 8 fold may be observed sometimes.[36] In contrast, solubility ratios of anhydrate/hydrate are observed to have a wider range and higher than the that of the non-solvated polymorphs.[36] Typically, the most stable polymorphic form presents the least solubility; however, these forms are still preferred in development as they result in robust formulations. Metastable forms are strictly avoided despite their higher solubility unless they are stabilized kinetically to achieve desired shelf-life window. From a formulation perspective, transitions among polymers are common, and may be accelerated under elevated conditions of temperature and humidity. It is important to understand the polymorphic transition that may occur during manufacturing and storage that may impact *in-vitro* and *in-vivo* behavior of the drug product.[37]

1.2.4 Salt formation and co-crystal approach

Salt formation has been used to improve aqueous solubility of ionizable compounds (anionic, cationic or zwitterionic) pharmaceutical active ingredients.[38] More than 50% of drugs that are available as salts, are typically prepared by combining a drug with its water-soluble

counterion. Putra, D. et. al., used this approach for an anti-ulcer drug Benexate to form salts such as Benexate Succinate Monohydrate and Benexate Cylcamate where the salts showed higher solubility and faster dissolution rates.[34]

The ability of certain acidic and basic drugs to form salt and ability of the salts to dissociate back into the free acid or free base form depends on factors such as intrinsic solubility, pH, pKa, solubility product and pH of maximum solubility.[39] It is desired to have a difference in pKa of about four units between a base and an acid to form salts, especially when forming salts of a drug that is either a weak acid or a weak base.[34] In addition to solubility, other properties such as ease of isolation, hygroscopicity, crystal purity, melting point, possibility of hydrate & polymorph formation, processability, and stability can also be optimized using salt formation.[30]

The approach is not feasible for all drugs. Salt formation is not a viable option for neutral compounds or a compound with very low pKa (for weak base) or high pKa (for weak acid), as disproportionation issues occur in these compounds during storage / processing. Serajuddin et. al. found that the tablets of the maleate salt of a basic drug showed a loss in potency and mass balance upon storage under accelerated stability testing conditions due to conversion of the salt form of a drug into its free base. The phenomena occurred due to pH micro-environment of drug in a tablet being higher than the maximum pH of solubilization.[40] Dissolution rate of Delveridine Mesylate was reduced by more than 20% at 60 min upon storage in accelerated stability conditions due to conversion into free crystalline form upon exposure to high humidity.[41] Moreover, salts may reconvert into their respective acid/base forms following administration; increased dissolution rate may therefore not be achieved in certain cases.[15]

1.2.5 Complexation

Complexation with Cyclodextrins has been used for improving solubility of poorly soluble drugs. Cyclodextrins have an ability to form physical complex with drugs and alter its physical, chemical and biological properties.[42] This technique is challenging to implement when drug properties don't allow formation of a strong interaction within the β-cyclodextrin cavity, and yields no solubility enhancement.[43] Aloisio, C., et al. formed ternary complexes of Sulfamerazine drug with β-cyclodextrin, Methyl β-cyclodextrin, and Hydroxypropyl β-cyclodextrin using Meglumine as a ternary component, and found that the ternary complex of Methyl β-cyclodextrin with Meglumine had the highest solubility.[44] Rawat et al. found that the solubility of an NSAID drug Celecoxib was increased linearly with concentration of β-cyclodextrin [45] However, because of its mechanism of formation of hydrogen bonds with drug, the degree to which β-cyclodextrin can improve solubility and dissolution rate is limited.[46] α-cyclodextrin, having a small internal diameter of 6°A, is not suitable for complexation of most pharmaceutical molecules, which tend to be larger in size compared, while γ-cyclodextrin has shown improvement in solubility of drugs such as Digoxin upon complexation due to its larger cavity size.[46]

1.2.6 Emulsion formulations

Techniques such as micro emulsions, nano-emulsions, oils, self-emulsifying drug delivery systems (SEDDS) and solid lipid nanoparticles (SLN) have become popular to improve bio availability of poorly soluble drugs.[47, 48] Lipid formulations for solubility enhancement consists of dissolving drugs in one or more lipid excipients such as triglyceride oils, partial glycerides,

surfactants, or co-surfactants.[49] Nano-emulsion and Solid Lipid Nanoparticles both are lipid based formulation techniques, which differ in the nature of the internal phase (liquid or solid).[48] In a study performed by Akhtar J. at. al., Repaglinide nano-emulsion was optimized using Sefsol-218 (Propylene Glycol Caprylate) as an oil phase, Tween-80 and Transcutol® as surfactants to control droplet size, and distilled water as an aqueous phase.[47] Lipid carriers such as Gelucire® 44/14, Kolliphor® TPGS and precipitation inhibitors such as Polyvinylpyrrolidone K30 (PVP K30) have been successfully used in self-emulsifying drug delivery systems for achieving sustained long-term supersaturation and higher absorption. [50] Porter C.J.H. et al. showed that PEG loaded nanoparticles of interferon α2 improved lymphatic exposure and antitumor efficacy against lymphatic breast cancer.[51]

1.3 Selection of carriers for solid dispersion

The choice of carrier and method of preparation are crucial steps in the formulation of solid dispersions.[50] Carriers may be hydrophilic or hydrophobic polymers and can influence the state of drug in the solid dispersion. Both types of carriers, water-soluble and water-insoluble, have been found to be useful in improving dissolution rate and stability of poorly soluble drugs.[52] Water-soluble carriers are moisture-sensitive, and might create more handling problems when compared to water-insoluble carriers. Water-insoluble carriers, such as microcrystalline cellulose are required in higher ratios, and may be used in combination with other hydrophilic carriers.[53, 54] Some widely explored water soluble carriers for solid dispersions are Polyvinylpyrrolidone (PVP), hydroxypropyl methylcellulose (HPMC), Polyethylene Glycol (PEG) and water insoluble carriers are HPMC Acetyl Succinate and polymethacrylates.[2, 55, 56] Stability of amorphous drug in carrier and solubility of the drug in solid dispersion are the two most important factors in

consideration for selection of excipients for solid dispersion. PVP is a strong lewis base with water-soluble tertiary amine groups, hence is widely used to prepare solid dispersions.[53] Kavitha R. et al. studied solid dispersions of Repaglinide using polyethylene glycol 6000 (PEG 6000), PVP K30, poloxamer 188 and crospovidone in different ratios; their studies showed that solid dispersion with water soluble carrier PVP K30 in the ratio of 1:4 had the highest solubility.[57] For water-soluble polymers that melt and form solid solution with a poorly soluble drugs, tend to crystallize drug at higher humidity conditions due to solubilizing in presence of water. Mitra et.al. studied the impact of HPMC Acetyl Succinate (HPMCAS) and Povidone on stability and solubility of a poorly water soluble investigational drug and found out that the solid dispersion prepared with Povidone absorbed significant amount of water at 40ºC75%RH conditions that the entire dispersion coalesced into a liquid mass.[58] While many polymers in solid dispersion technique show initial supersaturation and increase in solubility, it often follows precipitation. In this situation, hydrophobic polymers are effective in inhibiting moisture related crystallization and maintaining super saturation of the drug for longer time in dissolution. In the study performed by Mitra et. al. it was revealed that the molecular dispersion of hydrophobic drug was facilitated by hydrophobic polymer through hydrophobic-hydrophobic interactions, which also facilitated solubility by higher supersaturation and inhibiting precipitation.[58]

A combination of carriers is often used to obtain enhance solubility, stability, compressibility, and flowability of drug compounds. Polymers such as Eudragit E100 that has high solubility in acidic pH, is used along with other hydrophilic polymers to enhance dissolution.[56] Cong W. et. al. used PVP K30, microcrystalline cellulose and crospovidone to improve solubility of

Breviscapine, a cardiovascular drug.[53] Water insoluble carriers such as silica have been used in solid dispersions, either alone or in combination of other carriers. The solid dispersion of Baicalin prepared with colloidal silica and porous silica provided rapid drug release, with a dissolution rate of more than 80% in 60 minutes.[59] Based on the physicochemical properties of drug and carrier, a suitable manufacturing process may be chosen. Melt process, solvent process and melt-solvent process are most commonly used.[60]

1.4 Selection of drug

Repaglinide is a commonly used drug to treat non-insulin-dependent diabetes mellitus, and works by promoting insulin-release from pancreatic β-cells.[61] Repaglinide belongs to BCS Class II.[62] Repaglinide has poor solubility, but it has fast absorption and elimination, which allows a relatively fast onset and short duration of action.[61] Due to poor solubility and slow dissolution rate, drug absorption and hence bioavailability of Repaglinide is limited to only 45-65%.[44, 63]

Yin, L.F. et al. studied that solid dispersions of Repaglinide prepared with hydrophilic carriers such as polyvinyl pyrolidone K30 enhanced drug solubility, absorption, oral bioavailability, and mean plasma concentration compared to crystalline Repaglinide.[64] In a study comparing pharmacokinetic profiles of an oral tablet formulation vs IV preparation of Repaglinide in healthy male volunteers, a large variability in AUC and T_{max} was observed for tablets as compared to IV preparation owing to poor solubility of the drug.[65] Commercially available Repaglinide (Prandin®) tablets are in 0.5 mg, 1 mg and 2 mg dosage strengths. They contain Meglumine (a weakly basic counter ion) to enhance dissolution of Repaglinide via in-

situ salt formation. Meglumine has been shown to improve solubility of Sulfamerazine, which is a poorly soluble drug.[44] The *in-vivo* performance might be affected by inter and intra species variability in GI pH environment conditions.

Repaglinide is BCS Class II compound that has a low solubility value of 2.94 µg/mL in water at 37°C and high lipophilicity with log P value of 3.97.[56, 66] Repaglinide has a pH-dependent dissolution profile, where it has a greater aqueous solubility at higher pH. The use of Repaglinide is intended to regulate postprandial glucose levels, hence it is important that it dissolves rapidly in the stomach where the pH is low. Repaglinide has pKa values of 4.19 and 5.78 and it is a zwitterionic compound.[67] Repaglinide remains in the ionized form at higher pH values. Melting point of Repaglinide is reported to be 130 to 131°C.[68] Converting Repaglinide into amorphous form using solid dispersion technique may offer higher solubility and prevent crystallization over time, if stabilized.

Figure 5 Chemical structure of Repaglinide[63]

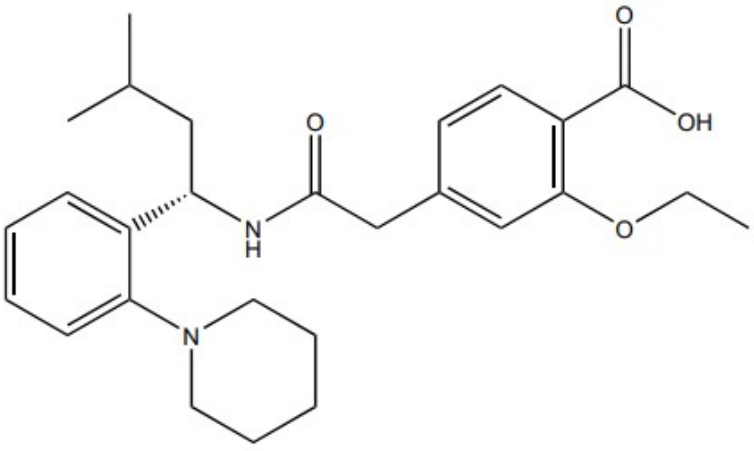

1.5 Selection of Carrier

1.5.1 Syloid®244FP

Surface-modifying carriers like fine silica particles are gaining attention in the pharmaceutical world for improving solid dispersion technology.[69] Studies have evaluated the value of porous vs. nonporous, and hydrophilic vs. hydrophobic fine silica particles for potential use as carriers for solid drug dispersions.[70, 71] Takeuchi et al. studied Indomethacin solid dispersions using porous and non-porous silica, and found that dissolution of Indomethacin was higher with porous silica (Sylysia® 350) compared to non-porous silica (Aerosil® 200).[72] Porous silica materials showed higher dissolution rates due to ability to lower drug crystallinity, compared to nonporous silica materials.[72]

Syloid® 244 FP is an insoluble, synthetic, amorphous, mesoporous silicon dioxide with a glass transition temperature of 1100°C.[73] Silica has multiple uses in food and medicinal products such as anti-caking agent, glidant, viscosity modifying agent, antifoaming agent, etc. Silica is considered as an essential component for health and deficiency could cause deformities in bones and skulls, joint weakness, and reduced collagen and cartilage.[74] Syloid® is nontoxic, biocompatible and biologically safe.[75] The large effective surface area and pore volume of Syloid can enhance drug loading, stability, and drug release.[76] Several grades of Syloid® are available that vary in surface area, bulk density, and pore volumes. Examples include 63FP, 72FP, 244FP. Syloid 244FP® has an average surface area of 300m^2/g, particle size of 2.5 – 3.7 μm and pore volume of 1.6ml/g.[69] The average pore diameter of Syloid® 244FP is 16nm[75]. Mesoporous materials like Syloid®, which provide high surface area for adsorption of amorphous drug, have

been explored for improving solubility and rate of drug dissolution.[69] Patel et al. adsorbed solid dispersion of Sulfathiazole- Plasdone® K-29/32 onto Syloid® 244FP and found increased solubility of this mixture compared to the binary mixture of sulfathiazole-Plasdone® K-29/32.[69]

1.5.2 Microcrystalline Cellulose (MCC)

Microcrystalline Cellulose (MCC) has been used for numerous decades as an excipient in pharmaceutical formulation. MCC is a purified and partially depolymerized cellulose, prepared by high-quality treatment with mineral acid to hydrolyze cellulose wood pulp and lower the degree of polymerization.[77] MCC is available in many grades; MCC PH 101 and 102 are semi crystalline with amorphous content of 64% and 51% respectively.[77] MCC PH 101 has low particle size and high surface area of 1.07m^2/g, and is used in applications such as granulation, roller compaction and spheronization.[78] MCC grade PH 102 is more suitable for processes involving direct compression. Patel et. al. increased dissolution of Furosemide in stomach pH in 30 mins by making a solid dispersion with Polyethylene Glycol 6000 and adsorbing the solid dispersion on MCC as another carrier, where MCC was helpful in converting a sticky dispersion into a free flowing powder.[54] MCC converted the sticky dispersion into a free flowing powder and provided high surface area, resulting in a higher dissolution rate.[54]

Figure 6 Chemical structure of Microcrystalline Cellulose[76]

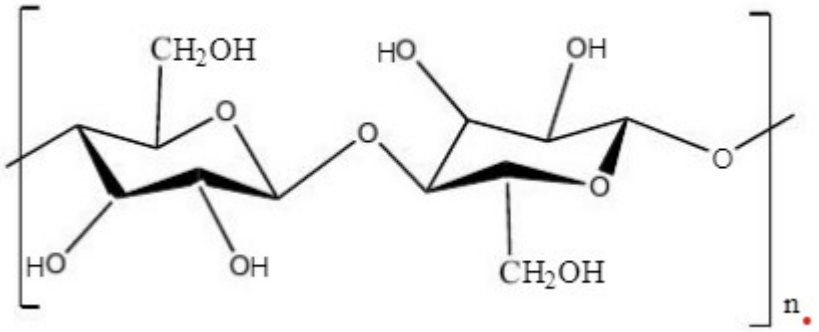

1.6 Methods of preparing solid dispersion

There are multiple approaches explored for overcoming solubility issues by converting drug into amorphous form.[79] Solid dispersion techniques widely used to convert drug in amorphous form are spray drying, melt cooling, solvent extraction, emulsification and complex coacervation.[79, 80] In some instances amorphous drug is formed inadvertently during processing such as mechanical milling, solution-based phase separation, and ultra-rapid freezing.[81]

1.6.1 Hot Melt Extrusion

Hot melt extrusion (HME) involves applying heat on a mixture of materials where heated materials are passed through an extrusion barrel and eventually forced out through a die.[82] Applying heat makes the material fluid and viscous which passes through the die.[83] Depending on the desired size and shapes such as pellets, rods, films, threads, etc., there are different type of dies available to choose from. Sometimes it may be desired to run an extruder without a die or can be coupled with other extruders toc make multilayer films via co-extrusion.[82] HME can be

operated as a continuous process with a consistent product flow at high throughput rates.[83] HME has been widely used to produce a variety of pharmaceutical dosage forms including melt granules, pellets, tablets, transdermals for controlled release, and solubility enhancement of therapeutics.[84] The HME barrel has different zones with a separate temperature control for each zone. The material is fed from a hopper and it passes through the barrel containing heating and extrusion zones where the molten mass moves by helical screws and exits through a die of smaller size.[83]

One of the most popular examples of commercial product that has used HME is Kaletra™, a combination of Lopinavir and Ritonavir, providing higher aqueous solubility and physical stability. [82] Djuris, J. et al. prepared Carbamazepine solid dispersions, using Soluplus® (polyethylene glycol-polyvinyl caprolactam-polyvinyl acetate grafted copolymer) and Poloxamer 407 (polyoxyethylene-polyoxypropylene block copolymer), and demonstrated that Poloxamer 407 as a plasticizer improved processing conditions and decreased the hardness of hot-melt extrudates.[85]

Paradkar et.al used polyvinylpyrrolidone (PVP) and hydroxypropyl methylcellulose acetate succinate (HPMCAS) for solid dispersions by two techniques, hot-melt extrusion and spray drying, and found that faster drug release was obtained for solid dispersions produced by spray drying as compared to corresponding melt extruded formulations while stability was improved in solid dispersions prepared by HME.[86]

Figure 7 Schematic of an extruder[82]

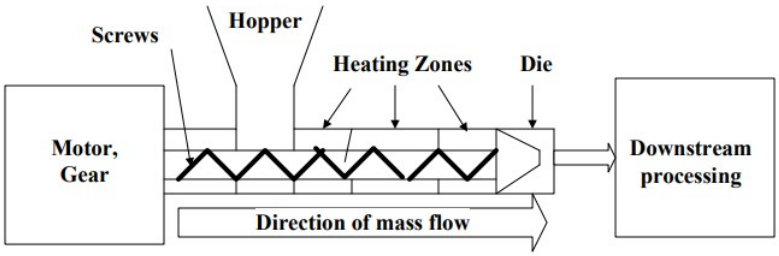

1.6.2 Spray Drying

Solid dispersion could also be achieved by the spray drying technique, where selected polymer and drug is dissolved in common solvents or solvent mixture, and evaporated to recover a solid dispersion with defined particle size.[87] This method has many advantages such as, cost effectiveness and simplicity for scale up.[88] The spray drying process has three major steps: (1) atomization of liquid, (2) drying, (3) collection and separation of dried particles.[89] An atomizer is used to convert colloidal dispersion into small drops, which are dried in a hot vertical column and microparticles are formed.[87, 90] Iskandar F. et al studied that the hydrodynamic effects during spray drying process and structure of droplets are important factors in determining the morphology of spray dried particles.[88] By controlling the parameters in spray drying, such as inlet air temperature, moisture content, inlet and liquid feed rates, the particle properties such as crystallinity, porosity, and density may be readily modified.[91]

Figure 8 Schematic of spray drying process

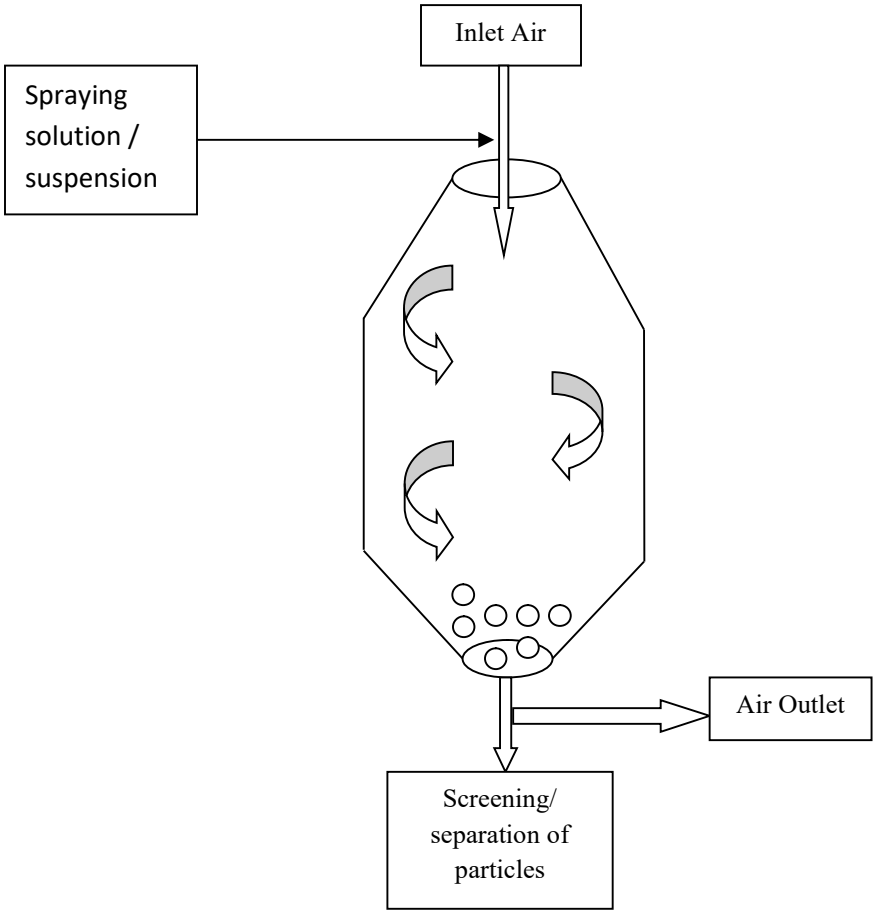

Spray-dried nano-particles may be obtained through the spraying of solutions, emulsions, or dispersions. [92] The use of emulsion/dispersion systems is particularly useful in the preparation of modified or delayed release particles.[91]

1.7 Methods for characterization of solid state of APIs

The formulation and stability of amorphous compounds can be studied using various analytical techniques such as Differential Scanning Calorimetry (DSC), Scanning Electron Microscopy (SEM), and Fourier Transform Infrared Spectroscopy (FTIR).[1]

1.7.1 Differential Scanning Calorimetry (DSC)

Differential scanning calorimetry (DSC) is used for analysis of the thermal properties such as melting and/or glass transition phenomena of compounds such as polymers, crystalline solids and nanoparticles.[93] Differential Scanning Calorimetry (DSC) monitors change in material's heat capacity (C_p) with change in temperature. Heat Capacity (C_p) of a compound is defined as the quantity of heat used by the material to achieve an increase of 1^{o}C temperature. Heat Capacity of a material changes as it goes through a phase transition. DSC records changes in heat capacity as heat flow when sample is heated or cooled at a desired rate. The DSC instrument has two pans: sample pan which contains the material to be tested, and an empty reference pan which is used as a control. The temperature of the pans is increased or decreased at a constant rate. The rate of temperature change for a given amount of heat will differ between the two pans. This difference depends on the material inside the pan and tends to be constant until the material undergoes a phase transition. DSC provides qualitative and quantitative information about the transitions such as endothermic or exothermic processes, and records changes in heat capacity as a function of time and temperature.[94] DSC has advantages such as simple sample preparation, application in both solids and liquids, fast analysis and broad temperature range. Some limitations of DSC are, the inability to separate from reversible vs. non-reversible heat flow, which leads to difficulty in

interpreting results when multiple transitions occur over the same temperature range. Such an example would be when at the glass transition temperature, an enthalpic relaxation peak is superimposed on the heat flow transition peak where the enthalpic relaxation peak can be so large that the transition is confused with a melting transition.[94]

1.7.2 X-Ray Diffraction (XRD)

X-Ray powder diffraction is a primary method to characterize crystal forms including polymorphs, salt forms, solvates, hydrates and co crystals. XRPD pattern is a fingerprint of a specific crystal form. It is widely used for compound identification and phase identification. XRD is used as an identification tool for the determination of crystalline and amorphous material, as well as to investigate phase transformations such as dehydration, hydration, polymorph conversion, melting and crystallization for variable temperature studies. It can be used for qualitative or quantitative analysis. X-Ray Diffraction analysis is done on the basis of Bragg's law.

Bragg's law: $n\lambda = 2d\sin\theta$ ---------- (3)

where, *d* = distance between atomic layers in a crystal, lambda (λ) = the wavelength of the incident X-ray beam; n = integer. The Bragg's law was developed by Bragg et al. and it explains that when an X-ray beam is applied on a crystal, the reflection of X-ray beams from different layers within the crystal would be at certain angles of incidence (theta, θ).[95]

Figure 9 Schematic diagram explaining X-Ray Diffraction

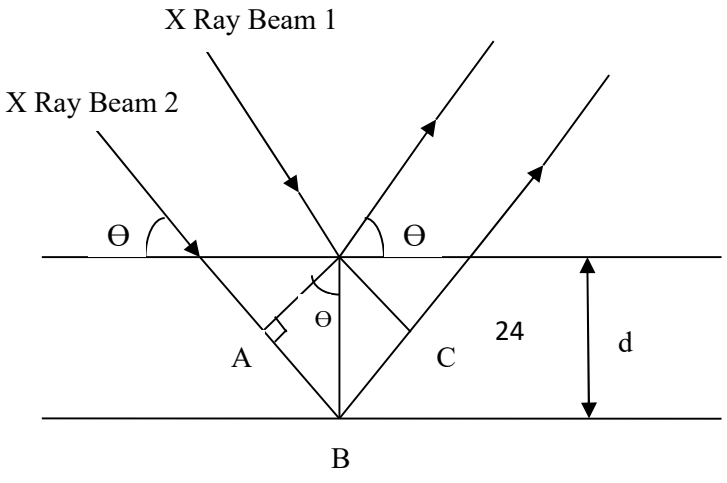

In the figure above, nλ (AB+BC) is an extra length travelled by X ray beam 2 while being reflected from the second layer of the crystal and d = the distance between the two layers of a crystal. XRD technique is used to understand crystalline behavior of material. In XRD, the sample preparation and data interpretation are simple. It requires a homogeneously mixed material when used in identification of material.

1.7.3 Scanning Electron Microscopy (SEM)

In scanning electron microscope (SEM) technique, a beam with high-energy electrons is applied on material. In SEM, the interaction between incident electron beam and the sample would produce secondary electrons. These secondary electrons provide information about the morphology of the sample, its chemical composition and physical structure. With SEM, higher magnification imaging compared to light microscopy is possible, as the wavelength of the electron beam can be modified to values significantly below that of the wavelength of visible light.

SEM is used for applications such as identification of polymorphic forms, physical forms of a compound and evaluation of surface of tablet/pellets after coating. SEM is easy to operate, quick and user-friendly technique, which requires minimal sample preparation. Limitations include the use of a high energy electron beam, which can degrade particles.

Figure 10 Schematic diagram of SEM analysis

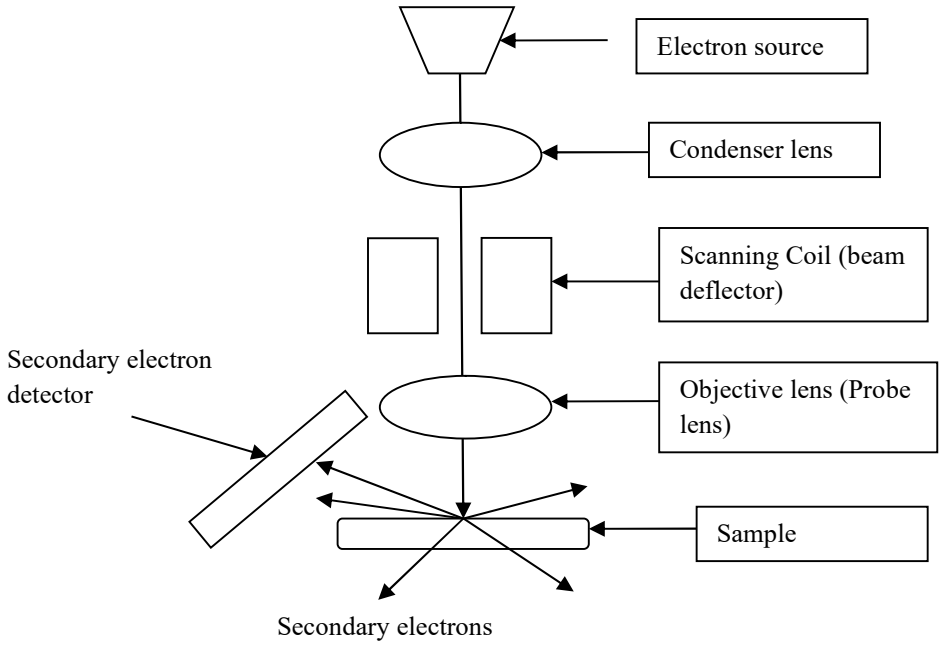

1.7.4 Fourier Transform Infrared Spectroscopy (FTIR)

Fourier Transform Infrared spectroscopy works on the principle of generating a molecular fingerprint based on absorption and transmission of IR rays by the molecules of the material through which the IR rays are passed through. The spectra collected is unique to a compound representing its molecular structure and bonds that exist within a sample. Infrared with Fourier transformation (FTIR) spectroscopy is a commonly used tool allowing recognition of structural modification in lattice by non-covalent bonding formation.[96]

FTIR technique studies interactions between compound and electromagnetic fields in the IR region. FTIR is a nondestructive method used for determination of the chemical composition of materials based on the bonds present in the sample.[97] McCool B. et al. measured the surface area of porous and non-porous silica using FT-IR technique.[98]

An FT-IR instrument contains an interferometer that performs spectral encoding, the beam that passes through the sample goes through the detector which can measure the interferogram signal. Some of the major advantages of FT-IR include speed of testing, simple sample preparation, high sensitivity of the instrument and reproducibility of the results.

1.8 Hypothesis and specific aims of research

The overall goal of this research is to develop a platform technology for the stabilization of amorphous forms of BCS Class II drugs within polymeric carriers to enable the formulation of stable, oral drug delivery systems. This research will evaluate Syloid®244FP and Microcrystalline Cellulose (MCC) as carriers for the amorphous form of Repaglinide. The hypothesis of this research is that the amorphous form Repaglinide can be introduced and stabilized within the structures of Syloid®244FP and microcrystalline cellulose to prepare amorphous solid dispersions (ASDs) with higher solubility compared to the crystalline form of the drug. The specific aims of this research are as follows:

1. To make amorphous solid dispersion by loading Repaglinide into the polymeric carriers Syloid® 244FP and Microcrystalline Cellulose in ratios of 25:75, 50:50, and 75:25% w/w using a hot-melt technique, and determination of amorphization as a function of drug to carrier ratio.

2. To evaluate the stability of the ASD prepared from specific aim 1, under accelerated stability conditions of 40ºC/75% RH and 30ºC/60% RH.
3. To evaluate the saturation solubility of the resulting ASDs compared to the corresponding crystalline form of repaglinide.

Chapter 2: Methodology

2.1 Materials and Methods

2.1.1 Materials

Repaglinide (lot no. PNORPGFL004, assay 99.98%) was received as a sample from Sun Pharma, India. Syloid® 244 FP (amorphous Silicon Dioxide) and Microcrystalline Cellulose PH 101 (Vivapur® 101) were received as a sample from Grace Chemicals and JRS Pharma, respectively. Citric acid monohydrate and Disodium hydrogen phosphate used to make pH 5.0 citro-phosphate buffer were received from Sigma-Aldrich.

2.1.2. Methods

2.1.2.1 Preparation of Solid Dispersion

Repaglinide and Syloid® 244FP were weighed and mixed in three weight ratios (1:3, 1:1, 3:1). Each sample was mixed by using a magnetic stirrer at 60 rpm for 2 minutes. An oil bath using mineral oil was heated in a stainless-steel pan to 160ºC. All three mixed samples were placed in this oil bath to ensure that the product reached a temperature of 140ºC. After visual confirmation of melting (melting point of Repaglinide is 131ºC), the product container was removed from the oil bath and placed in an ice bath for 15 minutes to ensure rapid cooling. Finally, the product was

secured in a 20 mL glass scintillation and stored at room temperature (25ºC) until further evaluation. Samples of Repaglinide in Microcrystalline Cellulose 101 (MCC) were prepared in the ratios of 1:3, 1:1 and 3:1 was prepared using same process. Repaglinide (control) was heated and cooled in the same manner as those described for polymer combinations.

Table 2.1 Composition of samples prepared by melting and quench cooling

Sample, Ratio	Drug	Carrier	Total wt (g)
Repaglinide: Syloid® 244FP (RS solid dispersion)			
1:3	0.251g	0.750g	1.001
1:1	0.500g	0.500g	1.000
3:1	0.749g	0.249g	0.998
Repaglinide: Microcrystalline Cellulose 101 (RMC solid dispersion)			
1:3	0.250g	0.750g	1.000
1:1	0.501g	0.502g	1.003
3:1	0.750g	0.251g	1.001
Repaglinide			
N/A	1.122g	N/A	1.122

The samples were divided into multiple scintillation vials with cap closed and placed in stability chambers as per below:

Table 2.2 Stability conditions and testing

Stability condition	Initial (T_0)	1 week	2 week	4 week
40ºC/75%RH	SEM, DSC, FT-IR, Solubility using UV			
30ºC/60%RH	SEM, DSC, FT-IR, Solubility using UV			

The samples were analyzed using DSC, SEM and FT-IR for physical state characteristics. At each time point, the solubility of samples was checked using UV spectrophotometer.

2.1.2.2 Differential Scanning Calorimetry (DSC) Analysis

DSC instrument used was a Mettler Toledo DSCQ100 (Mettler-Toledo; Ohio, USA) which was equipped with an intercooler. Each sample in weight range of approximately 3.5–7 mg, was individually placed inside aluminum pans, which were sealed by crimping. Thermal analysis was performed under a nitrogen purge in a temperature range of 25°C to 145°C, at a heating rate 10°C/min. The first scans were analyzed for glass transition using onset, midpoint, end set and enthalpy of relaxation; and melting transition using enthalpy of melting. Enthalpy of relaxation was measured using method explained by Shamblin e.t al.[99]

2.1.2.3 Scanning Electron Microscopy (SEM) Analysis

Scanning Electron Microscopy was performed on both the crystalline and amorphous structures of Repaglinide and solid dispersion samples to examine changes in physical form of repaglinide upon heating and subsequent quench cooling. Samples were non-coated and placed on a double-sided tape on a sample holder, and scanning was performed in magnification of 1000X for Repaglinide, 500-700X for Microcrystalline cellulose dispersions, 5000-9000X for Syloid dispersions.

2.1.2.4 Fourier Transform Infrared (FT-IR) Analysis

Fourier Transform Infrared was used to examine potential physicochemical reactions between Repaglinide and the polymeric carriers used in this study. Nicolet iZ 10 from Thermofisher was used. Samples were placed on a diamond sample holder, and scanned from 400 to 4000 nm range in transmission mode with 16 no. of scans and resolution of 4.

2.1.2.5 Solubility studies

Dissolution media, pH 5.0 citro-phosphate buffer was prepared by mixing 10.2 g citric acid monohydrate (0.05M) and 18.2g dibasic sodium phosphate (0.1M) in 1 L Water. The media was prepared as per USP method. Solubility of crystalline Repaglinide is known to be 2.94 µg/ml in water at 25°C.[56] For solubility studies, samples were added to the dissolution media, equivalent to the weight of Repaglinide that would make 500 µg/ml of Repaglinide concentration. Each sample was prepared in a 20 ml scintillation vial by vortexing the solution for 2 minutes, followed by shaking on a water-bath for 24 hours, 37°C with water filled in the bath. After 24 (± 2) hours, the solution was withdrawn into a syringe, filtered through 0.45-micron Whatman filter to eliminate dispersed particles, and evaluated for dissolved content using a UV spectrometer (SpectraMaxPlus, Molecular Devices). A UV absorption spectrum was collected, and 265 nm wavelength was chosen for absorption measurements.

Repaglinide is highly soluble in Methanol. Solution of Repaglinide in Methanol at various known concentrations (0.25, 0.5, 1, 2, 4, 6, 8, 10 µg/ml) was prepared and the absorbance value was plotted to derive a calibration curve. This calibration curve was used to determine Repaglinide solubility in all the samples analyzed.

Chapter 3: Results

3.1 Scanning Electron Microscopy (SEM) Analysis

Scanning electron micrographs of Repaglinide original sample, quench cooled Repaglinide, and solid dispersions prepared using Syloid® 244FP and MCC are shown below. The SEM image of Repaglinide showed needle-shaped crystals, which could not be observed in the quench cooled

sample. The quench cooled Repaglinide showed irregular shaped cubes of different sizes instead of needle like crystals.

Figure 11 SEM images of Repaglinide original sample

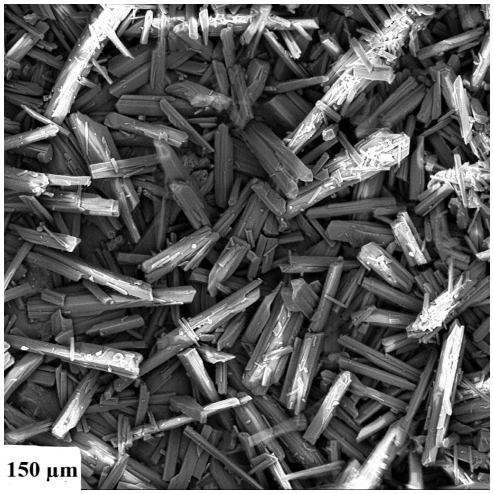

Figure 12 SEM images of quench cooled Repaglinide

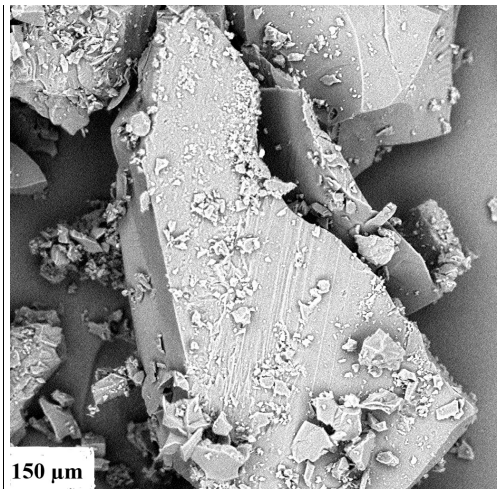

The morphology of both Syloid® 244FP showed fluffy particles of irregular shapes. Microcrystalline Cellulose PH 101 showed some crystals along with amorphous particulates. The morphology of both Syloid® 244FP and Microcrystalline Cellulose were different than that of the

crystalline needle-shaped crystals, suggesting a higher degree of amorphous structure in these polymers.

Figure 13 SEM images of Syloid®244FP (A) and MCC PH101 (B)

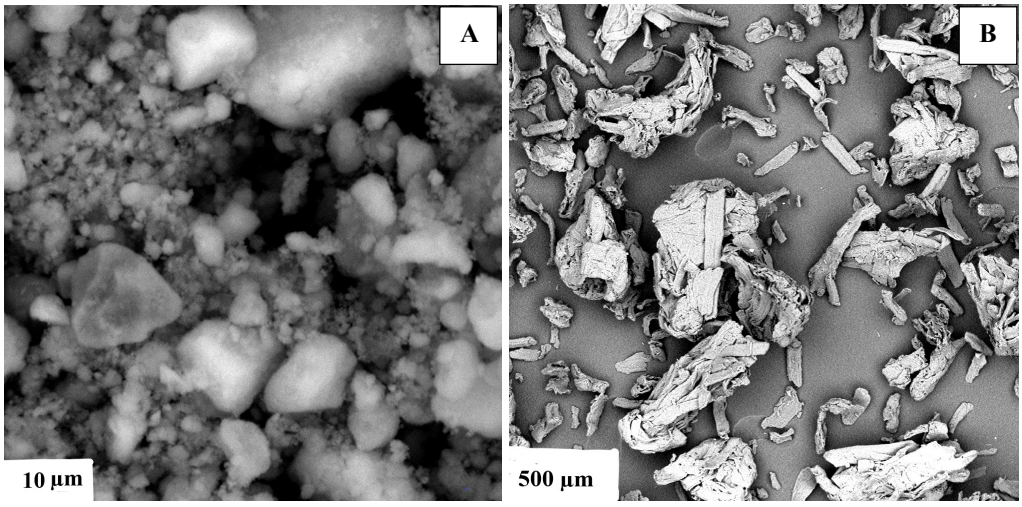

The SEM images of RS solid dispersions did not show any defined structures comparable to those of the crystalline, unformulated Repaglinide sample. Evidence of crystallization could be found in the RMC solid dispersions containing the highest drug load (ratio 3:1).

Figure 14 SEM images of RS 1:3 (A), RS 1:1 (B) and RS 3:1 (C) solid dispersion

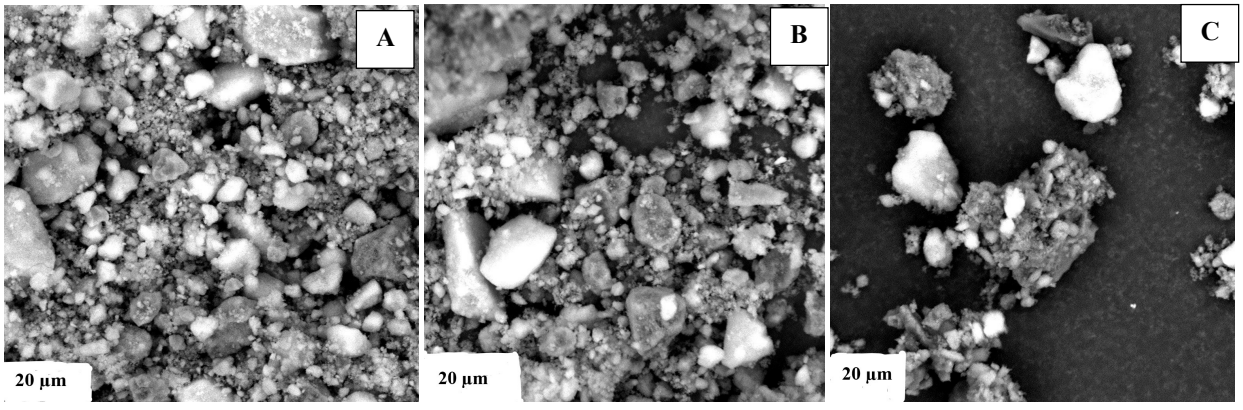

Figure 15 SEM images of RMC 1:3 (A), RMC 1:1 (B) and RMC 3:1 (C) solid dispersion

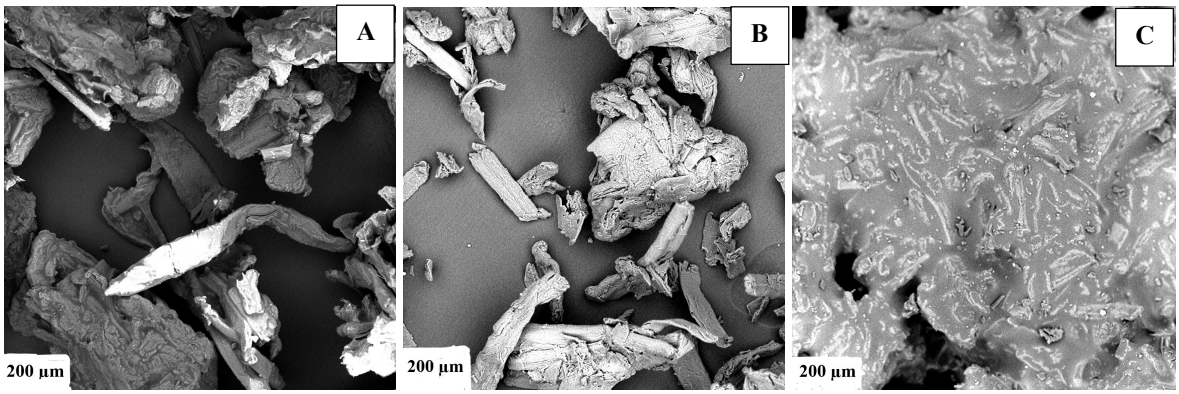

3.2 DSC thermograms on stability

3.2.1 Physical Stability of Repaglinide:

The DSC analysis on unformulated (original) and the quench-cooled samples (Initial, T0) was performed, and the graphs shown below.

Figure 16 DSC overlay of Repaglinide original and quench cooled forms (A), glass transition (B), Melting (C)

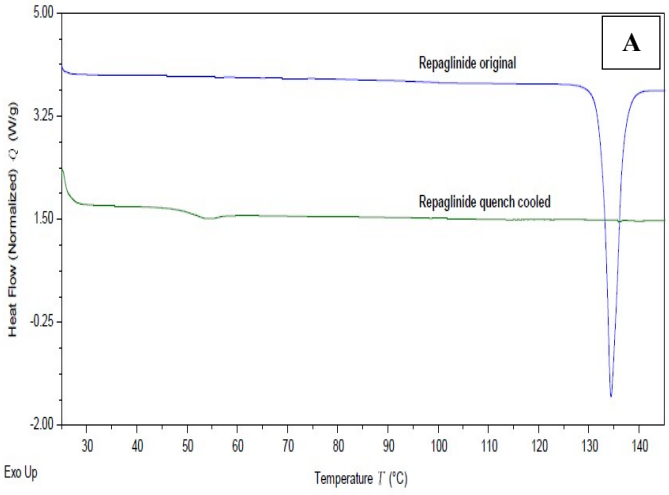

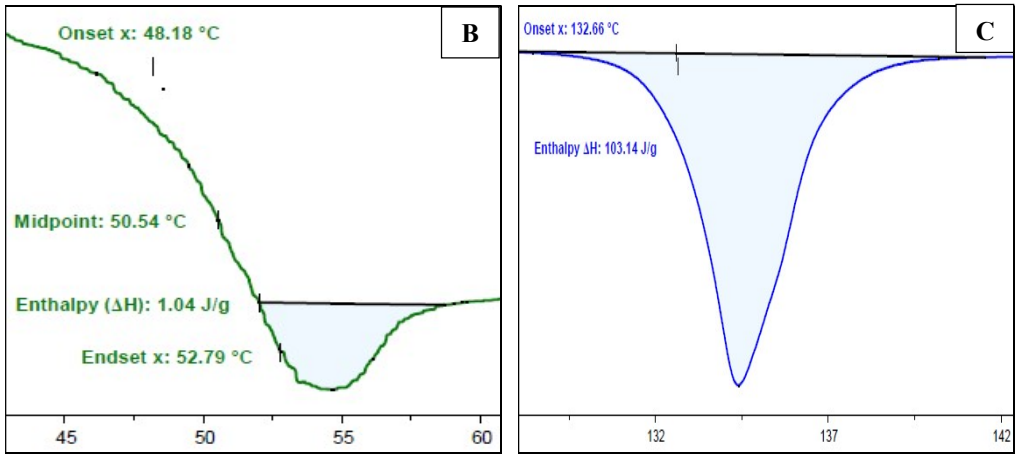

The DSC thermograms of the Repaglinide original sample, as received from the manufacturer, showed a melting point of 132.6ºC and no glass transition. This indicates the predominant crystalline character of the original sample, and is consistent with the crystalline needle-shaped morphology observed in the SEM. Upon heating followed by quench cooling, the melting transition was not observed; rather, a clear glass transition temperature at 50.5ºC could be seen. Figure 16A shows glass transition event and Figure 16B shows melting event with characterization of the peaks and calculating enthalpy values.

Table 3.1 Summary of thermal events on DSC graphs for Repaglinide original and quench cooled samples

Sample	Time	Glass Transition				Melting	
		Onset ºC	Midpoint ºC	Endset ºC	Enthalpy J/g	Onset ºC	Enthalpy J/g
Repaglinide Quench cooled	Initial	48.18	50.5	52.79	1.04	N/A	N/A
Repaglinide Original	Initial	N/A	N/A	N/A	N/A	132.6	103.14

Figures 17A below shows DSC patterns for Repaglinide quench cooled samples on stability at 30ºC/60%RH conditions.

Figure 17 DSC overlay of Repaglinide quench cooled samples stored up to 4 weeks at 30ºC/60%RH conditions (A), glass transition temperature (B), melting temperature(C)

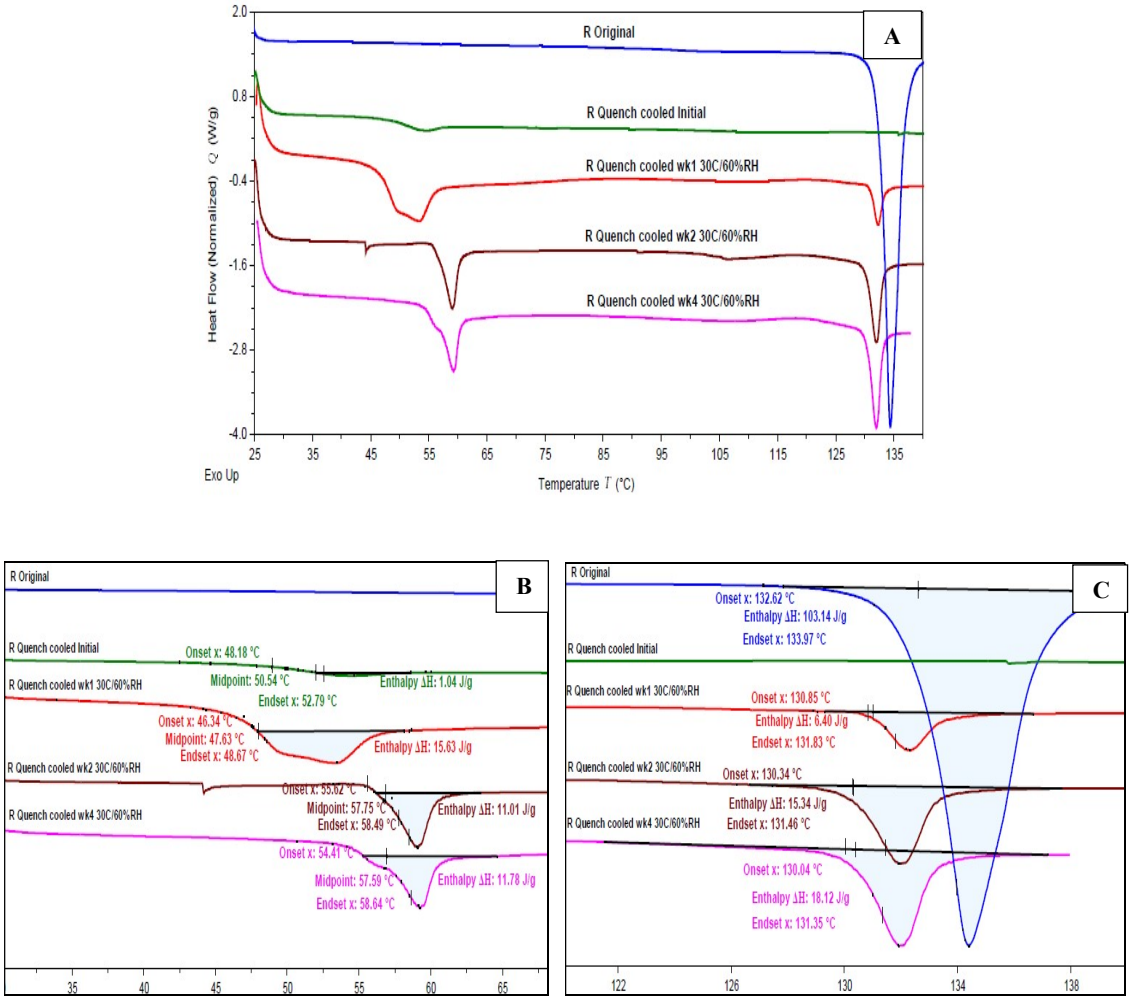

Repaglinide quench cooled sample was stored at 30ºC/60%RH conditions in a tightly closed 20 ml glass scinitilation vial. Figure 17B shows glass transition event and Figure 17C shows melting event with peaks and enthalpy values. From figure 17B, it could be observed that the glass transition temperature was broad at week 1 and shifted towards higher temperatures in week 2 to week 4. Figure 17C shows that the melting enthalpy progressively increased from the initial quench cooled sample to as much as 18 J/g at week 4 of the accelerated stability study, suggesting instability of the amorphous phase and subsequent recrystallization of repaglinide.

Table below summarizes values pertaining to glass transition and melting for quench cooled samples stored at 30ºC/60%RH.

Table 3.2 Summary of thermal events on DSC graphs for Repaglinide original and quench cooled samples stored at 30ºC/60%RH

Sample	Time point	Glass Transition				Melting	
		Onset, ºC	Midpoint, ºC	Endset, ºC	Enthalpy, J/g	Onset, ºC	Enthalpy, J/g
Repaglinide Original	Initial	N/A	N/A	N/A	N/A	132.66	103.14
Repaglinide Quench cooled	Initial	48.18	50.54	52.79	1.04	N/A	N/A
	1 week	46.34	47.63	48.67	15.63	130.85	6.40
	2 week	55.62	57.75	58.49	11.01	130.34	15.34
	4 week	54.41	57.59	58.64	11.78	130.04	18.12

Figures 18 below shows DSC patterns for Repaglinide quench cooled samples on stability at 40ºC/75%RH conditions. Repaglinide quench cooled sample was stored at 40ºC/75%RH conditions in a tightly closed 20 ml glass scinitilation vial. Figure 18B shows glass transition event and Figure 18C shows melting event with characterization of the peaks and calculating enthalpy values. From Figure 18B, the enthalpy of relaxation was seen to be increasing in week 2 and week 4 samples, with a broader peak resulting in a larger increase in the enthalpy of relaxation at week 1. A similar trend was observed in samples stored at 30ºC/60%RH conditions. It could be observed that the glass transition peak broadened at week 1 followed by a slight shift towards higher in glass transition temperature from week 2 to week 4 as the melting peak area increased from initial time point to week 4 as seen in Figure 18C. The increase in melting enthalpy with time was higher than the values obtained at 30ºC/60%RH conditions. It can also be seen that there is a recrystallization occurring at 112ºC before melting. The recrystallization was

more pronounced with increase in storage time from week 1 to week 4 and was higher in 40ºC/75%RH compared to 30ºC/60%RH.

Figure 18 DSC overlay of Repaglinide quench cooled samples stored for 4 weeks at 40ºC/75%RH conditions (A), glass transition (B), melting (C)

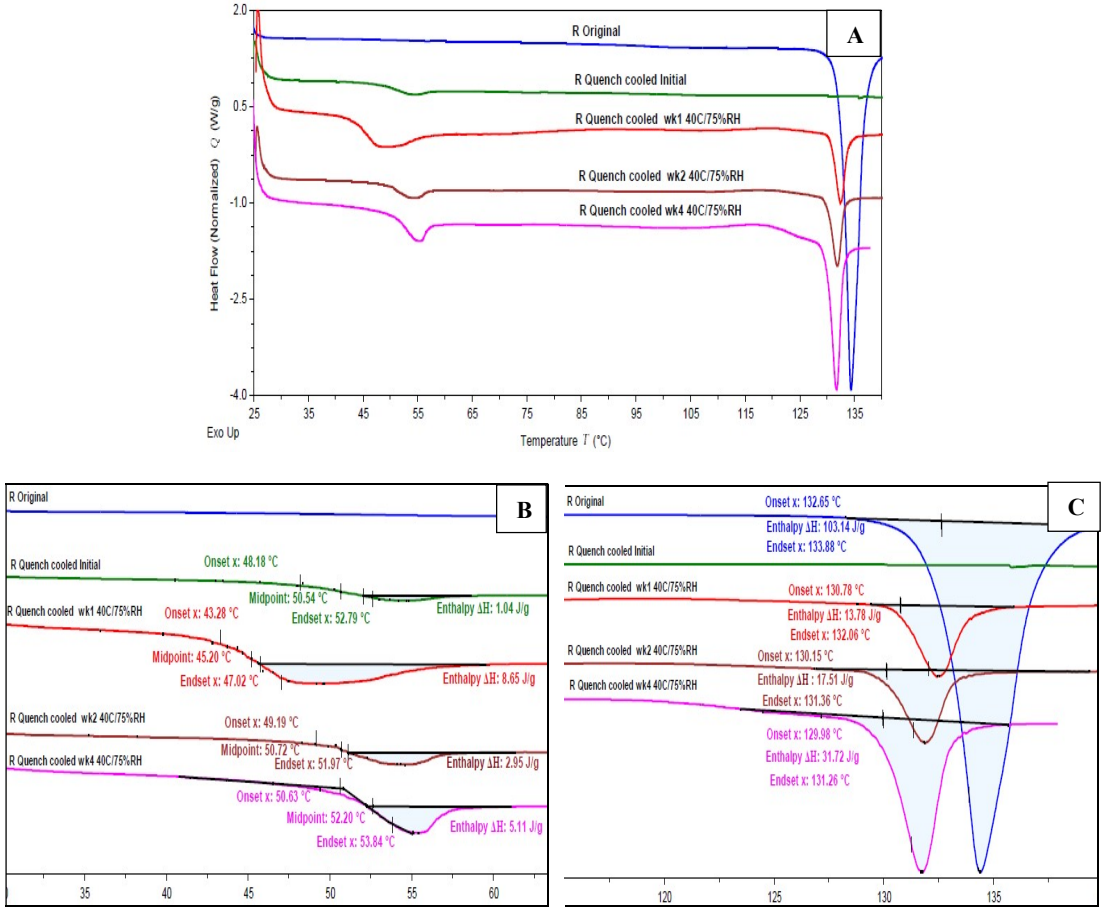

Table below summarizes values pertaining to glass transition and melting for quench cooled samples stored at 40ºC/75%RH. Glass transition, enthalpy of relaxation and melting enthalpy has been summarized in Table 3.3 for both stability conditions from initial to 4 weeks old samples.

Table 3.3 Summary of thermal events on DSC graphs for Repaglinide original and quench cooled samples stored at 40°C/75%RH

Sample	Time point	Glass Transition				Melting	
		Onset, °C	Midpoint, °C	Endset, °C	Enthalpy, J/g	Onset, °C	Enthalpy, J/g
Repaglinide Original	Initial	N/A	N/A	N/A	N/A	132.66	103.14
Repaglinide Quench cooled	Initial	48.18	50.54	52.79	1.04	N/A	N/A
	1 week	43.28	45.20	47.02	8.65	130.78	13.78
	2 week	49.19	50.72	51.97	2.95	130.15	17.51
	4 week	50.63	52.20	53.84	5.11	129.98	31.72

Table 3.4 below summarizes the enthalpy of melting peak for original Repaglinide sample and quench cooled Repaglinide at all stability time points. Percentage of crystalline component in samples with time has been plotted in Figure 19A and Figure 19B.

Table 3.4 Calculated percentage of crystalline Repaglinide in quench cooled Repaglinide samples stored in Enthalpy in 30°C/60%RH and 40°C/75%RH conditions

		30°C/60%RH conditions		40°C/75%RH conditions	
Sample	Time Point	Enthalpy of melting, J/g	% Crystalline Drug	Enthalpy of melting, J/g	% Crystalline Drug
Repaglinide Original	Initial	103.14	100%	103.14	100%
Repaglinide Quench cooled	Initial	0.0	0%	0.0	0%
	week 1	6.40	6%	13.78	13%
	week 2	15.34	15%	17.54	17%
	week 4	18.12	18%	31.72	31%

Repaglinide Original sample had a melting enthalpy of 103.14 J/g with no glass transition. Percentage of crystalline drug in each sample was derived using enthalpy (J/g) of melting of each quench cooled sample with respect to that of the 100% crystalline drug sample. It further shows that the percent crystalline component of drug increased with time in quench cooled samples subjected to 40°C/75%RH and 30°C/60%RH conditions. This suggests that there is a need for a

stabilization technique such as solid dispersion to stabilize the amorphous form. Percentage of crystalline drug increased from 0% to 18% in 4 weeks at 30ºC/60%RH condition and from 0% to 31% in 4 weeks at 40ºC/75%RH condition. The trend of increase in crystalline component in quench cooled Repaglinide sample can be clearly seen from the figures below.

Figure 19 Crystalline component of drug in quench cooled Repaglinide (RQC) samples placed on 30ºC/60%RH (A) and 40ºC/75%RH condition for stability (B)

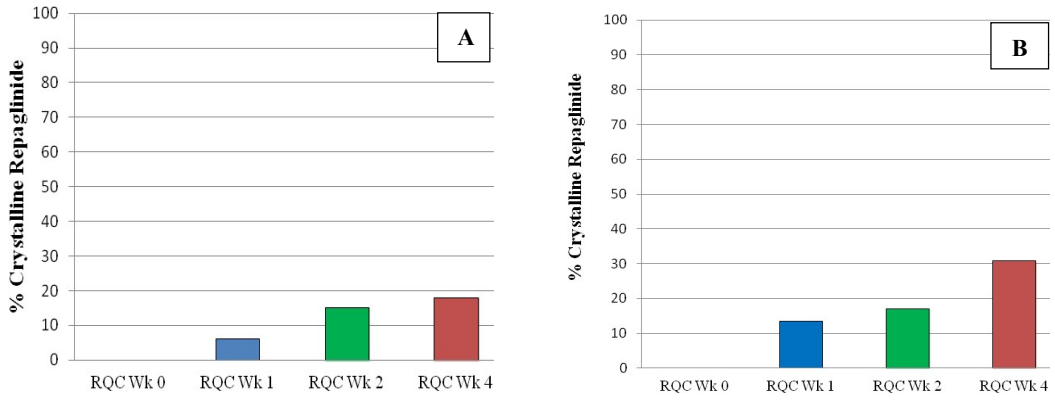

3.2.2 Solid dispersions prepared in 1:3 Repaglinide: Carrier ratio

Figures 20 shows DSC graphs of quench cooled Repaglinide: Syloid® 244FP solid dispersion (RS dispersion) prepared in 1:3 ratio and stored at 30ºC/60%RH conditions. Figure 20B shows glass transition event and Figure 20C shows melting event with the peaks and enthalpy values. From Figure 20B, it can be observed that the enthalpy of relaxation is increasing from initial time point to week 4. The enthalpy relaxation values were much lower than that of the Quench cooled Repaglinide samples. The values of melting enthalpy were significantly lower than the values obtained for quench cooled Repaglinide and recrystallization peak was not seen in any samples. Table below summarizes values pertaining to glass transition and melting for quench cooled samples stored at 30ºC/60%RH.

Figure 20 DSC overlay of Repaglinide: Syloid® 244FP solid dispersion (Ratio 1:3) stored up to 4 weeks at 30ºC/60%RH conditions (A), glass transition (B), melting (C)

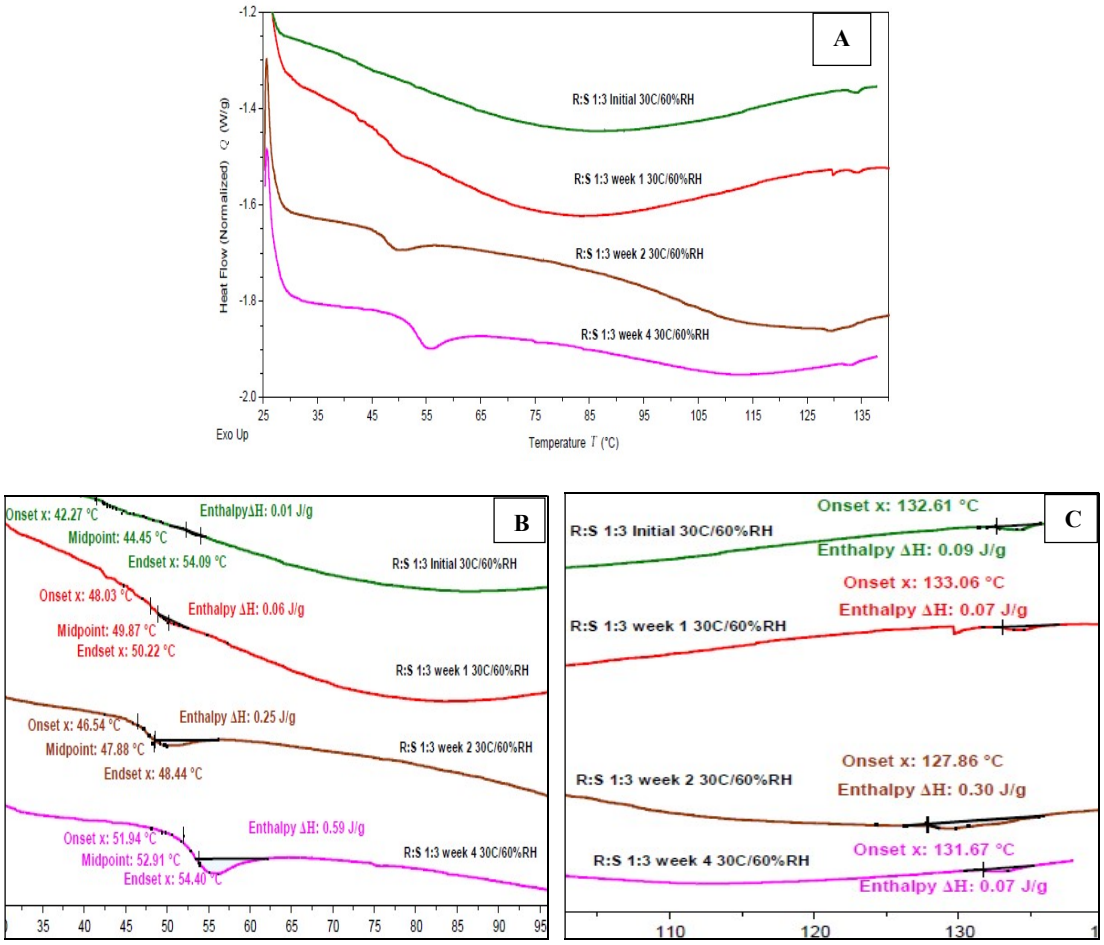

Table 3.5 Summary of thermal events on DSC graphs for Repaglinide: Syloid® 244FP solid dispersion (Ratio 1:3) at 30ºC/60%RH (enthalpy values adjusted for concentration of API in the sample)

Sample	Time point	Glass Transition				Melting	
		Onset, ºC	Midpoint, ºC	Endset, ºC	Enthalpy, J/g	Onset, ºC	Enthalpy, J/g
Repaglinide: Syloid 1:3 Ratio at 30ºC/60% RH	Initial	42.27	44.45	54.09	0.04	132.61	0.36
	1 week	48.03	49.87	50.22	0.24	133.06	0.28
	2 week	46.54	47.88	48.44	1.00	127.86	1.20
	4 week	51.94	52.91	54.40	2.36	131.67	0.28

Figures 21 shows DSC graphs of quench cooled Repaglinide: Syloid® 244FP solid dispersion (RS dispersion) prepared in 1:3 ratio and stored at 40ºC/75%RH conditions. Figure 21B shows glass transition event and Figure 21C shows melting event with peaks and enthalpy values.

Figure 21 DSC overlay of Repaglinide: Syloid® 244FP (Ratio 1:3) solid dispersion stored up to 4 weeks at 40ºC/75%RH conditions (A), glass transition (B), melting (C)

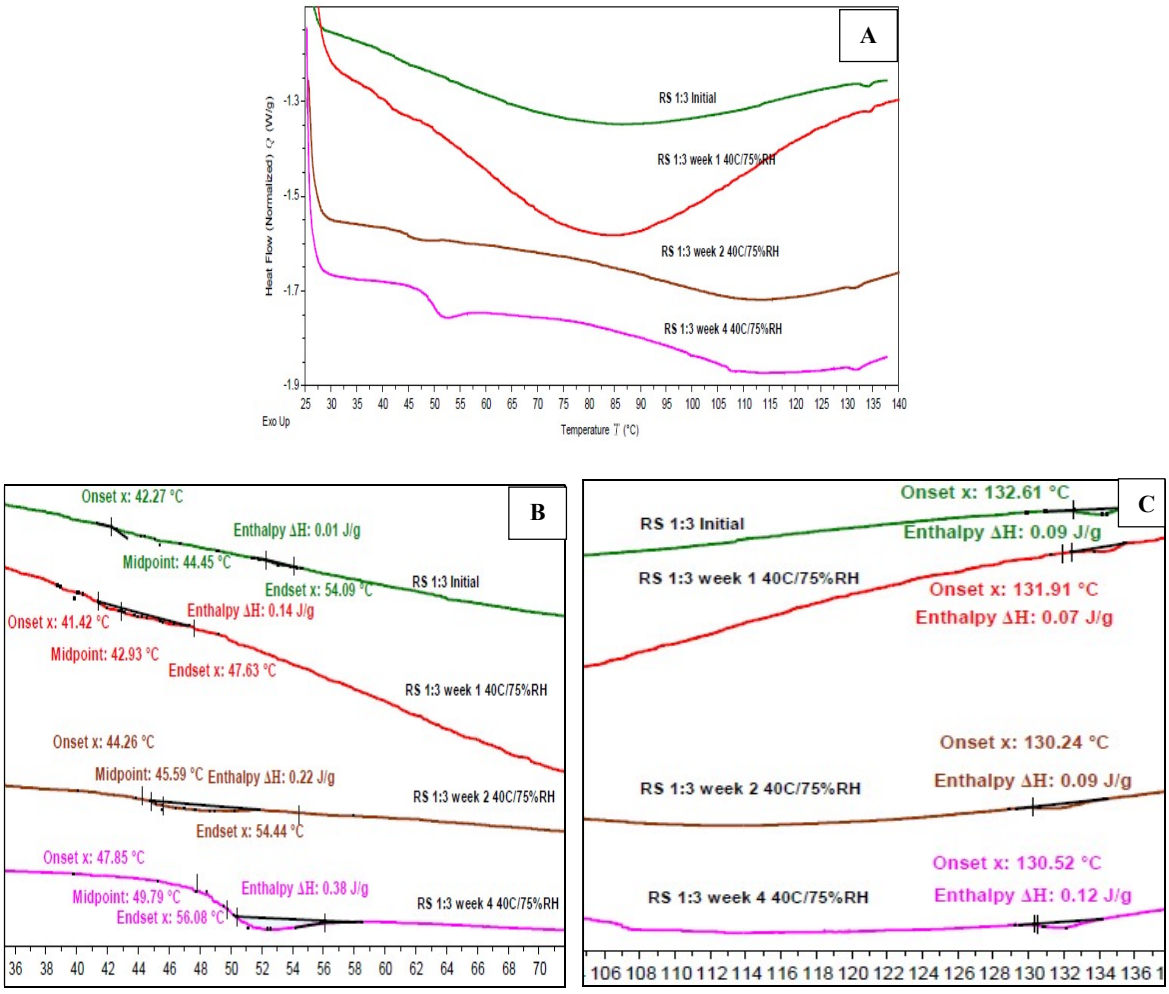

From Figure 21B, it can be seen that the enthalpy of relaxation is increasing from initial time point to week 4. The enthalpy of relaxation was much lower compared to that of 30ºC/60%RH condition. The values of melting enthalpy were significantly lower than the values obtained for quench cooled Repaglinide and similar to the values obtained for RS 1:3 dispersion stored at

30ºC/60%RH condition. The recrystallization peak was not seen in any samples. Table below summarizes values pertaining to glass transition and melting for quench cooled samples stored at 40ºC/75%RH.

Table 3.6 Summary of thermal events on DSC graphs for Repaglinide: Syloid® 244FP solid dispersion (Ratio 1:3) samples stored at 40ºC/75%RH (enthalpy values adjusted for concentration of API in the sample)

Sample	Time point	Glass Transition				Melting	
		Onset, ºC	Midpoint, ºC	Endset, ºC	Enthalpy, J/g	Onset, ºC	Enthalpy, J/g
Repaglinide: Syloid 1:3 Ratio at 40ºC/75% RH	Initial	42.27	44.45	54.09	0.04	132.61	0.36
	1 week	41.42	42.93	47.63	0.56	131.91	0.28
	2 week	44.26	45.59	54.44	0.88	130.24	0.36
	4 week	47.85	49.79	56.08	1.52	130.52	0.48

Figures 22 shows DSC graphs of Repaglinide: MCC PH101 solid dispersion (RMC dispersion) prepared in 1:3 ratio and stored at 30ºC/60%RH conditions up to 4 weeks. Figure 22B shows glass transition event and Figure 22C shows melting event with characterization of the peaks and calculating enthalpy values.

Figure 22 DSC overlay of Repaglinide: MCC (Ratio 1:3) solid dispersion stored up to 4 weeks at 30ºC/60%RH conditions (A), glass transition (B), melting (C)

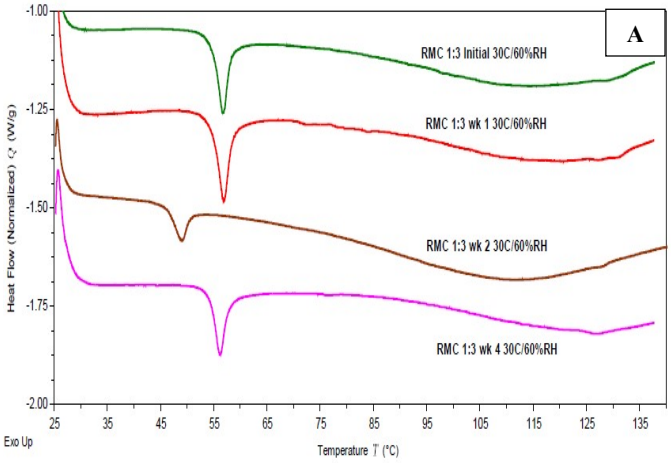

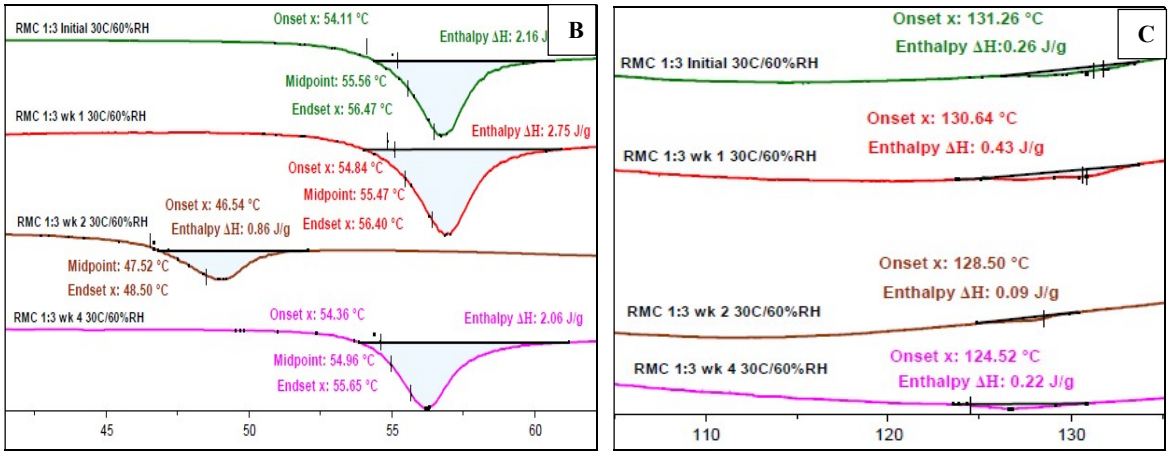

Enthalpy of relaxation values and glass transition temperatures as observed in figure 22B for RMC 1:3 dispersion stored at 30ºC/60%RH was similar for all time points except week 2 where the enthalpy of relaxation was less, and glass transition temperature was less for this sample. The enthalpies of relaxation values were higher than that of the corresponding RS 1:3 dispersion samples. The melting enthalpy seen from figure 22C was lesser compared to that of the quench cooled Repaglinide samples. It was seen that the melting point values was lowered for RMC 1:3 dispersions and lowering with time was observed. Table 3.7 below summarizes the thermal events and enthalpies observed for RMC 1:3 dispersions stored at 30ºC/60%RH conditions.

Table 3.7 Summary of thermal events on DSC graphs for Repaglinide: Microcrystalline Cellulose PH101 solid dispersion (Ratio 1:3) stored up to 4 weeks at 30ºC/60%RH conditions (enthalpy values adjusted for concentration of API in the sample)

Sample	Time point	Glass Transition				Melting	
		Onset, ºC	Midpoint, ºC	Endset, ºC	Enthalpy, J/g	Onset, ºC	Enthalpy, J/g
Repaglinide: MCC 1:3 Ratio at 30ºC/60% RH	Initial	54.11	55.56	56.47	8.64	131.26	1.04
	1 week	54.84	55.47	56.40	11.00	130.64	1.72
	2 week	46.54	47.52	48.50	3.44	128.50	0.36
	4 week	54.36	54.96	55.65	8.24	124.52	0.88

Figures 23 shows DSC graphs of quench cooled Repaglinide: MCC solid dispersion (RS dispersion) prepared in 1:3 ratio and stored at 40ºC/75%RH conditions. Figure 23B shows glass transition event and Figure 23C shows melting event with peaks and enthalpy values.

Figure 23 DSC overlay of Repaglinide: MCC solid dispersion (Ratio 1:3) stored up to 4 weeks at 40ºC/75%RH conditions (A), glass transition (B), melting (C)

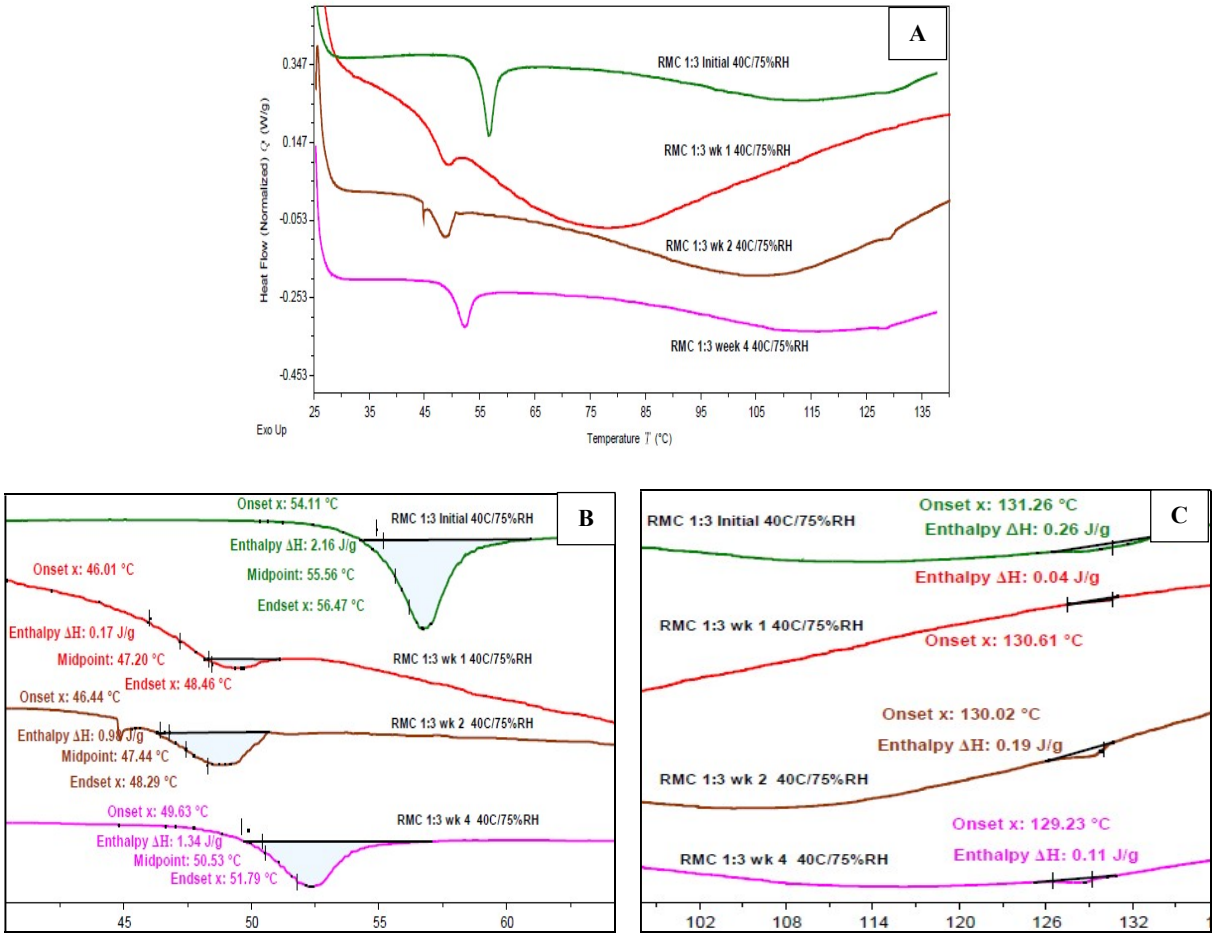

Figures 23B shows that the enthalpy of relaxation increased with time from week 1 to week 4 timepoint with a higher value observed for initial sample. It can be observed from Figure 23C that the enthalpy of melting peaks is smaller with less enthalpy of melting. For RMC 1:3 dispersions stored at 40ºC/75% RH condition, the enthalpy of relaxation was lesser than that observed for 30ºC/60% RH condition. Melting enthalpy values were low and comparable to the

values of RS 1:3 dispersions. It was observed that the solid dispersion of Repaglinide: Syloid® 244FP and Repaglinide: MCC 101 prepared in 1:3 ratio does not have a sharp melting peak of Repaglinide in both stability conditions, albeit a very small melting transition was noticed.

Table 3.8 Summary of thermal events on DSC graphs for Repaglinide: Microcrystalline Cellulose PH101 solid dispersion (Ratio 1:3) stored up to 4 weeks at 40ºC/75%RH conditions (enthalpy values adjusted for concentration of API in the sample)

Sample	Timepoint	Glass Transition				Melting	
		Onset, ºC	Midpoint, ºC	Endset, ºC	Enthalpy, J/g	Onset, ºC	Enthalpy, J/g
Repaglinide: MCC 1:3 Ratio at 40ºC/75% RH	Initial	54.11	55.56	56.47	8.64	131.26	1.04
	1 week	46.01	47.20	48.46	0.68	130.1	0.16
	2 week	46.44	47.44	48.29	3.92	130.02	0.76
	4 week	49.63	50.53	51.79	5.36	129.23	0.44

Percent crystalline component calculated for all the 1:3 ratio samples is summarized in the table below. It can be observed that the crystalline component in both RS and RMC solid dispersions is significantly less for all time points as compared to that of the quench cooled Repaglinide samples.

Table 3.9 Enthalpy of melting peak and percent crystallinity of drug in 1:3 solid dispersion samples in 30ºC/60%RH and 40ºC/75%RH conditions

		30ºC/60%RH conditions		40ºC/75%RH conditions	
Sample	Time point	Enthalpy, J/g	% Crystalline Drug	Enthalpy, J/g	% Crystalline Drug
RS 1:3 Ratio	Initial	0.36	0.35	0.36	0.35
	week 1	0.28	0.27	0.28	0.27
	week 2	1.20	1.16	0.36	0.35
	week 4	0.28	0.27	0.48	0.47
RMC 1:3 Ratio	Initial	1.04	1.00	1.04	1.00
	week 1	1.72	1.67	0.16	0.16
	week 2	0.36	0.35	0.76	0.74
	week 4	0.88	0.85	0.44	0.43

3.2.3 Solid dispersions prepared in 1:1 Drug: Carrier ratio:

Figures 24 shows DSC graphs of Repaglinide: Syloid® 244FP solid dispersion (RS dispersion) prepared in 1:1 ratio and stored at 30ºC/60%RH conditions.

Figure 24 DSC overlay of Repaglinide: Syloid® 244FP (Ratio 1:1) solid dispersion stored up to 4 weeks at 30ºC/60%RH conditions (A), glass transition (B), melting (C)

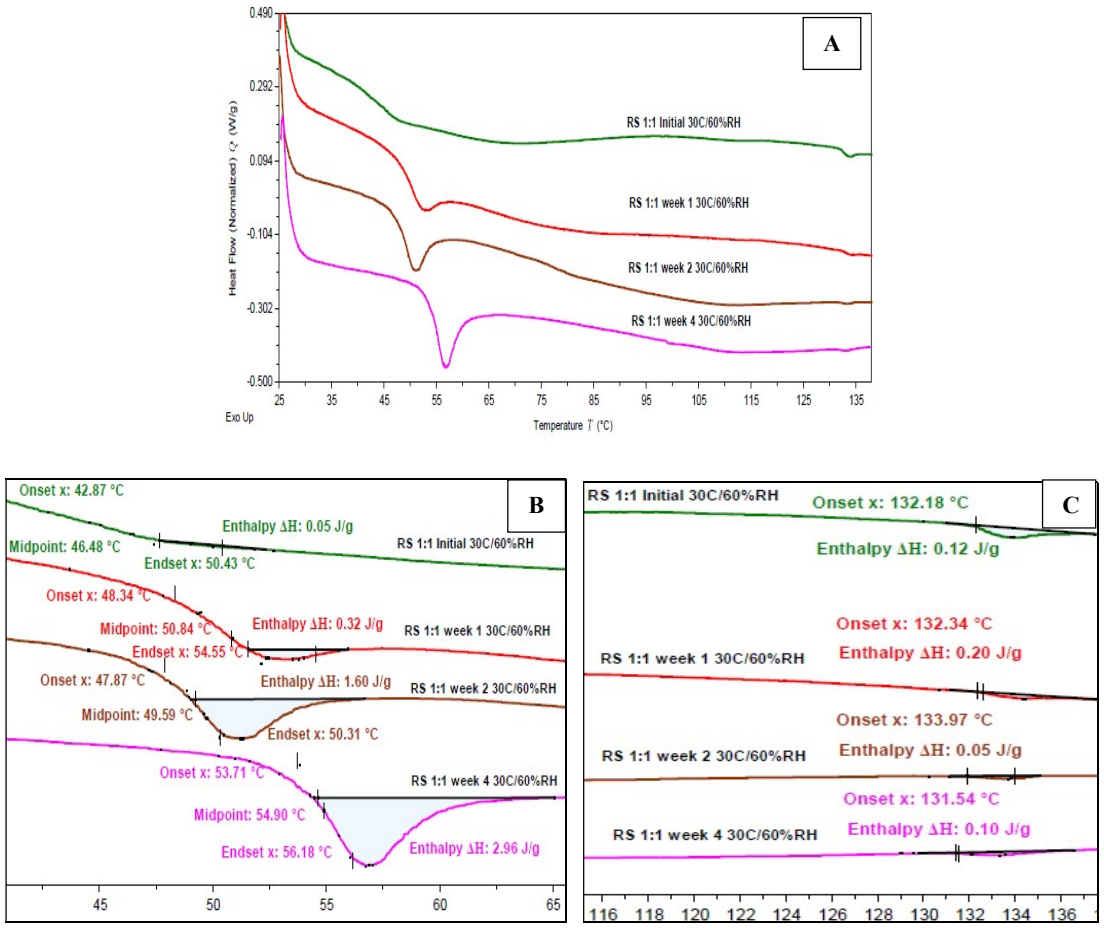

Figure 24B shows glass transition event and Figure 24C shows melting event with characterization of the peaks and calculating enthalpy values. Figure 24B shows that for RS 1:1 solid dispersion stored at 30ºC/60% RH, there was an increase in enthalpy of relaxation from initial time point to week 4. The melting enthalpy was less compared to that of the quench cooled

Repaglinide samples. Table 3.10 summarizes the temperatures of thermal transitions and enthalpies.

Table 3.10 Summary of thermal events on DSC graphs for Repaglinide: Syloid® 1:1 Ratio stored at 30ºC/60% RH conditions (enthalpy values adjusted for concentration of API in the sample)

ample	Time point	Glass Transition				Melting	
		Onset, ºC	Midpoint, ºC	Endset, ºC	Enthalpy, J/g	Onset, ºC	Enthalpy, J/g
Repaglinide: Syloid 1:1 Ratio at 30ºC/60% RH	Initial	42.87	46.48	50.43	0.10	132.18	0.24
	1 week	48.34	50.84	54.55	0.64	132.34	0.40
	2 week	47.87	49.59	50.31	3.2	133.97	0.10
	4 week	53.71	54.90	56.18	5.92	131.54	0.20

Figures 25 shows DSC graphs of Repaglinide: Syloid® 244FP solid dispersion (RS dispersion) prepared in 1:1 ratio and stored at 40ºC/75%RH conditions.

Figure 25 DSC overlay of Repaglinide: Syloid® 244FP (Ratio 1:1) solid dispersion stored up to 4 weeks at 40ºC/75%RH conditions (A), glass transition (B), melting (C)

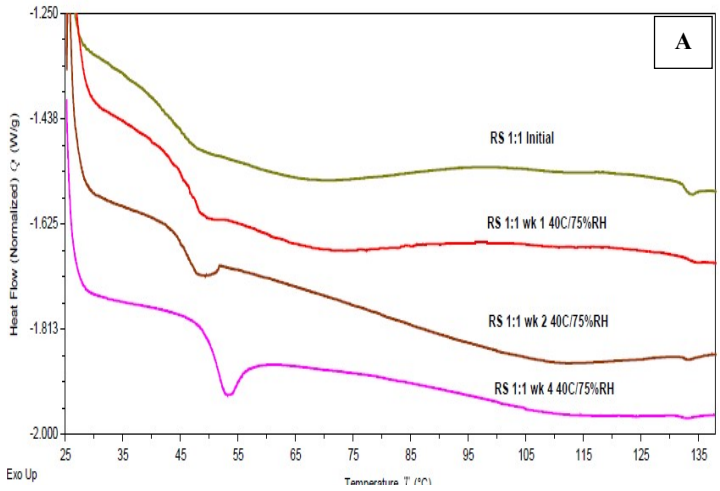

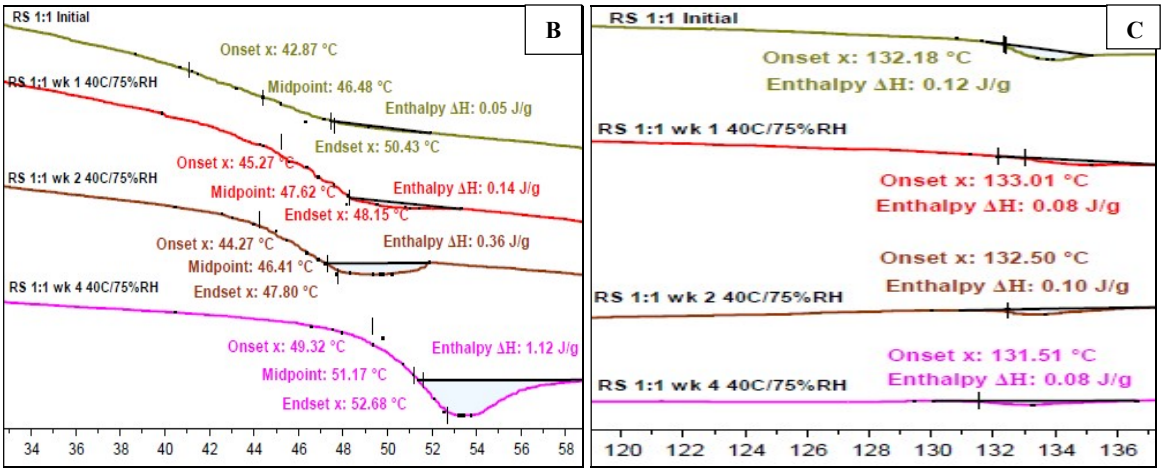

Figure 25B shows glass transition event and Figure 25C shows melting event with characterization of the peaks and calculating enthalpy values. From figure 25B, it can be observed that there is an increase in enthalpy of relaxation with time. The enthalpy of relaxation was lesser than that of the 30ºC/60% RH condition for the same solid dispersion. The enthalpy of melting values as seen in figure 25B are smaller as compared to that of the quench cooled Repaglinide samples.

Table 3.11 Summary of thermal events on DSC graphs for Repaglinide: Syloid® 1:1 Ratio stored at 40ºC/75% RH conditions (enthalpy values adjusted for concentration of API in the sample)

Sample	Timepoint	Glass Transition				Melting	
		Onset, ºC	Midpoint, ºC	Endset, ºC	Enthalpy, J/g	Onset, ºC	Enthalpy, J/g
Repaglinide: Syloid 1:1 Ratio at 40ºC/75% RH	Initial	42.87	46.48	50.43	0.10	132.18	0.24
	1 week	45.27	47.62	48.15	0.28	133.01	0.16
	2 week	44.27	46.41	47.80	0.72	132.50	0.20
	4 week	49.32	51.17	52.68	2.24	131.51	0.16

Figure 26 shows DSC graphs of Repaglinide: MCC PH101 solid dispersion (RMC dispersion) prepared in 1:1 ratio and stored at 30ºC/60%RH conditions.

Figure 26 DSC overlay of Repaglinide: Microcrystalline Cellulose PH101 solid dispersion (Ratio 1:1) stored up to 4 weeks at 30ºC/60%RH conditions (A), glass transition (B), melting (C)

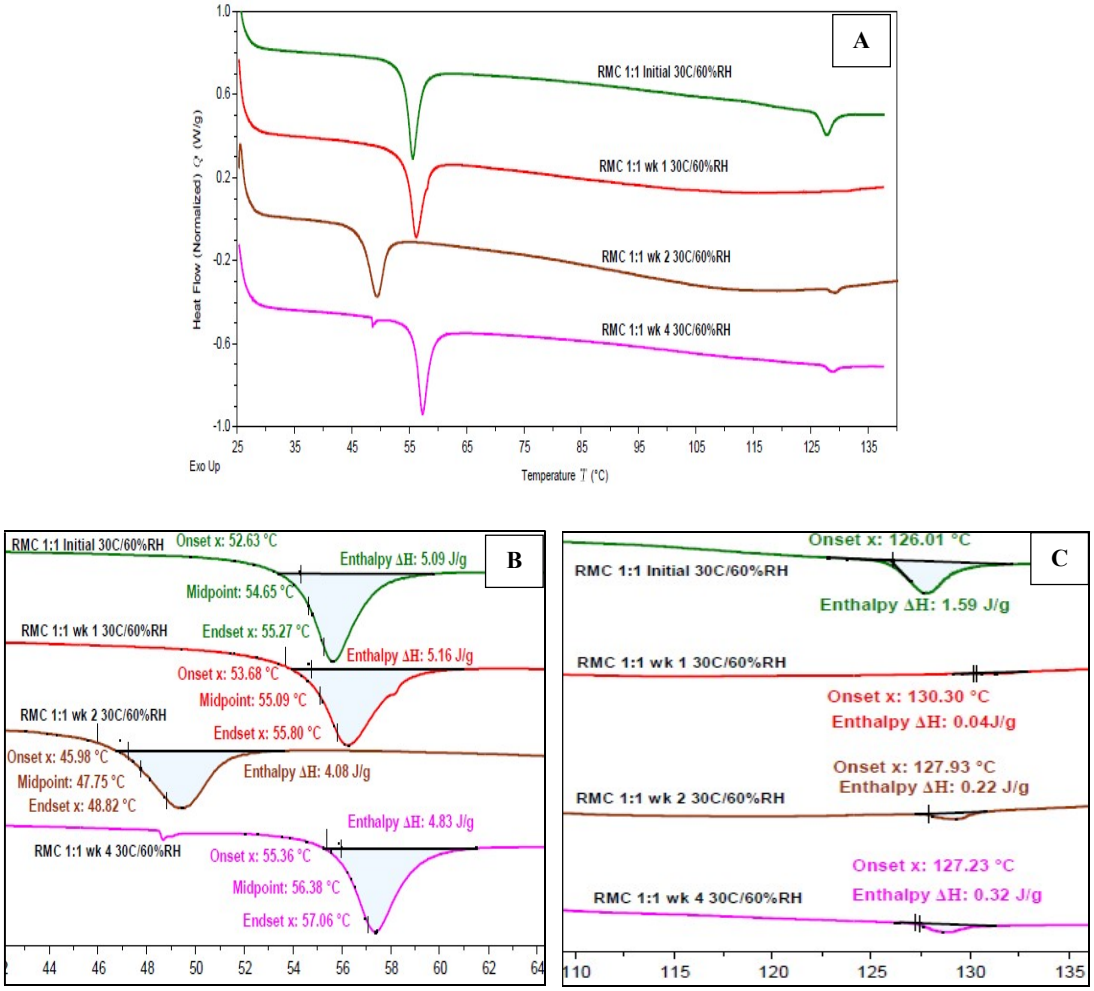

Figure 26B shows glass transition event and Figure 26C shows melting event with characterization of the peaks and calculating enthalpy values. It can be observed in figure 26B that the enthalpy of relaxation is variable and does not show a trend of an increase or decrease with time. There are small melting transition peaks as observed in figure 26C.

Table 3.12 summarizes the temperatures of thermal events and enthalpies. For RMC 1:1 solid dispersion stored at 30ºC/60% RH, the enthalpy of relaxation was higher than that of the RS 1:1

dispersion stored at the same condition. The melting enthalpy was less compared to that of the quench cooled Repaglinide samples.

Table 3.12 Summary of thermal events on DSC graphs for Repaglinide: : Microcrystalline Cellulose PH101 solid dispersion (Ratio 1:1) stored up to 4 weeks at 30ºC/60%RH conditions (enthalpy values adjusted for concentration of API in the sample)

Sample	Time point	Glass Transition				Melting	
		Onset, ºC	Midpoint, ºC	Endset, ºC	Enthalpy, J/g	Onset, ºC	Enthalpy, J/g
Repaglinide: MCC 1:1 Ratio at 30ºC/60% RH	Initial	52.63	54.65	55.27	10.18	126.01	3.18
	1 week	53.68	55.09	55.80	10.32	130.30	0.08
	2 week	45.98	47.75	48.82	8.16	127.93	0.44
	4 week	55.36	56.38	57.06	9.66	127.23	0.64

Figure 27 shows DSC graphs of Repaglinide: MCC PH101 solid dispersion (RMC dispersion) prepared in 1:1 ratio and stored at 40ºC/75%RH conditions. Figure 27B shows glass transition event and Figure 27C shows melting event with peaks and enthalpy values.

Figure 27 DSC overlay of Repaglinide: MCC PH101 solid dispersion (Ratio 1:1) stored up to 4 weeks at 40ºC/75%RH conditions (A), glass transition (B), melting (C)

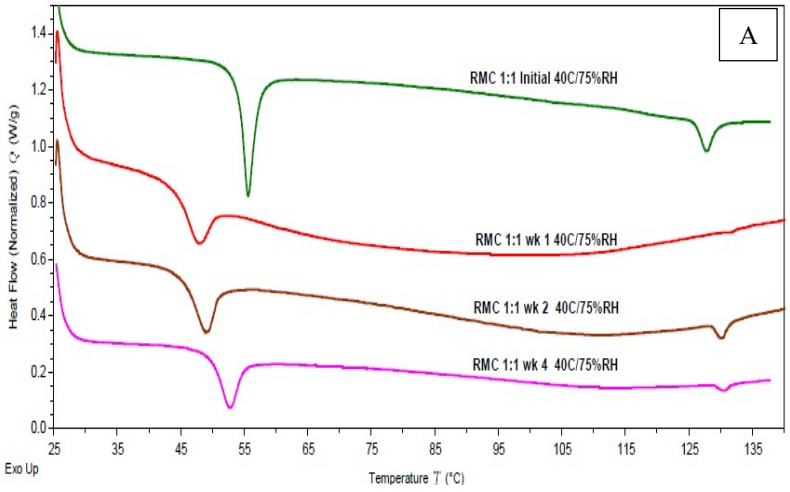

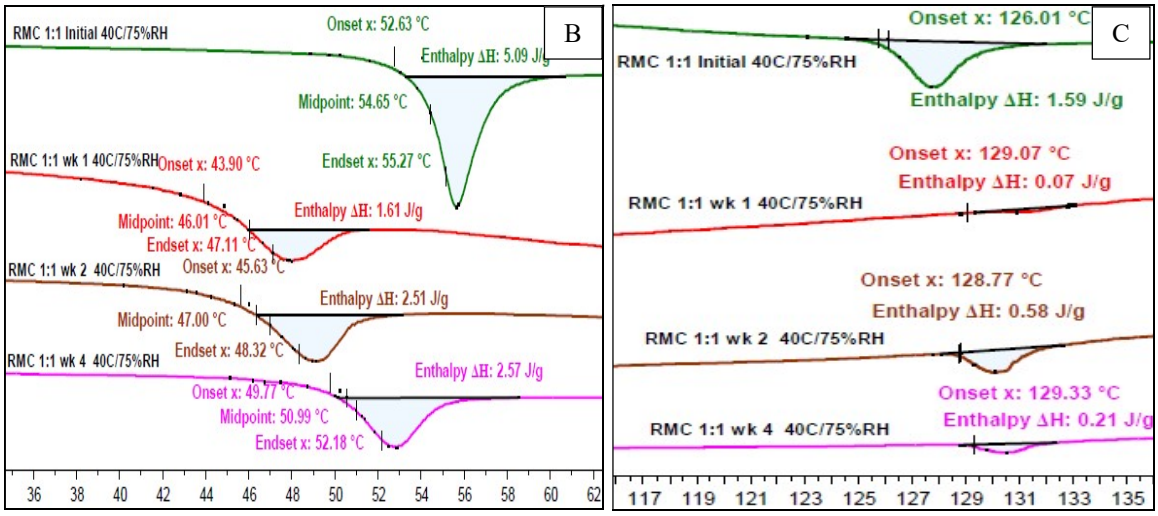

It can be observed in figure 27B that the enthalpy of relaxation is variable and doesn't show a trend of an increase or decrease with time. There are small melting transition peaks as observed in figure 27C. For RMC 1:1 solid dispersion stored at 40ºC/75% RH, the enthalpy of relaxation was lower than that of the same samples stored in 30ºC/60% RH condition. The melting enthalpy was less compared to that of the quench cooled Repaglinide samples and lowered melting point was observed. The summary of events for RMC sample stores at 40ºC/75%RH condition is provided in table 3.13.

Table 3.13 Summary of thermal events on DSC graphs for Repaglinide: : Microcrystalline Cellulose PH101 solid dispersion (Ratio 1:1) stored up to 4 weeks at 40ºC/75%RH conditions (enthalpy values adjusted for concentration of API in the sample)

Sample	Time point	Glass Transition				Melting	
		Onset, ºC	Midpoint, ºC	Endset, ºC	Enthalpy, J/g	Onset, ºC	Enthalpy, J/g
Repaglinide: MCC 1:1 Ratio at 40ºC/75% RH	Initial	52.63	54.65	55.27	10.18	126.01	3.18
	1 week	43.90	46.01	47.11	3.22	129.07	0.14
	2 week	45.63	47.00	48.32	5.02	128.77	1.16
	4 week	49.77	50.99	52.18	5.14	129.33	0.42

Percent crystalline component of Repaglinide in RS and RMC solid dispersions in 1:1 ratio is calculated in table 3.14. It can be observed that there is a small percentage of drug converted in crystalline form.

Table 3.14 Enthalpy of melting peak and percent crystallinity of drug in 1:1 solid dispersion samples in 30ºC/60%RH and 40ºC/75%RH and conditions

		30ºC/60%RH conditions		40ºC/75%RH conditions	
Sample	**Time point**	**Enthalpy, J/g**	**% Crystalline Drug**	**Enthalpy, J/g**	**% Crystalline Drug**
RS 1:1 Ratio	Initial	0.24	0.23	0.24	0.23
	week 1	0.40	0.39	0.16	0.16
	week 2	0.10	0.10	0.20	0.19
	week 4	0.20	0.19	0.16	0.16
RMC 1:1 Ratio	Initial	3.18	3.08	3.18	3.08
	week 1	0.08	0.08	0.14	0.14
	week 2	0.44	0.43	1.16	1.12
	week 4	0.64	0.62	0.42	0.41

3.2.4 Solid dispersions prepared in 3:1 Drug: Carrier ratio:

Figures 28 shows DSC graphs of Repaglinide: Syloid®244FP solid dispersion (RS dispersion) prepared in 3:1 ratio and stored at 30ºC/60%RH conditions. Figure 28B shows glass transition event and Figure 28C shows melting event with characterization of the peaks and calculating enthalpy values. The enthalpy of relaxation in RS 3:1 sample stored at 30ºC/60%RH conditions was higher than that of the other ratio. Enthalpy of melting was not much different that the samples containing lower drug ratios. There was a slight increase in melting enthalpy and lowered melting point at week 4 compared to earlier time points.

Figure 28 DSC overlay of Repaglinide: Syloid®244FP (Ratio 3:1) solid dispersion stored up to 4 weeks at 30ºC/60%RH conditions (A), glass transition (B), melting (C)

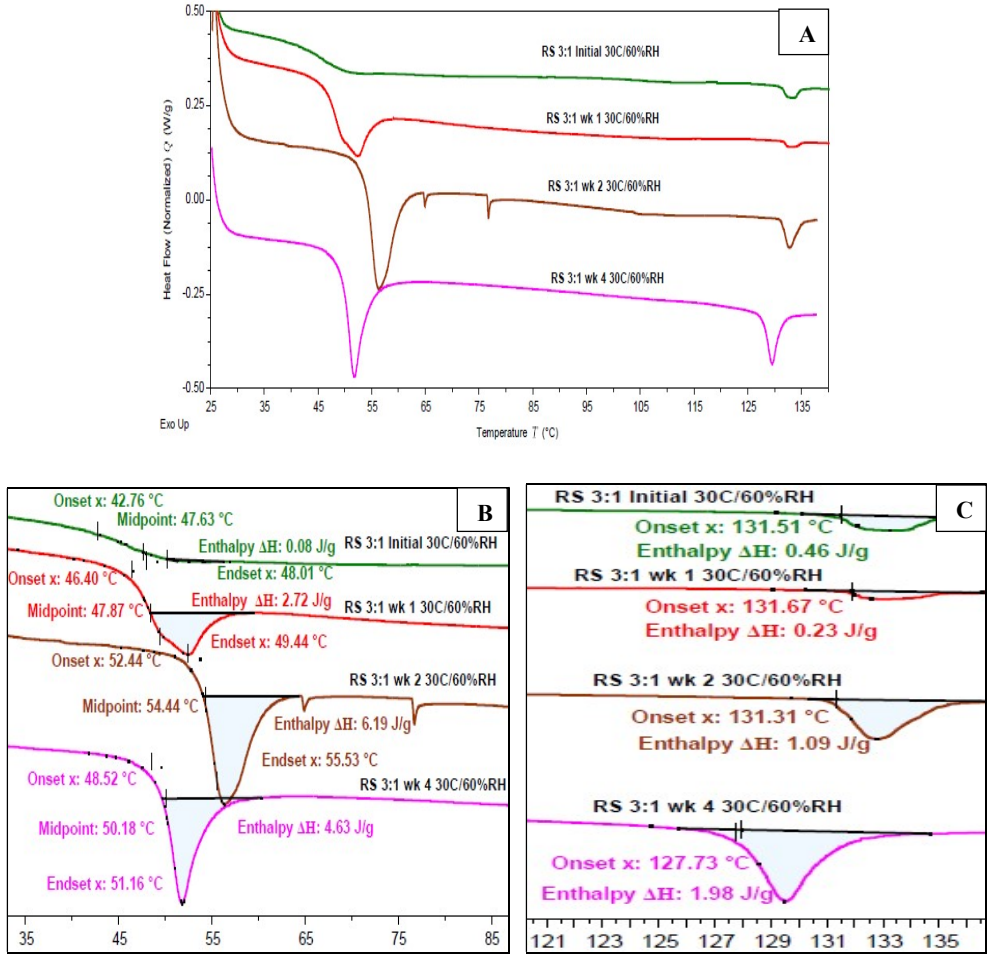

Table 3.15 Summary of thermal events on DSC graphs for Repaglinide: Syloid® 244FP (Ratio 3:1) solid dispersion stored up to 4 weeks at 30ºC/60%RH conditions

Sample	Timepoint	Glass Transition				Melting	
		Onset, ºC	Midpoint, ºC	Endset, ºC	Enthalpy, J/g	Onset, ºC	Enthalpy, J/g
Repaglinide: Syloid 3:1 Ratio at 30ºC/60% RH	Initial	42.76	47.63	48.01	0.11	131.51	0.61
	1 week	46.40	47.87	49.44	3.62	131.67	0.31
	2 weeks	52.44	54.44	55.53	8.23	131.31	1.45
	4 weeks	48.52	50.18	51.16	6.16	127.73	2.63

From the table above, it could be observed that the enthalpy of melting increases with time from initial timepoint to 4 weeks, but it is less than that observed for Repaglinide quench cooled sample.

Figures 29 shows DSC graphs of Repaglinide: Syloid®244FP solid dispersion (RS dispersion) prepared in 3:1 ratio and stored at 40ºC/75%RH conditions.

Figure 29 DSC overlay of Repaglinide: Syloid® 244FP (Ratio 3:1) solid dispersion stored up to 4 weeks at 40ºC/75%RH conditions (A), glass transition (B), melting (C)

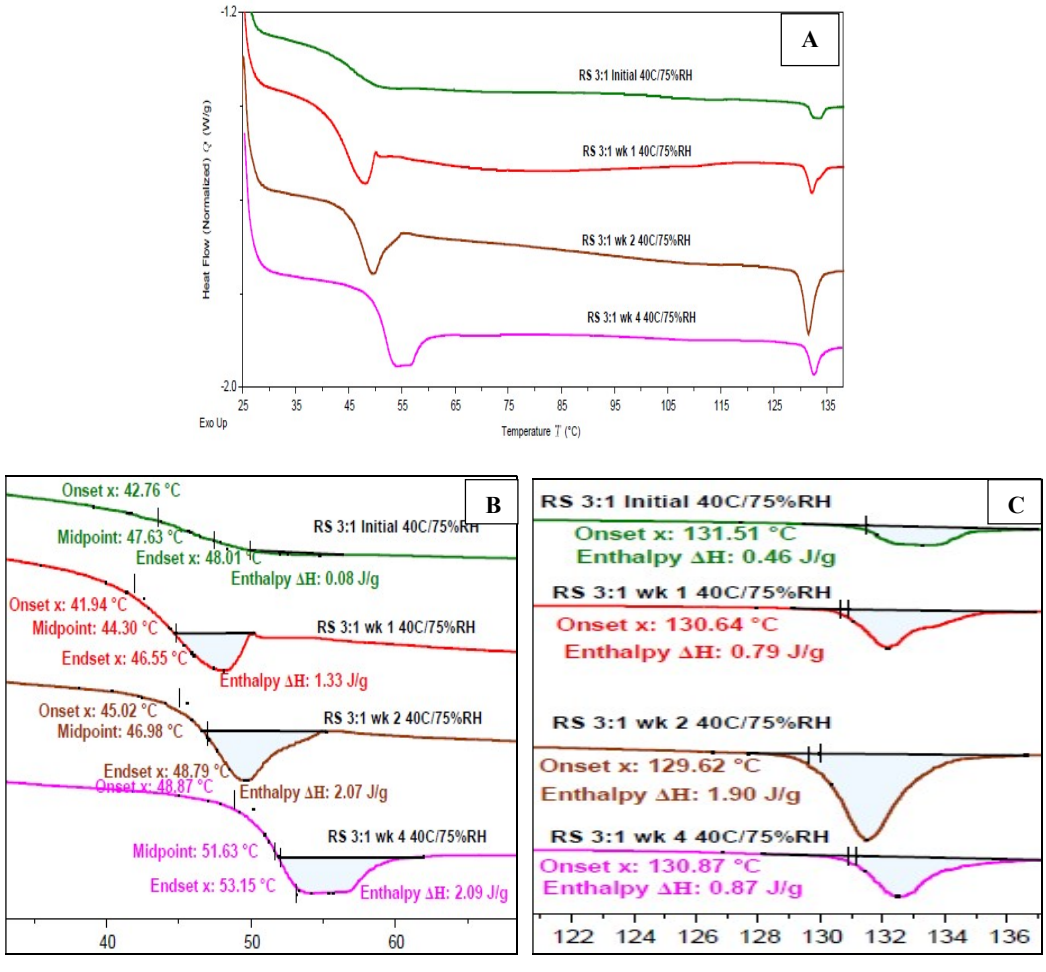

Figure 29B shows glass transition event and Figure 29C shows melting event with peaks and enthalpy values. The enthalpy of relaxation in RS 3:1 sample stored at 40ºC/75%RH conditions

was higher than that of the samples at 30ºC/60%RH storage condition. Enthalpy of melting was not much different than the samples containing lower drug ratios.

Table 3.16 Summary of thermal events on DSC graphs for Repaglinide: Syloid® 244FP (Ratio 3:1) solid dispersion stored up to 4 weeks at 40ºC/75%RH conditions

Sample	Time point	Glass Transition				Melting	
		Onset, ºC	Midpoint, ºC	Endset, ºC	Enthalpy, J/g	Onset, ºC	Enthalpy, J/g
Repaglinide: Syloid 3:1 Ratio at 40ºC/75% RH	Initial	42.76	47.63	48.01	0.11	131.51	0.61
	1 week	41.94	44.30	46.55	1.77	130.64	1.05
	2 week	45.02	46.98	48.79	2.75	129.62	2.53
	4 week	48.87	51.63	53.15	2.78	130.87	1.16

Figures 30 shows DSC graphs of Repaglinide: MCC PH101 solid dispersion (RMC dispersion) prepared in 3:1 ratio and stored at 30ºC/60%RH conditions. Figure 30B shows glass transition event and Figure 30C shows melting event with peaks and enthalpy values. For RMC 3:1 solid dispersion stored at 30ºC/60% RH, there was variation in enthalpy of relaxation and enthalpy in melting. The melting point was lowered.

Figure 30 DSC thermograms of Repaglinide: MCC solid dispersion (Ratio 3:1) stored up to 4 weeks at 30ºC/60%RH conditions (A), glass transition (B), melting (C)

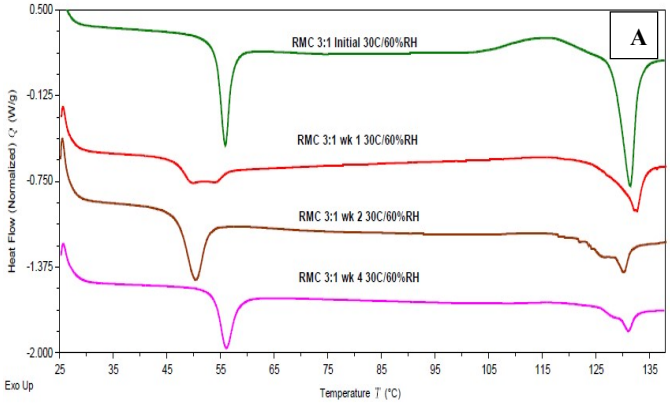

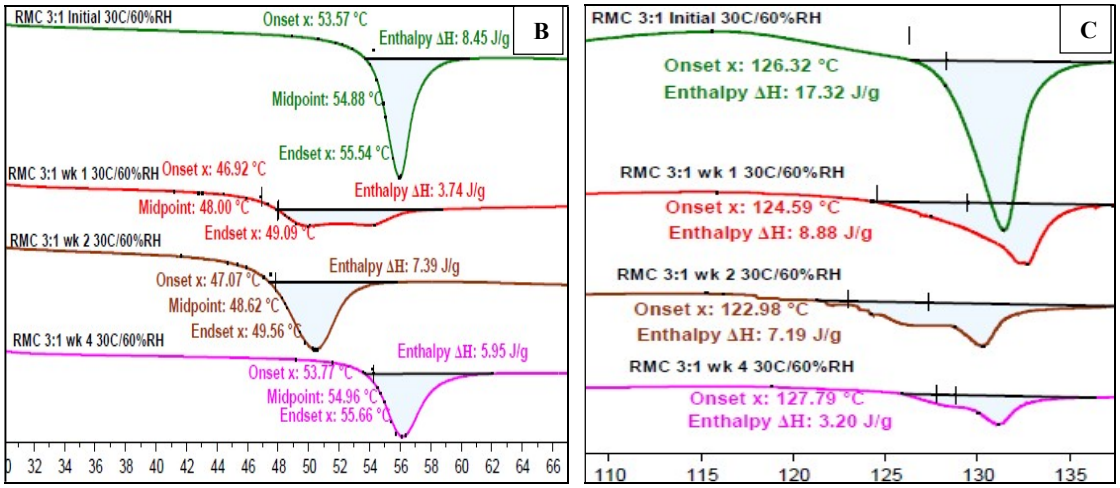

Table 3.17 Summary of thermal events on DSC graphs for Repaglinide: Microcrystalline Cellulose PH101 solid dispersion (Ratio 3:1) stored up to 4 weeks at 30ºC/60%RH conditions

Sample	Time point	Glass Transition				Melting	
		Onset, ºC	Midpoint, ºC	Endset, ºC	Enthalpy, J/g	Onset, ºC	Enthalpy, J/g
Repaglinide: MCC 3:1 Ratio at 30ºC/60% RH	Initial	53.57	54.88	55.54	11.24	126.32	23.04
	1 week	46.92	48.00	49.09	4.97	124.59	11.81
	2 week	47.07	48.62	49.56	9.83	122.98	9.56
	4 week	53.77	54.96	55.66	7.91	127.79	4.26

Figures 31 shows DSC graphs of Repaglinide: MCC PH101 solid dispersion (RMC dispersion) prepared in 3:1 ratio and stored at 40ºC/75%RH conditions. Figure 31B shows glass transition event and Figure 31C shows melting event with peaks and enthalpy values.

For RMC 3:1 solid dispersion stored at 40ºC/75% RH, there was variation in enthalpy of relaxation and enthalpy in melting. The enthalpy of relaxation was lower than that of the same samples in 30ºC/60% RH condition. The melting point was lowered.

Figure 31 DSC overlay of Repaglinide: MCC solid dispersion (Ratio 3:1) stored up to 4 weeks at 40ºC/75%RH conditions (A), glass transition (B), melting (C)

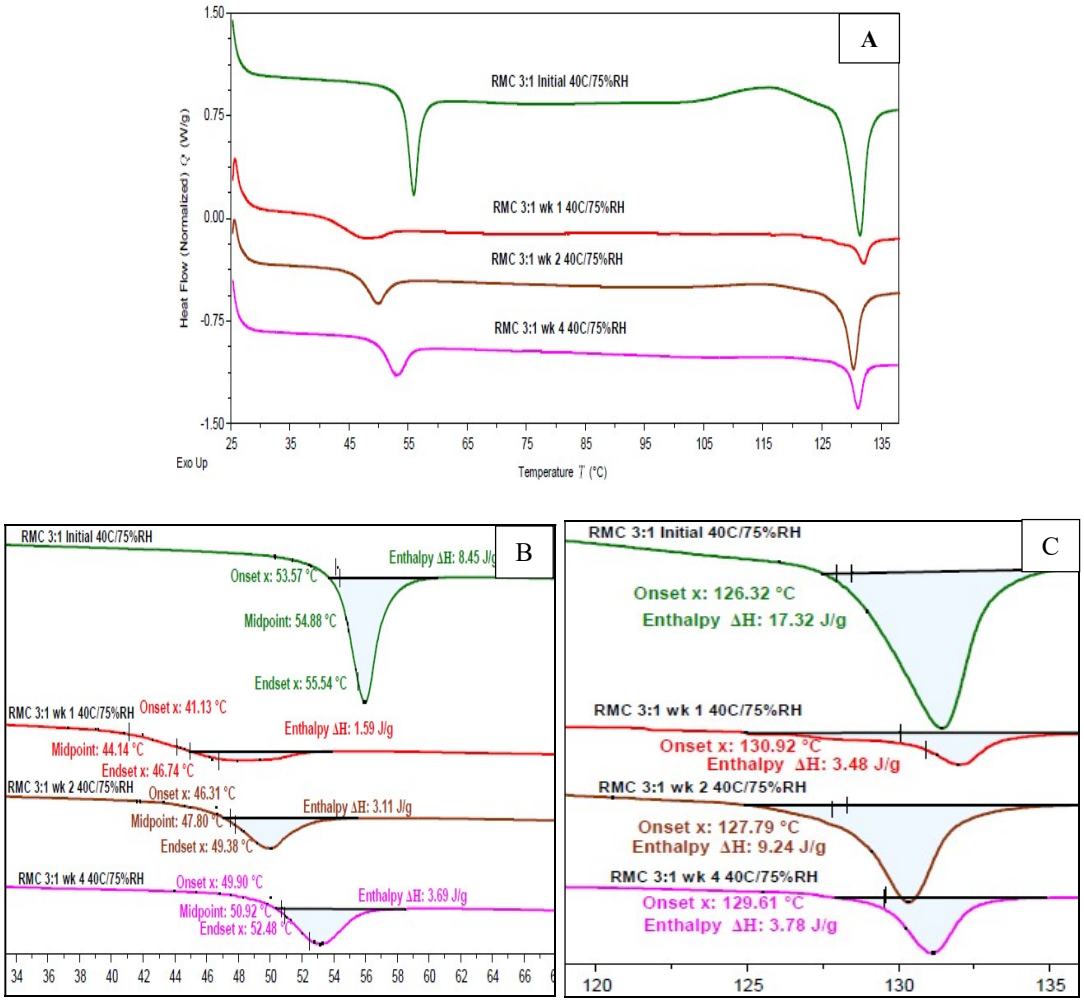

Table 3.18 Summary of thermal events on DSC graphs for Repaglinide: Microcrystalline Cellulose PH101 solid dispersion (Ratio 3:1) stored up to 4 weeks at 40ºC/75%RH conditions

Sample	Time point	Glass Transition				Melting	
		Onset, ºC	Midpoint, ºC	Endset, ºC	Enthalpy, J/g	Onset, ºC	Enthalpy, J/g
Repaglinide: MCC 3:1 Ratio at 40ºC/75% RH	Initial	53.57	54.88	55.54	11.24	126.32	23.04
	1 week	41.13	44.14	46.74	2.11	130.92	4.63
	2 week	46.31	47.80	49.38	4.14	127.79	12.29
	4 week	49.90	50.92	52.48	4.91	129.61	5.03

Percent crystalline component in solid dispersions was calculated and provided in the table below. It could be observed that there was a lot of variability in crystallinity of drug in RMC sample while the RS samples showed much less crystalline component in the mixture.

Table 3.19 Enthalpy of melting peak and percent crystallinity of drug in 3:1 solid dispersion samples in 40ºC/75%RH and 30ºC/60%RH conditions

		30ºC/60%RH conditions		40ºC/75%RH conditions	
Sample	**Time point**	**Enthalpy, J/g**	**% Crystalline Drug**	**Enthalpy, J/g**	**% Crystalline Drug**
RS 3:1 Ratio	Initial	0.61	0.59	0.61	0.59
	week 1	0.31	0.30	1.05	1.02
	week 2	1.45	1.41	2.53	2.45
	week 4	2.63	2.55	1.16	1.12
RMC 3:1 Ratio	Initial	23.04	22.34	23.04	22.34
	week 1	11.81	11.45	4.63	4.49
	week 2	9.56	9.27	12.29	11.92
	week 4	4.26	4.13	5.03	4.88

3.3 Fourier Transform Infrared (FT-IR) Analysis

Shown in figure 32 is the FTIR analysis overlay Repaglinide, Syloid® 244FP and Solid dispersion of Repaglinide and Syloid® 244FP in three ratios.

FTIR analysis of Repaglinide shows peaks at 3304 cm^{-1} (-N-H stretching in secondary amine group), 1685 cm^{-1} (strong) (>C=O stretching in carboxylic acid group), 2500–3000 cm^{-1} (weak) (-O-H stretching), 2934 cm^{-1} (medium) (-CH stretching), and 1450–1650 cm^{-1} (weak) (>C=C stretching in aromatic ring).[63] Syloid® 244FP shows peaks at 2359 cm^{-1} (Weak) (-Si-H stretching) and 1089 cm^{-1} (strong) (-Si-OR stretching).

Figure 32 FTIR overlay of Repaglinide, Syloid® 244FP and solid dispersions of Repaglinide and Syloid® 244FP in 1:3, 1:1 and 3:1 ratio

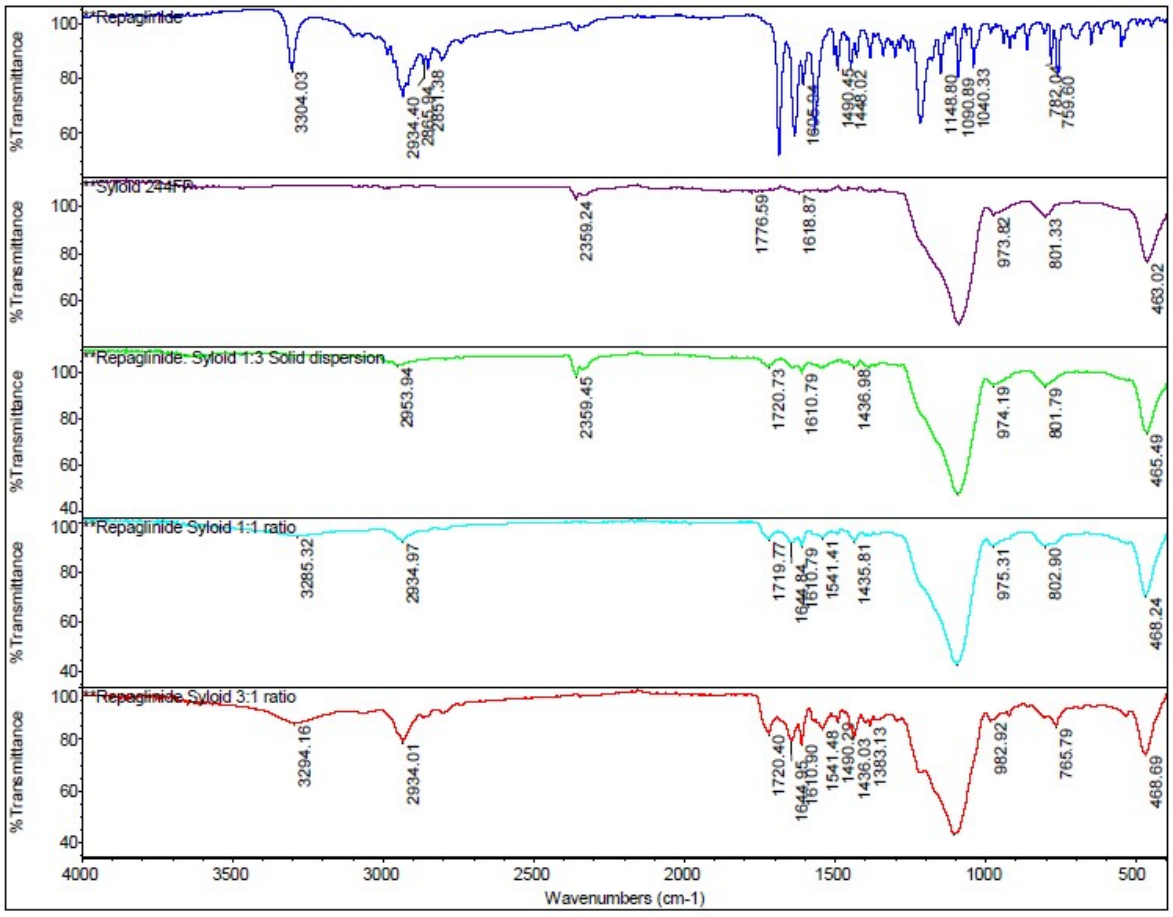

In Repaglinide: Syloid 244FP (1:3) solid dispersion, the peak due –N-H stretching at 3304cm^{-1} disappeared, a broadening of –CH stretching peak and shifting at 2953cm^{-1} was observed and the smaller peaks of –CH stretching at 2865 and 2851 cm^{-1} disappeared. Peaks at 2359 cm^{-1} (Weak) (-Si-H stretching) and 1089 cm^{-1} (strong) (-Si-OR stretching) due to Syloid 244FP were retained. The >C=O stretching in carboxylic acid group observed at 1685cm^{-1} was shifted to 1720 cm^{-1} (weak). In Repaglinide: Syloid 244FP (1:1) solid dispersion, a broad –N-H stretching peak (weak) was broadened and observed at 3285 cm^{-1}, a –C-H stretching (weak) was seen at 2934cm^{-1} and >C=O stretching peak (weak) due to carboxylic acid group was observed at

1720 cm^{-1}. For Repaglinide: Syloid 244FP (3:1) solid dispersion, –N-H stretching peak was medium with less broadening and observed at 3294 cm^{-1}, a –C-H stretching (strong) was seen at 2934cm^{-1} and >C=O stretching peak (strong) due to carboxylic acid group was observed at 1720 cm^{-1}.

Figure 33 FTIR overlay of Repaglinide, Microcrystalline Cellulose PH 101 and solid dispersions of Repaglinide and Microcrystalline Cellulose PH 101 in 1:3, 1:1 and 3:1 ratio

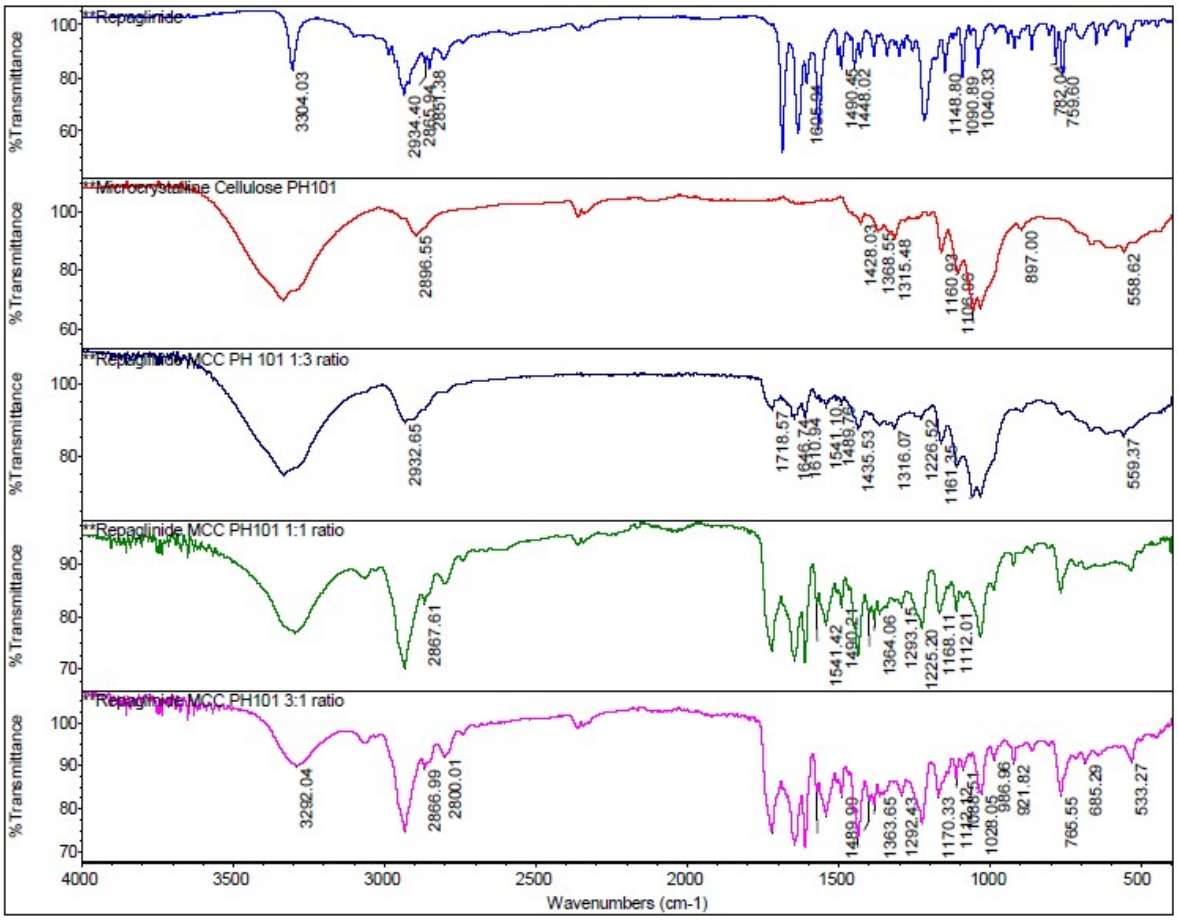

Shown in figure 33 is the FTIR analysis overlay Repaglinide, MCC and Solid dispersion of Repaglinide and MCC in three ratios.

Microcrystalline cellulose PH 101 shows peaks at 3334 cm^{-1} (Strong, broad) (-O-H stretching), 2896 cm^{-1} (medium) (-C-H stretching) and a band at 1428 cm^{-1} (-O-H bending) due to adsorbed water.[100, 101]

In Repaglinide: MCC dispersion of 1:3, the –N-H stretching peak of Repaglinide at 3304cm^{-1} was disappeared and a broad peak was observed instead, a –C-H stretching peak (weak) was observed at 2932cm^{-1} and >C=O stretching peak (strong) due to carboxylic acid group was observed at 1718 cm^{-1}. Broadening of weak peaks in the region of >C=O was also observed. In RMC dispersions of 1:1 ratio, a broad –N-H stretching peak was observed. A –CH stretching peak (weak) was observed at 2934cm^{-1} and >C=O stretching peak (strong) due to carboxylic acid group was observed at 1720 cm^{-1}. For solid dispersion containing Repaglinide and MCC in the ratio of 3:1, a broad peak at 3292cm^{-1} in –N-H stretching region, more defined –C-H stretching peaks at 2934cm^{-1}, 2866cm^{-1}, 2800cm^{-1} and >C=O stretching peak (strong) due to carboxylic acid group was observed at 1720 cm^{-1}.

3.4 Solubility of Drug in samples:

3.4.1 Calibration curve of Repaglinide in Methanol using UV spectrometer

1 mg Repaglinide was dissolved in 100ml Methanol to make 10 µg/ml concentration of Repaglinide in Methanol. From this stock solution, 8ml, 6ml, 4ml, 2ml, 1ml, 0.5 ml and 0.025ml of the solution was taken and diluted to 10 ml to make up 8 µg /ml, 6 µg/ml, 4 µg/ml, 2 µg/ml, 1 µg/ml, 0.5 µg/ml and 0.25 µg/ml concentration respectively. UV absorbance of each sample was recorded. Using the known concentration and absorbance data, a calibration curve was established. Absorbance of blank Methanol solvent was also recorded and this value was

deducted from samples' measured absorbance to get actual absorbance value of each Repaglinide solution. Using the calibration curve, slope and intercept were calculated. These values were used in determining solubility of Repaglinide in samples placed on stability.

Table 3.20 Absorbance Values of various Repaglinide concentrations in Methanol

Concentration of Repaglinide	Absorbance	Blank Absorbance	Actual Absorbance (Measured Absorbance – Blank Absorbance)
10 µg/ml	0.292	0.081	0.211
8 µg/ml	0.255	0.081	0.174
6 µg/ml	0.229	0.081	0.148
4 µg/ml	0.179	0.081	0.098
2 µg/ml	0.128	0.081	0.047
1 µg/ml	0.104	0.081	0.023
0.5 µg/ml	0.093	0.081	0.012
0.25 µg/ml	0.086	0.081	0.005

Figure 34 Calibration of curve of UV absorbance of Repaglinide at various concentrations

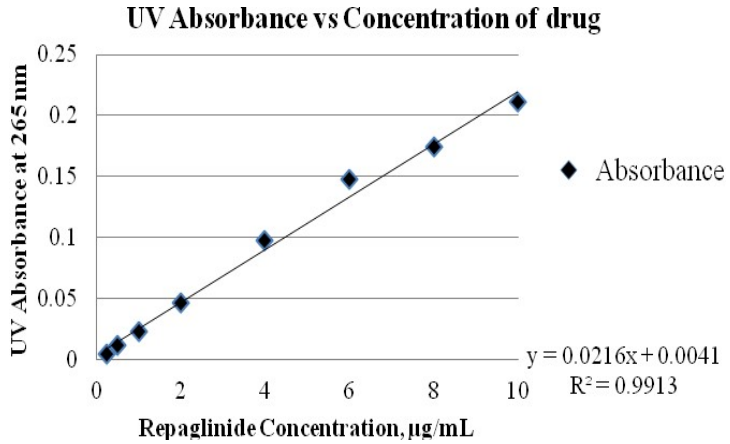

3.4.2 Saturation solubility of Repaglinide

The saturation solubility results of quench cooled Repaglinide stored at 30ºC/60%RH conditions and measured in pH 5.0 citro-phosphate buffer are summarized below in table 3.21 and plotted in figure 35.

Table 3.21 Saturation solubility of Repaglinide (µg/ml) for samples on stability at 30ºC/60%RH in pH 5.0 citro-phosphate buffer at 37ºC

Sample	Average Solubility, µg/ml (range, n=3)
Repaglinide Original	4.5(2.7-6.2)
Repaglinide Quench cooled T0	4.9(2.9-6.0)
Repaglinide Quench cooled week 2	3.8(2.5-6.0)
Repaglinide Quench cooled week 4	4.1(2.1-6.2)

It was observed that there was not much difference in solubility of original Repaglinide as received from the supplier and quench cooled Repaglinide at initial timepoint and on stability up to 4 weeks in 30ºC/60%RH conditions.

Figure 35 Saturation solubility of Repaglinide (µg/ml) for samples on stability at 30ºC/60%RH in pH 5.0 Citrophosphate buffer at 37ºC, n=3

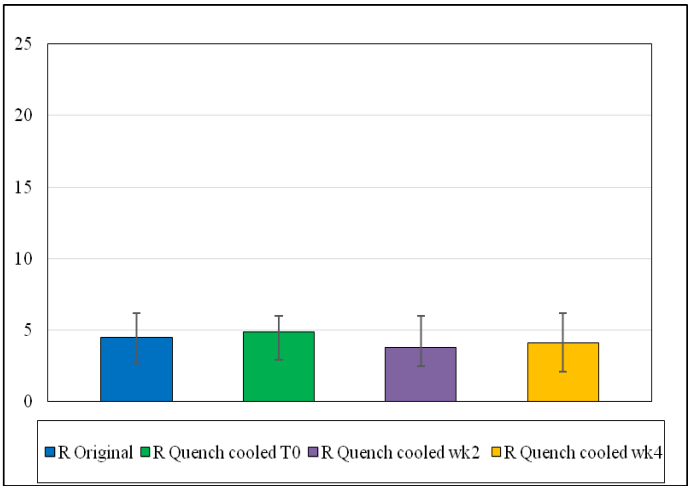

The saturation solubility results of quench cooled Repaglinide stored at 30ºC/60%RH conditions and measured in pH 5.0 citro-phosphate buffer are summarized below in table 3.22 and plotted in figure 36.

Table 3.22 Saturation solubility of Repaglinide (µg/ml) for samples on stability at 40ºC/75%RH in pH 5.0 Citrophosphate buffer at 37ºC

Sample	Average Solubility, µg/ml (range, n=3)
Repaglinide Original	4.5(2.7-6.2)
Repaglinide Quench cooled T0	4.9(2.9-6.0)
Repaglinide Quench cooled week 2	3.9(2.9-5.2)
Repaglinide Quench cooled week 4	3.8(2.2-5.8)

Figure 36 Saturation solubility of Repaglinide (µg/ml) for samples on stability at 40ºC/75%RH in pH 5.0 Citrophosphate buffer at 37ºC, n=3

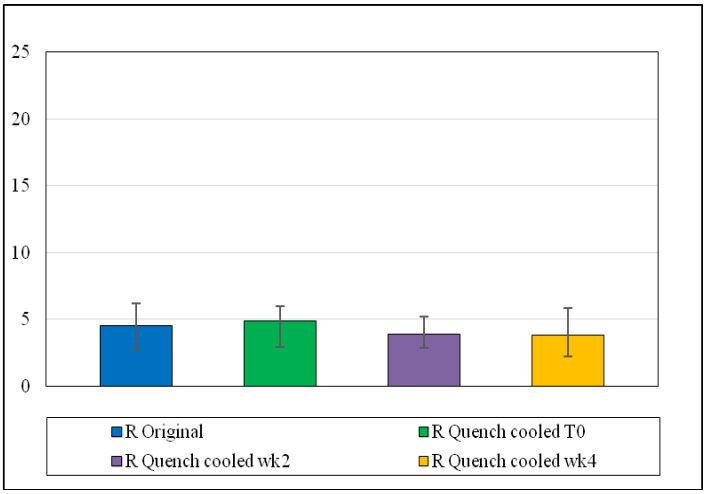

It was observed that there was not much difference in solubility of original Repaglinide as received from the supplier and quench cooled Repaglinide at initial timepoint and on stability up to 4 weeks in 40ºC/75%RH conditions. A slight decrease in solubility was observed at week 2 and 4 but was within the standard deviation of the data points. Table below indicates t-test values showing no significance in values obtained for Repaglinide original and Repaglinide quench cooled samples, Repaglinide quench cooled sample and quench cooled samples on stability in both conditions.

Table 3.23 Statistical comparison of Repaglinide solubility data using t-test.

Stability conditions	Sample set 1	Sample set 2	P-Value	T-Value
Initial	R original	R quench cooled	1.00	0.00
30C/60%RH	R quench cooled	R QC Week 2	0.49	0.66
	R quench cooled	R QC Week 4	0.81	0.27
40C/75%RH	R quench cooled	R QC Week 2	0.49	0.65
	R quench cooled	R QC Week 4	0.81	0.27

Saturation solubility of RS and RMC dispersions placed on stability at 30°C/60%RH condition was measured. The table below summarizes the solubility data. Figures 37 to 40 are plots of solubility per timepoint from initial (T_0) to week 4.

Table 3.24 Saturation solubility of solid dispersions of Repaglinide for samples stored at 30°C/60%RH condition in pH 5.0 Citrophosphate buffer at 37°C

Repaglinide solubility, µg/ml (range, n=3)				
Sample	**Initial**	**Week 1**	**Week 2**	**Week 4**
R Original	4.47(2.7-6.2)			
RS 1:3	16.4(14.8-17.3)	14.6(14.3-14.9)	16.9(16.0-17.6)	16.5(15.6-17.2)
RMC 1:3	8.6(8.2-8.9)	9.4(7.9-10.5)	6.3(6.0-6.6)	7.9(7.5-8.4)
RS 1:1	19.7(19.1-20.0)	17.0(15.8-19.4)	20.8(20.2-21.1)	23.5(23.0-23.9)
RMC 1:1	5.5(4.9-6.5)	8.8(8.1-9.3)	10.8(10.4-11.3)	8.2(7.7-8.4)
RS 3:1	2.9(1.7-3.7)	2.9(2.8-3.1)	2.1(1.8-2.6)	3.9(3.2-4.8)
RMC 3:1	2.8(2.3-3.8)	3.4(2.8-4.0)	5.5(5.0-6.2)	2.0(1.5-2.3)

The solid dispersions showed more solubility as compared to that of original Repaglinide sample as received from supplier. RS dispersion had higher solubility values compared to RMC dispersion at all timepoints. The solubility values of RMC dispersion were lower than that of the RS dispersion but was higher than the solubility of original Repaglinide sample.

Figure 37 Solubility of Repaglinide (µg/ml) for samples at T0 time point in pH 5.0 Citrophosphate buffer at 37ºC, n=3

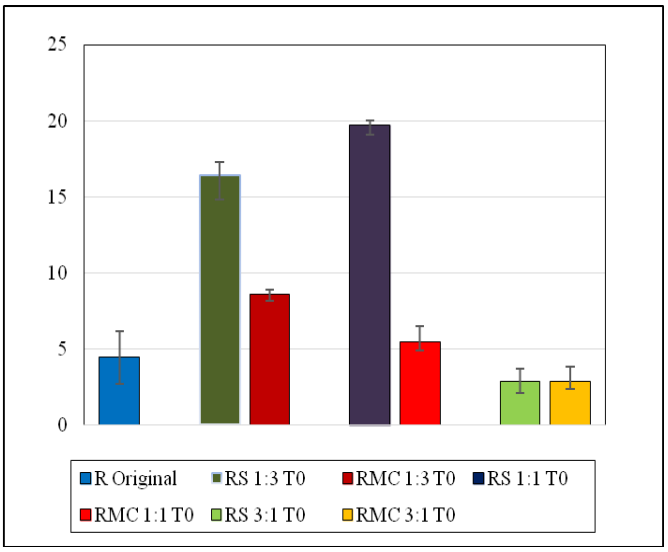

Figure 38 Solubility of Repaglinide (µg/ml) for samples stored in 30ºC/60%RH condition at 1 week time point in pH 5.0 Citrophosphate buffer at 37ºC, n=3

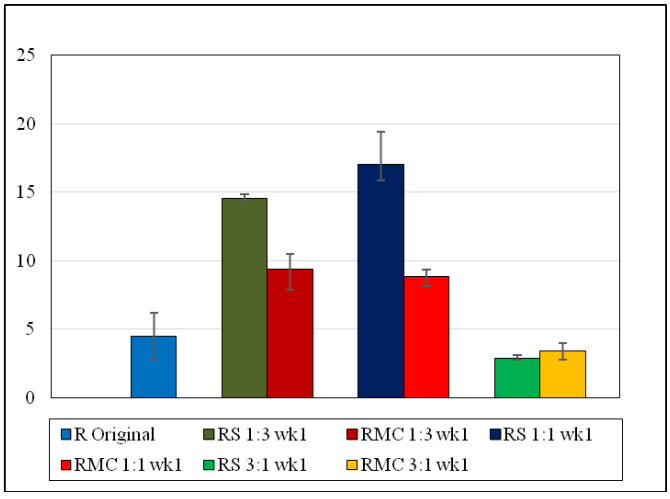

It could be observed from the graphs that amongst the RS dispersions, 1:1 ratio had higher solubility than the 1:3 ratio. RS dispersion prepared in 3:1 ratio had the least solubility that was comparable to the solubility of original Repaglinide sample considering the standard deviation of the analysis. For the RMC dispersions, the solubility data was variable for different timepoints

where the variability could be attributed to dispersion preparation. However, for the most timepoints solubility of 1:3 and 1:1 ratio was similar while solubility for 3:1 timepoint was much lower. The solubility values did not change with time for all the samples.

Figure 39 Solubility of Repaglinide (µg/ml) for samples stored in 30ºC/60%RH condition at 2 week time point in pH 5.0 Citrophosphate buffer at 37ºC, n=3

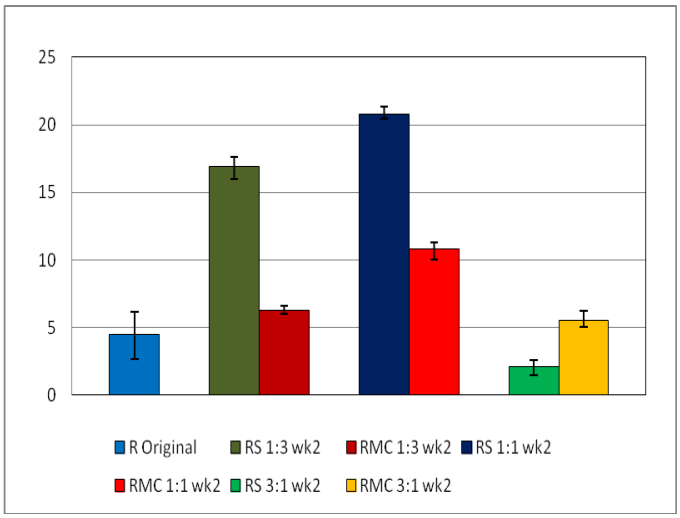

Figure 40 Solubility of Repaglinide (µg/ml) for samples in 30°C/60%RH condition at 4 week time point in pH 5.0 Citrophosphate buffer at 37°C, n=3

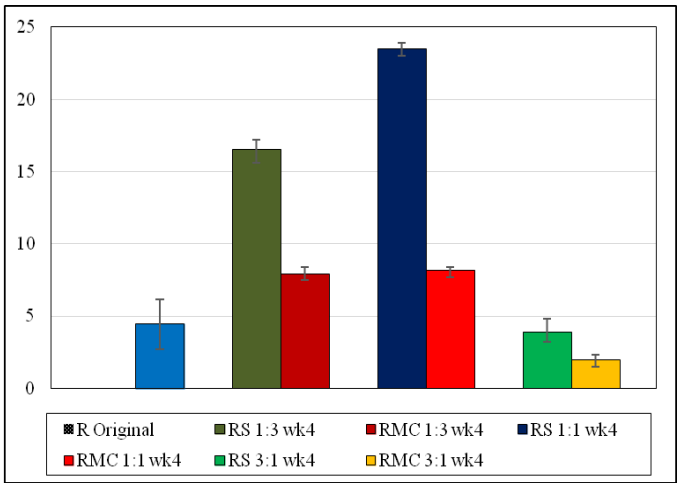

Saturation solubility of RS and RMC dispersions placed on stability at 40°C/75%RH condition was measured. The table below summarizes the solubility data. Figures 41 to 44 are plots of solubility per timepoint from week 1 to week 4.

Table 3.25 Saturation solubility of solid dispersions of Repaglinide for samples stored at 40°C/75%RH condition in pH 5.0 Citrophosphate buffer at 37°C

	Repaglinide solubility, µg/ml (range, n=3)			
Sample	**Initial**	**Week 1**	**Week 2**	**Week 4**
R Original	4.5(2.7-6.2)			
RS 1:3	16.4(14.8-17.3)	16.4(16.2-16.6)	15.3(14.7-15.6)	15.8(15.3-16.6)
RMC 1:3	8.6(8.2-8.9)	5.0(4.1-5.6)	7.8(7.4-8.2)	7.1(6.5-7.9)
RS 1:1	19.7(19.1-20.0)	21.7(21.0-22.6)	22.3(21.6-22.9)	19.0(18.4-19.3)
RMC 1:1	5.5(4.9-6.5)	9.3(8.9-9.7)	4.8(4.5-5.2)	6.5(6.0-7.5)
RS 3:1	2.9(1.7-3.7)	3.9(3.1-4.4)	4.8(3.7-5.4)	4.9(3.9-5.5)
RMC 3:1	2.8(2.3-3.8)	2.5(1.8-3.0)	4.2(3.7-4.5)	4.3(3.7-4.6)

Figure 41 Saturation solubility of solid dispersions of Repaglinide for samples stored in 40°C/75%RH condition at 1 week time point in pH 5.0 Citrophosphate buffer at 37°C, n=3

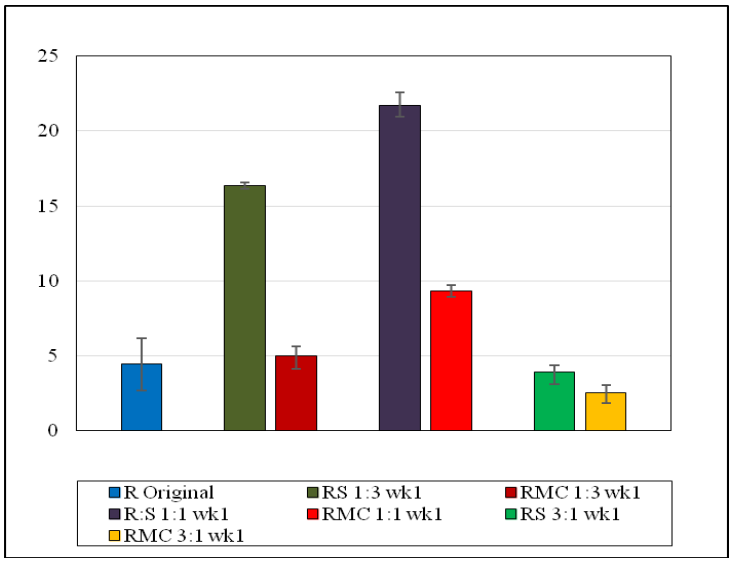

The solid dispersions showed more solubility as compared to that of original Repaglinide sample as received from supplier. RS dispersion had higher solubility values compared to RMC dispersion at all timepoints. The solubility values of RMC dispersion were lower than that of the RS dispersion but was higher than the solubility of original Repaglinide sample.

Figure 42 Saturation solubility of solid dispersions of Repaglinide for samples stored in 40°C/75%RH condition at 2 week time point in pH 5.0 Citrophosphate buffer at 37°C, n=3

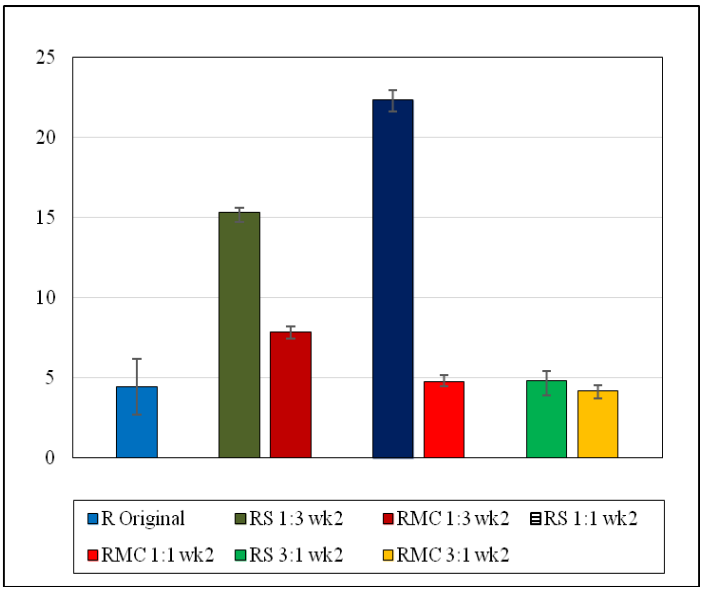

Figure 43 Saturation solubility of solid dispersions of Repaglinide for samples stored in 40°C/75%RH condition at 4 week time point in pH 5.0 Citrophosphate buffer at 37°C, n=3

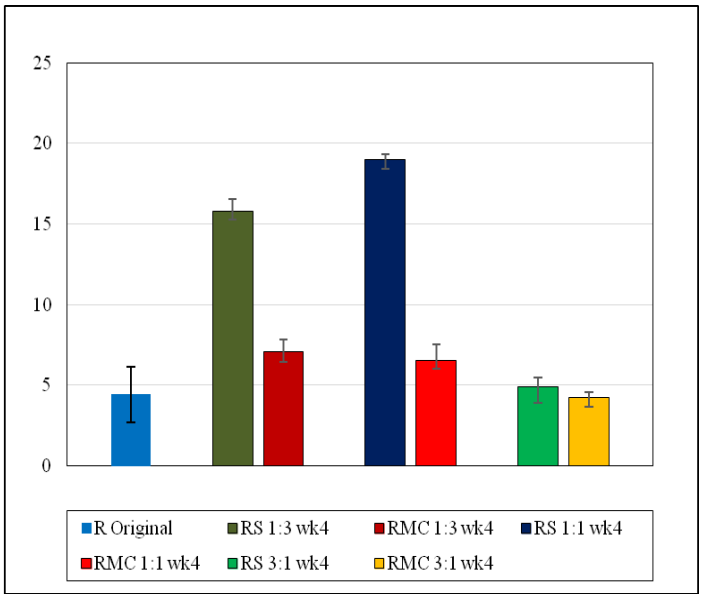

It could be observed from the graphs that amongst the RS dispersions, 1:1 ratio had higher solubility than the 1:3 ratio. RS dispersion prepared in 3:1 ratio had the least solubility that was comparable to the solubility of original Repaglinide sample considering the standard deviation of

the analysis. For the RMC dispersions, the solubility of drug in RS solid dispersion prepared in 1:3 and 1:1 ratio was higher than that of the RMC solid dispersion prepared in the same ratio. The same phenomenon was not observed for 3:1 ratio where the solubility was lower than the other two ratios of both dispersions.

Chapter 4: Discussion

Original sample of Repaglinide has a melting point of 132.66ºC that was confirmed by DSC and had no glass transition peak (figure 16). This suggests that the sample received from the manufacturer was in 100% crystalline form. The sample prepared by heating the Repaglinide sample above the melting point of Repaglinide and rapidly cooling it on an ice bath showed a glass transition around 50.54ºC without any melting peak. It can be inferred that the melt cooling technique utilized in the experiment converts Repaglinide from crystalline to amorphous form.

4.1 Enthalpy of relaxation and glass transition temperature

Figure 44 was plotted using enthalpy of relaxation near glass transition observed in samples stored at 30ºC/60%RH and 40ºC/75%RH conditions up to 4 weeks. It was observed that there was an increase in enthalpy of relaxation from initial time point to 4 weeks in both conditions.

Figure 44 Enthalpy of relaxation with time, quench cooled Repaglinide (A), Repaglinide and Syloid® 244FP solid dispersion stored at 30ºC/60%RH conditions (B), Repaglinide and Syloid®244FP solid dispersion stored at 40ºC/75%RH conditions (C)

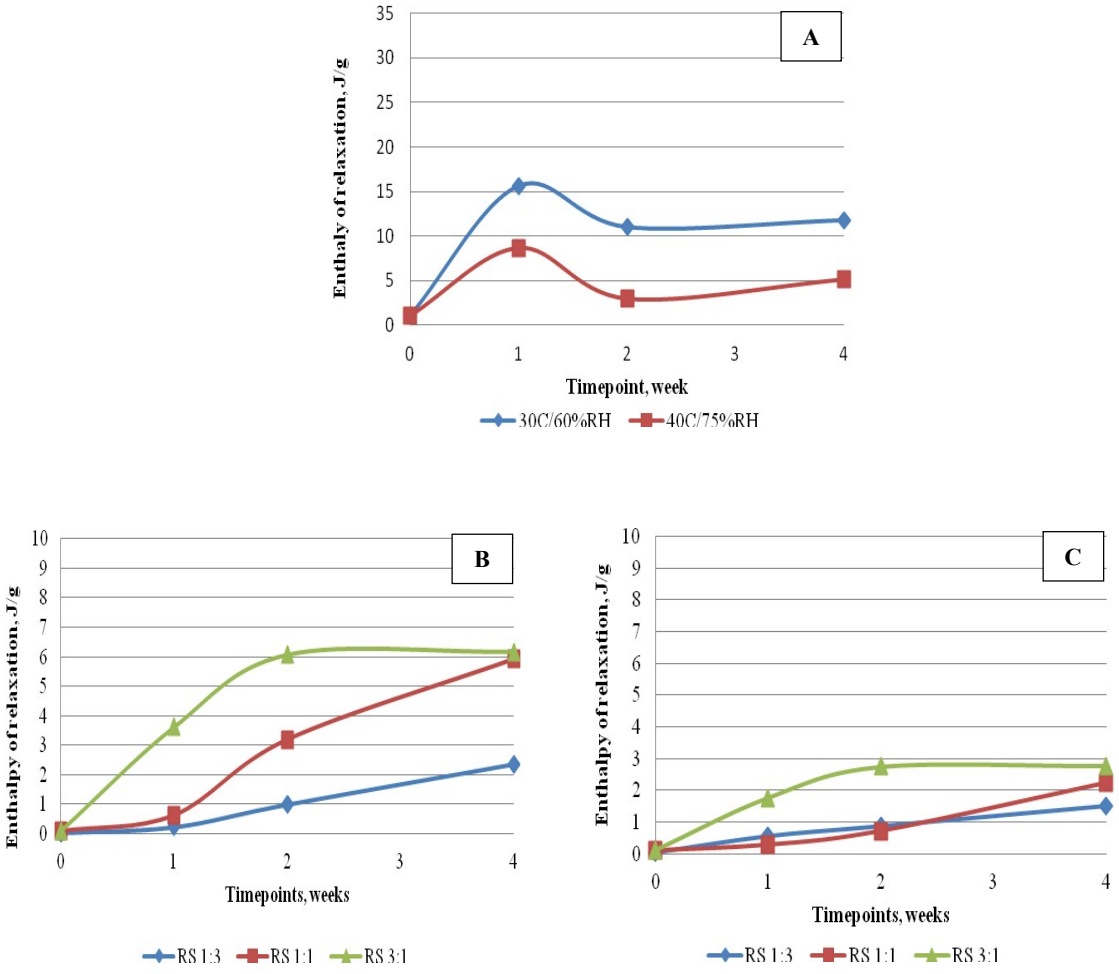

From figure 44A it could be observed that the enthalpy of relaxation observed for quench cooled Repaglinde in 30ºC/60%RH was greater than that of 40ºC/75%RH condition. The enthalpy of relaxation in an amorphous material occurs over storage time when this material is maintained at temperatures below their T_g and it depends on the rate at which the material is allowed to cool from temperatures above their T_g. Materials that are allowed to cool slowly from

temperatures above their T_g exhibit less enthalpy of relaxation, as their molecular chains had the opportunity to find energetically favorable orientations. They are closer to thermodynamic equilibrium than those cooled rapidly. Quench cooled amorphous system is in a thermodynamically non equilibrium state with a long range translational order.[102] Hence, the relaxation occurs over time in the form of molecular arrangements at room temperature. Within an amorphous system, the super-cooled liquid state is comparatively at more equilibrium than glassy state, regarding that is actually a pseudo equilibrium state and only crystal is in equilibrium state. Hence, the enthalpy change is required for the material to relax from glassy state to super-cooled liquid state.[99] The relaxation time is significantly reduced while storing the material at temperatures near but not exceeding the T_g. The liquid shows a single peak relaxation frequency at high temperature which is indicative of one relaxation mechanism. A moderately supercooled liquid shows peaks split into α relaxation and β relaxation. α relaxation is slow and exhibits non-Arrhenious behavior and it disappears at Tg while β relaxation is fast and exhibits Arrhenious behavior.[9] Since 40ºC storage condition is closer to T_g of Repaglinide, the enthalpy of relaxation observed is less than that observed in material stored at 30ºC. In figure 17 and 18, at week 1, the glass transition endotherm had a broader peak compared to other samples. In a regular DSC technique, when glass transition and enthalpy relaxation both occur, it is difficult to isolate the glass transition temperature and calculate correct enthalpy of relaxation. The enthalpy of relaxation values seen at 1 week is higher in both conditions which could be due to a long endothermic event that may have led to higher estimation of enthalpy of relaxation at this time point. Thermally modulated DSC technique could provide the correct estimation of enthalpy relaxation and glass transition in these cases. There was an increase in glass transition

temperature with an increase in crystalline component as well due to coexistence of amorphous and crystalline components in the sample.

For Repaglinide and Syloid® 244FP (RS) solid dispersion stored at 30ºC/60%RH conditions (figure 44B), the enthalpy of relaxation was more than that observed in samples stored in 40ºC/75%RH conditions (figure 44C). Repaglinide and Syloid dispersions prepared in the ratio of 3:1 had higher enthalpy of relaxation values and rate followed by 1:1 ratio and 1:3 ratio in both conditions. The highest value of enthalpy of relaxation for RS dispersion in the ratio of 3:1 was achieved in both conditions at week 2 and it plateau showing no further increase from week 2 to week 4. For RS 1:1 ratio, the enthalpy value increased from week 2 to week 4 and the value attained at week 4 was similar to that of the RS 3:1 dispersion. The enthalpy value for RS 1:3 dispersion increases from time zero to 4 weeks and the value at week 4 lesser than the value of RS 3:1 and 1:1 ratio at week 4. This observation suggests that the rate of enthalpy relaxation increased with the higher amount of drug in the solid dispersion, with the 3:1 ratio having the fastest enthalpy relaxation followed by 1:1 and 1:3 ratio. The rate of enthalpy relaxation was higher for the 30ºC/60%RH condition than the 40ºC/75%RH condition due to 40ºC being close to T_g of Repaglinide, a phenomenon that was observed for the quench cooled Repaglinide sample as well.

For Repaglinide and Microcrystalline Cellulose (RMC) solid dispersions, the enthalpy of relaxation values were seen as variable from time zero to week 4 for all three ratio for 30ºC/60%RH condition (summarized in tables 3.7, 3.12, 3.17 and 40ºC/75%RH condition (summarized in tables 3.8, 3.13 and 3.18). The values of enthalpy of relaxation did not show the correlation with the concentration of API in the sample or the temperature of storage, a trend that was seen for quench cooled Repaglinide and RS solid dispersions. This variability in the values

for enthalpy of relaxation could be due to non-homogeneity of Repaglinide API in the mixtures. The samples were prepared by physical mixing while being heated above the melting point of Repaglinide and mixing further after cooling. In the heating process the carriers do not melt and are in the form of solid powders. Since Syloid has glidant properties and is known to aid uniformity of APIs in solid powder blends, this variability of API concentration was not exhibited in RS dispersion as it was seen in RMC dispersions (figure 45A). Due to this variability, the average values from Time zero to week 4 for all the solid dispersion was plotted (figure 45B) in place of each time point. The enthalpy of relaxation was higher for 30°C/60%RH condition as compared to that of 40°C/75%RH condition samples. The samples containing 1:1 ratio of Repaglinide and Microcrystalline Cellulose were more uniform in terms of API concentration compared to 1:3 and 3:1 ratio as observed from the enthalpy values for this ratio.

Figure 45 Enthalpy of relaxation from initial to week 4 for Repaglinide and Microcrystalline Cellulose solid dispersion (A), Average enthalpy values for all timepoints per ratio (B)

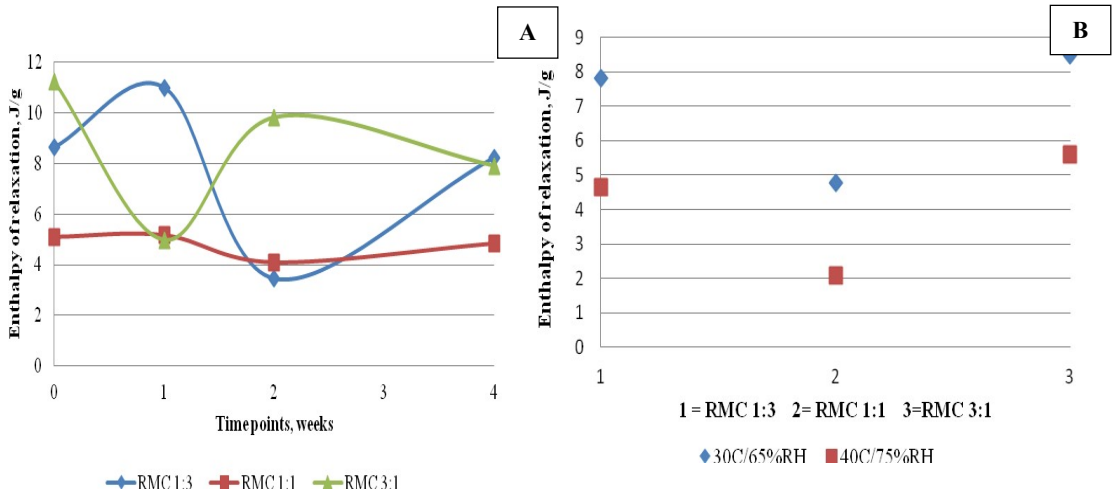

4.2 Enthalpy of melting and crystallization of Repaglinide

From figure 16, it could be derived that the original Repaglinide has no glass transition but a sharp melting curve, suggesting that it is 100% crystalline. The quench cooled Repaglinide showed a glass transition which characteristic of an amorphous material with no melting peak. The percentage of crystalline component in API was calculated for quench cooled samples placed on stability by using the enthalpy of melting for the original Repaglinide sample as 100%. Figure 46 shows that the crystalline component in quench cooled Repaglinide sample increased with time in both conditions. This indicates that there is a need to improve stability of the amorphous Repaglinide. The rate of increase and amount of crystalline component for 40ºC/75%RH was higher than that of 30ºC/60%RH condition. This phenomenon shows an effect of higher temperature and humidity in converting amorphous material to crystalline with time.

Figure 46 Crystalline component in quench cooled Repaglinide with time

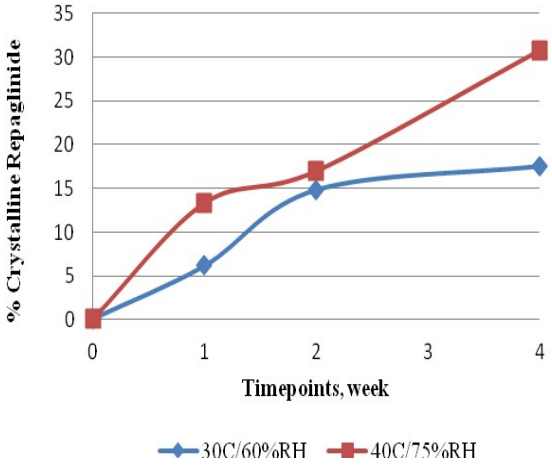

The samples of Repaglinide and carriers prepared by the same quench cooling technique showed a glass transition as well as a small transition in the melting range. Yoshioka et al. showed using

Indomethacin as a model drug, that a completely dry amorphous material at 30°C which is below its Tg, had an increased rate of crystallization over the period of 3 weeks which suggests that the rate of crystallization was increased at higher temperatures due to an increased molecular mobility.[103] It was also established that water acts as a plasticizer and water absorption by amorphous solids lowers the Tg of the solid.[104] The samples prepared as solid dispersions of Repaglinide and Syloid 244FP prepared in three drug: carrier ratios (1:3, 1:1, 3:1) showed negligible conversation to crystalline state on stability as confirmed by DSC.

Figure 47 Crystalline Repaglinide content in Repaglinide solid dispersions at 30ºC/60% RH conditions (A), 40ºC/75% RH conditions (B)

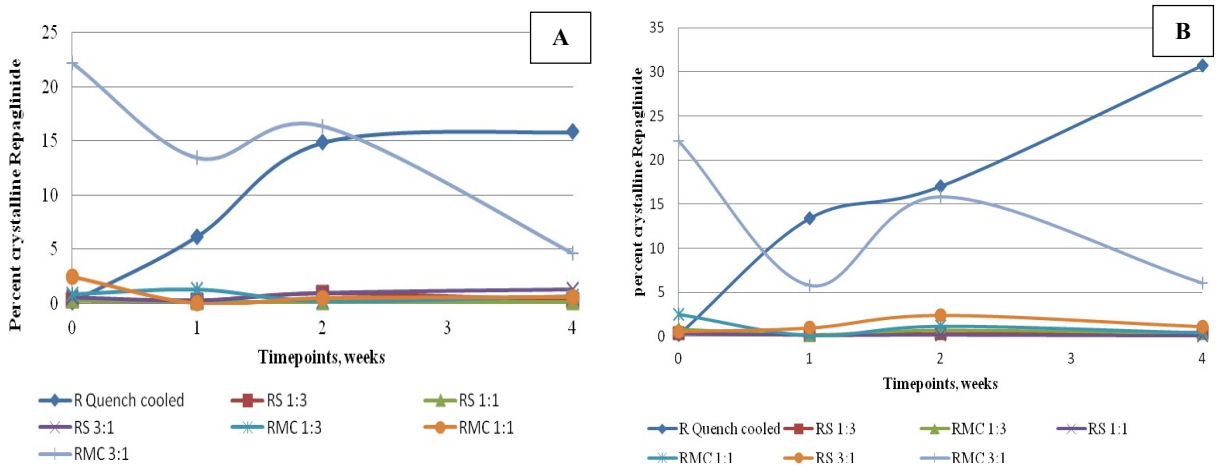

In both stability conditions, the crystalline component values of Repaglinide found in the RS dispersions was significantly small compared to Quench cooled Repaglinide and the difference in crystalline values between the ratio was found to be statistically insignificant as analyzed using paired t- test (Table 4.1). For RMC dispersions in ratio of 1:3 and 1:1, the crystalline Repaglinide amount was small and not statistically different in both conditions. For RMC 3:1 ratio, the crystalline Repaglinide values were significantly higher and variable. The variability

could be because the in-homogeneity of the API in the mixtures containing microcrystalline cellulose.

Table 4.1 Statistical significance from t-test of crystalline API percentage in solid dispersions

Stability conditions	Sample set 1	Sample set 2	P-Value	T-Value
30°C/60%RH	RS 1:3	RS 1:1	0.23	1.51
	RS 1:1	RS 3:1	0.08	-2.59
	RS 1:3	RS 3:1	0.29	-1.20
	RMC 1:3	RMC 1:1	0.78	-0.30
40°C/75%RH	RS 1:3	RS 1:1	0.25	1.29
	RS 1:1	RS 3:1	0.07	-2.69
	RS 1:3	RS 3:1	0.10	-2.41
	RMC 1:3	RMC 1:1	0.39	-1.01

4.3 Appearance of particles from scanning electron microscopy

It was observed in scanning electron microscopy that the original Repaglinide (figure 11) had needle shaped crystals that disappeared in the quench cooled Repaglinide (figure 12) suggesting that the quench cooled Repaglinide lacked the crystalline structure. The same lack of crystallinity was observed in solid dispersions of Repaglinide and Syloid 244FP in 1:3, 1:1 and 3:1ratio (figure 14) and the images were similar to that of the Syloid 244FP (figure 13A). The SEM images of the Repaglinide and MCC solid dispersions in the ratio of 1:3, 1:1 and 3:1 (figure 15) were similar to that of the Microcrystalline Cellulose (figure 13B) with some crystals owing to a partial crystalline nature of MCC, albeit some needle shaped structure was observed in 3:1 ratio that was different from 1:3 and 1:1 ratio.

4.4 Drug-carrier interaction study

Upon comparing the FTIR spectra it was observed that Repaglinide has a strong peak at 3304cm^{-1} due to –N-H stretching in secondary amine group that disappeared in RS 1:3 dispersion, shifted to 3285cm^{-1} and 3294cm^{-1} in RS1:1 and RS 3:1 dispersion, respectively. This indicates a hydrogen bond formation.[105] Repaglinide has hydrogen bond acceptor count of 6 and donor count of 2.[106] Due to which it could form a hydrogen bond with Syloid®244FP which is also a hydrogen donor and acceptor due to silanol groups (-Si-OH). In Repaglinide: Syloid® 244FP (3:1) solid dispersion, –N-H stretching peak (medium) was observed with a slight shift to 3294 cm^{-1}. This being a small shift with intensity being higher, the hydrogen bond formed is weaker.[107] The >C=O stretching in carboxylic acid group observed at 1685cm^{-1} was shifted to 1720 cm^{-1} in RS dispersions indicating hydrogen bond formation.[63] – C-H absorption peak that appeared in the Repaglinide at 2934 cm^{-1}, shifted to 2953cm^{-1} in RS 1:3 dispersion. For RS 3:1 dispersion, smaller more intensified peaks appeared around 2934cm^{-1} like in the original Repaglinide sample.

In Repaglinide: MCC dispersion of 1:3 and 1:1, the –N-H stretching peak of Repaglinide at 3304cm^{-1} and –O-H peak at 3330cm^{-1} observed in MCC was disappeared and a single broad peak was observed instead indicating a hydrogen bond formation between the –NH group of Repaglinide and –OH group of MCC. For solid dispersion containing Repaglinide and MCC in the ratio of 3:1, a broad peak at 3292cm^{-1} in –N-H stretching region suggests a weaker bond formation. A –C-H stretching peak appeared in For RMC 1:3 was broad at 2932cm-1 while for RMC 3:1 ratio, more defined –C-H stretching peaks at 2934cm^{-1}, 2866cm^{-1}, 2800cm^{-1} were

observed and 1685 cm^{-1} due to >C=O stretching in carboxylic acid group observed in Repaglinide shifted to 1720 cm^{-1} suggesting bond interaction.

4.5 Saturation solubility of Repaglinide

The saturation solubility of original Repaglinide sample in pH 5.0 citrophosphosphate buffer was 4.5µg/mL. The saturated solubility of quench cooled Repaglinide sample at initial time point was 4.9µg/mL, which was similar to the original Repaglinide sample and did not change on stability. The values obtained from 1 week to 4 week were similar to the initial quench cooled sample taking into account the variability.

A pH – solubility study performed on Repaglinide, showed that the crystalline form and amorphous form displayed the lowest solubility at pH 5.0 due to the zwitterionic structure of Repaglinide containing a carboxylic acid group and a tertiary amine group and the solubility value obtained at this pH confirmed with the literature.[66] Repaglinide has each of a weakly basic and a weakly acidic group with two protonation sites, hence, there is a possibility of four species in equilibrium with each other. At isoelectric pH, two neutral forms of Repaglinide may exist: i) zwitterionic ii) uncharged form.[66]

The saturated solubility is an equilibrium concentration of solute between solution and the bulk powder which was measured after letting the super saturated solution of Repaglinide to settle for 24 hours. The drug is thermodynamically unstable in a supersaturated system and it has the tendency to return to the equilibrium state by drug precipitation.[108] When concentration of Repaglinide with time was measured in supersaturated conditions in pH 3.8 phosphate buffer, it was found that the metastable dissolution of Repaglinide was high at 1 hour followed by a sharp decline to approach dissolution profile of its crystalline counterpart. This significant decline in

dissolution is due to precipitation of more stable crystalline form which is less soluble.[67] This was confirmed by birefringence in solid samples collected during supersaturated dissolution tests suggesting that the supersaturation was the driver of nucleation and growth of crystals.[67] This explains, it is likely that the quench cooled Repaglinide which was amorphous had higher solubility initially in the supersaturated solution that declined to approach solubility value of original crystalline Repaglinide samples over the prolonged time of 24 hours due to precipitation in crystalline form. All the samples stored in both stability conditions precipitated to yield solubility of the crystalline Repaglinide. Hence, no difference in solubility values were seen at 24 hours, albeit there may have been differences in the solubility values at 1 to 2 hours. Guzman et al. described this concept by using the term 'spring and parachute approach where the higher solubility can be achieved initially for higher energy / metastable state of compounds followed by decline to that of its crystalline counterpart as spring approach and increase in length of time in decline in solubility by help of precipitation inhibitors, steric effect or hydrogen bond formation as spring with parachute approach.[109] It can be inferred that the quench cooled Repaglinide may have exhibited a higher apparent solubility with a spring effect followed by a decline in solubility due to precipitation induced by supersaturation, hence, the saturated solubility values obtained were similar to that of the crystalline form of Repaglinide. The apparent solubility can be described as the solubility of the metastable form and is different from equilibrium solubility which is the thermodynamic equilibrium between the drug in solution and the stable solid form.[108] Higher apparent solubility is achieved in amorphous forms, solid dispersions, co-crystals and crystalline salt forms can be achieved in higher energy.[17 110]

Solubility of RS dispersion prepared in 1:3 and 1:1 ratio in pH 5.0 Citro-phosphate buffer was 4 times and 5 times higher respectively, than that of original Repaglinide and quench cooled

Repaglinide in both stability storage conditions suggesting the interaction between the drug and carrier is improving solubility. There was not much difference in solubility values from time zero to week 4 in both conditions because the drug remained in amorphous form and no increase in crystalline component was observed on stability conditions. The solubility of Repaglinide in RMC 1:3 and 1:1 solid dispersions was about 1.7 – 2 folds higher than that of the Repaglinide original and quench cooled samples due to interactions between the drug and carrier suggesting effect of hydrogen bond formation between MCC and Repaglinide but solubility in RS dispersions of same ratio had higher solubility suggesting that the hydrogen bond formation and higher surface are of Silica is improving solubility of Repaglinide. Patel V. I. et al. had studied in solid dispersions containing Syloid244FP that during the dissolution process, due to the large specific surface area, as soon as the sample comes in contact with the dissolution media, the particles are immediately dispersed preventing further crystal growth. This phenomenon had prevented the crystal growth during dissolution, and a higher dissolution rate was rapidly achieved.[69] There was a combined effect of hydrogen bond formation due to Silanol groups present in Syloid and large surface area. The formation of hydrogen bond and steric effect of Silica helped in preventing crystallization in the solution exhibiting higher solubility for RS dispersions (1:3, 1:1 ratio). A similar effect of increase in solubility was seen with MCC in RMC dispersions (1:3, 1:1 ratio) but the extent was lesser than that of the RS dispersions due less surface area and difference in steric effect. Also, there was some variability in the solubility values of RMC dispersion due to non-uniformity of API in samples during processing. While the effect of hydrogen bond formation and surface area can be seen in RMC dispersions, Syloid® offers much higher surface area than MCC.

The carrier may serve as precipitation inhibitor and inhibit precipitation of the drug from the supersaturated solution. It has also been speculated that, even if the drug precipitates, it does so as a metastable polymorph which has higher solubility compared to that of its most stable form.[111]

Solubility of Repaglinide in RS 3:1 and RMC 3:1 dispersion was much lower and was comparable to that of the original Repaglinide sample. This could be explained by a weaker hydrogen bond formation in the high drug composition. The 3:1 ratio in both solid dispersions had a weaker hydrogen bond formation as seen in FTIR analysis. Also, due to higher amount of Repaglinide drug which is weakly acidic in nature in 3:1 ratio would make the solution acidic.

Chapter 5: Conclusion

Repaglinide can be converted into amorphous form by quench cooling method but it crystallizes rapidly on storage. The rate of crystallization is more at higher temperature and humidity. By forming solid dispersions with carriers, Syloid (mesoporous silica) and Microcrystalline Cellulose, crystallization was prevented on storage. Both the carriers formed hydrogen bond with Repaglinide which stabilized the drug in amorphous form and prevented recrystallization on storage.

Mesoporous silica offers a unique advantage in improving solubility of the poorly soluble drugs by enabling hydrogen bond formation and inhibiting crystallization. The optimal ratio of drug and carrier is required to obtain desired properties of solid dispersion. In the present study, the Repaglinide: Syloid® ratio of 3:1 did not result in higher solubility of the drug. Repaglinide is a zwitterionic compound with low solubility at pH 5. The amorphous Repaglinide could have higher solubility than crystalline Repaglinide but in a few minutes of going in solution, it

undergoes precipitation resulting in lower saturation solubility. Syloid®, due to its high surface area, enables the drug to go in solution quickly acting as crystallization inhibitor.

Microcrystalline Cellulose formed hydrogen bond with Repaglinide and increased saturation solubility of Repaglinide in 1:3 and 1:1 drug: MCC ratio. MCC also inhibited precipitation by molecularly dispersing the drug in solution. The effect of hydrogen bonding and higher surface area keeping the drug in solution was more pronounced with Syloid® as compared to MCC.

Future studies

This study revealed the effect of carriers in preventing recrystallization of Repaglinide and increasing saturation solubility of the drug. As part of the future studies, the effect on solubility can be confirmed in finished dosage form by performing hot melt extrusion followed by quench cooling and compressing tablet. Also, the dissolution profile of Repaglinide in different pH media could be performed to understand if the drug shows a pH dependent solubility in solid dispersions and compare the dissolution rate of amorphous drug and drug in solid dispersions at various ratios. The role of sample heterogeneity could be explored further in preparation of solid dispersions. A correlation could be established between enthalpy of relaxation and extent of recrystallization with long term stability studies. Use of mDSC could help differentiating reversible and non-reversible heatflow around T_g and enthalpy of relaxation in more clarified way. It could be studied using caco-2 cells if there is a correlation between solubility and absorption of the drug.

Abbreviations

API, active pharmaceutical ingredient; BCS, biopharmaceutics classification system; DSC, Differential Scanning Calorimetry; FTIR, Fourier Transformed Infrared (FTIR); IVIVC, in vitro/in vivo correlation; SEM, Scanning Electron Microscopy; RQC, Repaglinide Quench cooled; RS, Repaglinide Syloid solid dispersion; RMC, Repaglinide Microcrystalline solid dispersion; MCC, Microcrystalline Cellulose.

References

1. Yu, L. Amorphous pharmaceutical solids: preparation, characterization and stabilization. *Adv Drug Deliv Rev* **48**, 27-42 (2001).

2. Gao, P. Amorphous pharmaceutical solids: characterization, stabilization, and development of marketable formulations of poorly soluble drugs with improved oral absorption. *Mol Pharm* **5**, 903-904 (2008).

3. Sareen, S., Mathew, G. & Joseph, L. Improvement in solubility of poor water-soluble drugs by solid dispersion. *Int J Pharm Investig* **2**, 12-17 (2012).

4. Amidon, G.L., Lennernas, H., Shah, V.P. & Crison, J.R. A theoretical basis for a biopharmaceutic drug classification: the correlation of in vitro drug product dissolution and in vivo bioavailability. *Pharm Res* **12**, 413-420 (1995).

5. Cook, J., Addicks, W. & Wu, Y.H. Application of the biopharmaceutical classification system in clinical drug development--an industrial view. *AAPS J* **10**, 306-310 (2008).

6. Buckley, S.T., Frank, K.J., Fricker, G. & Brandl, M. Biopharmaceutical classification of poorly soluble drugs with respect to "enabling formulations". *Eur J Pharm Sci* **50**, 8-16 (2013).

7. Hancock, B.C. & Zografi, G. Characteristics and significance of the amorphous state in pharmaceutical systems. *J Pharm Sci* **86**, 1-12 (1997).

8. Stillinger, F.H. & Debenedetti, P.G. Phase transitions, Kauzmann curves, and inverse melting. *Biophys Chem* **105**, 211-220 (2003).

9. Debenedetti, P.G. & Stillinger, F.H. Supercooled liquids and the glass transition. *Nature* **410**, 259-267 (2001).

10. Bates, S. et al. Analysis of amorphous and nanocrystalline solids from their X-ray diffraction patterns. *Pharm Res* **23**, 2333-2349 (2006).

11. Kawabata, Y., Wada, K., Nakatani, M., Yamada, S. & Onoue, S. Formulation design for poorly water-soluble drugs based on biopharmaceutics classification system: basic approaches and practical applications. *Int J Pharm* **420**, 1-10 (2011).

12. Lakshman, J.P., Cao, Y., Kowalski, J. & Serajuddin, A.T. Application of melt extrusion in the development of a physically and chemically stable high-energy amorphous solid dispersion of a poorly water-soluble drug. *Mol Pharm* **5**, 994-1002 (2008).

13. Hancock, B.C. & Zografi, G. The relationship between the glass transition temperature and the water content of amorphous pharmaceutical solids. *Pharm Res* **11**, 471-477 (1994).

14. Chiou, W.L. & Riegelman, S. Pharmaceutical applications of solid dispersion systems. *J Pharm Sci* **60**, 1281-1302 (1971).

15. Serajuddin, A.T. Solid dispersion of poorly water-soluble drugs: early promises, subsequent problems, and recent breakthroughs. *J Pharm Sci* **88**, 1058-1066 (1999).

16. Leleux, J. & Williams, R.O., 3rd Recent advancements in mechanical reduction methods: particulate systems. *Drug Dev Ind Pharm* **40**, 289-300 (2014).

17. Mosharraf, M., Sebhatu, T. & Nystrom, C. The effects of disordered structure on the solubility and dissolution rates of some hydrophilic, sparingly soluble drugs. *Int J Pharm* **177**, 29-51 (1999).

18. Dokoumetzidis, A. & Macheras, P. A century of dissolution research: from Noyes and Whitney to the biopharmaceutics classification system. *Int J Pharm* **321**, 1-11 (2006).

19. Liu, M. & Frechet, J.M. Designing dendrimers for drug delivery. *Pharm Sci Technolo Today* **2**, 393-401 (1999).

20. Rasenack, N. & Muller, B.W. Micron-size drug particles: common and novel micronization techniques. *Pharm Dev Technol* **9**, 1-13 (2004).

21. Horn, D. & Rieger, J. Organic Nanoparticles in the Aqueous Phase-Theory, Experiment, and Use. *Angew Chem Int Ed Engl* **40**, 4330-4361 (2001).

22. Jinno, J. et al. Effect of particle size reduction on dissolution and oral absorption of a poorly water-soluble drug, cilostazol, in beagle dogs. *J Control Release* **111**, 56-64 (2006).

23. Almalik, A., Alradwan, I., Kalam, M.A. & Alshamsan, A. Effect of cryoprotection on particle size stability and preservation of chitosan nanoparticles with and without hyaluronate or alginate coating. *Saudi Pharm J* **25**, 861-867 (2017).

24. Sigfridsson, K., Nordmark, A., Theilig, S. & Lindahl, A. A formulation comparison between micro- and nanosuspensions: the importance of particle size for absorption of a model compound, following repeated oral administration to rats during early development. *Drug Dev Ind Pharm* **37**, 185-192 (2011).

25. Merisko-Liversidge, E. & Liversidge, G.G. Nanosizing for oral and parenteral drug delivery: a perspective on formulating poorly-water soluble compounds using wet media milling technology. *Adv Drug Deliv Rev* **63**, 427-440 (2011).

26. Lippacher, A., Muller, R.H. & Mader, K. Liquid and semisolid SLN dispersions for topical application: rheological characterization. *Eur J Pharm Biopharm* **58**, 561-567 (2004).

27. Wu, Y. et al. The role of biopharmaceutics in the development of a clinical nanoparticle formulation of MK-0869: a Beagle dog model predicts improved bioavailability and diminished food effect on absorption in human. *Int J Pharm* **285**, 135-146 (2004).

28. Junghanns, J.U. & Muller, R.H. Nanocrystal technology, drug delivery and clinical applications. *Int J Nanomedicine* **3**, 295-309 (2008).

29. Mukherjee, A. & Desiraju, G.R. Synthon polymorphism and pseudopolymorphism in co-crystals. The 4,4'-bipyridine-4-hydroxybenzoic acid structural landscape. *Chem Commun (Camb)* **47**, 4090-4092 (2011).

30. Healy, A.M., Worku, Z.A., Kumar, D. & Madi, A.M. Pharmaceutical solvates, hydrates and amorphous forms: A special emphasis on cocrystals. *Adv Drug Deliv Rev* **117**, 25-46 (2017).

31. Aaltonen, J. et al. Solid form screening--a review. *Eur J Pharm Biopharm* **71**, 23-37 (2009).

32. Aitipamula, S., Chow, P.S. & Tan, R.B. Solvates of the antifungal drug griseofulvin: structural, thermochemical and conformational analysis. *Acta Crystallogr B Struct Sci Cryst Eng Mater* **70**, 54-62 (2014).

33. Maeno, Y. et al. Novel pharmaceutical cocrystal consisting of paracetamol and trimethylglycine, a new promising cocrystal former. *Int J Pharm* **473**, 179-186 (2014).

34. Dwichandra Putra, O. et al. Solubility Improvement of Benexate through Salt Formation Using Artificial Sweetener. *Pharmaceutics* **10** (2018).

35. Cruz-Cabeza, A.J., Reutzel-Edens, S.M. & Bernstein, J. Facts and fictions about polymorphism. *Chem Soc Rev* **44**, 8619-8635 (2015).

36. Pudipeddi, M. & Serajuddin, A.T. Trends in solubility of polymorphs. *J Pharm Sci* **94**, 929-939 (2005).

37. Zhang, G.G., Law, D., Schmitt, E.A. & Qiu, Y. Phase transformation considerations during process development and manufacture of solid oral dosage forms. *Adv Drug Deliv Rev* **56**, 371-390 (2004).

38. Wen, H., Jung, H. & Li, X. Drug Delivery Approaches in Addressing Clinical Pharmacology-Related Issues: Opportunities and Challenges. *AAPS J* **17**, 1327-1340 (2015).

39. Serajuddin, A.T. Salt formation to improve drug solubility. *Adv Drug Deliv Rev* **59**, 603-616 (2007).

40. Zannou, E.A., Ji, Q., Joshi, Y.M. & Serajuddin, A.T. Stabilization of the maleate salt of a basic drug by adjustment of microenvironmental pH in solid dosage form. *Int J Pharm* **337**, 210-218 (2007).

41. Stephenson, G.A., Aburub, A. & Woods, T.A. Physical stability of salts of weak bases in the solid-state. *J Pharm Sci* **100**, 1607-1617 (2011).

42. Tiwari, G., Tiwari, R. & Rai, A.K. Cyclodextrins in delivery systems: Applications. *J Pharm Bioallied Sci* **2**, 72-79 (2010).

43. Moyano, J.R. et al. Nuclear magnetic resonance investigations of the inclusion complexation of gliclazide with beta-cyclodextrin. *J Pharm Sci* **86**, 72-75 (1997).

44. Aloisio, C., de Oliveira, A.G. & Longhi, M. Solubility and release modulation effect of sulfamerazine ternary complexes with cyclodextrins and meglumine. *J Pharm Biomed Anal* **100**, 64-73 (2014).

45. Rawat, S. & Jain, S.K. Solubility enhancement of celecoxib using beta-cyclodextrin inclusion complexes. *Eur J Pharm Biopharm* **57**, 263-267 (2004).

46. Horter, D. & Dressman, J.B. Influence of physicochemical properties on dissolution of drugs in the gastrointestinal tract. *Adv Drug Deliv Rev* **46**, 75-87 (2001).

47. Akhtar, J. et al. Nanoemulsion: for improved oral delivery of repaglinide. *Drug Deliv* **23**, 2026-2034 (2016).

48. Shakeel, F. & Faisal, M.S. Nanoemulsion: a promising tool for solubility and dissolution enhancement of celecoxib. *Pharm Dev Technol* **15**, 53-56 (2010).

49. Pouton, C.W. Lipid formulations for oral administration of drugs: non-emulsifying, self-emulsifying and 'self-microemulsifying' drug delivery systems. *Eur J Pharm Sci* **11 Suppl 2**, S93-98 (2000).

50. Barea, S.A. et al. Solid dispersions enhance solubility, dissolution, and permeability of thalidomide. *Drug Dev Ind Pharm* **43**, 511-518 (2017).

51. Kaminskas, L.M. et al. PEGylation of interferon alpha2 improves lymphatic exposure after subcutaneous and intravenous administration and improves antitumour efficacy against lymphatic breast cancer metastases. *J Control Release* **168**, 200-208 (2013).

52. Chutimaworapan, S., Ritthidej, G.C., Yonemochi, E., Oguchi, T. & Yamamoto, K. Effect of water-soluble carriers on dissolution characteristics of nifedipine solid dispersions. *Drug Dev Ind Pharm* **26**, 1141-1150 (2000).

53. Cong, W. et al. Solid dispersion tablets of breviscapine with polyvinylpyrrolidone K30 for improved dissolution and bioavailability to commercial breviscapine tablets in beagle dogs. *Eur J Drug Metab Pharmacokinet* **39**, 203-210 (2014).

54. Patel, R.C., Keraliya, R.A., Patel, M.M. & Patel, N.M. Formulation of furosemide solid dispersion with micro crystalline cellulose for achieve rapid dissolution. *J Adv Pharm Technol Res* **1**, 180-189 (2010).

55. Zawar, L.R. & Bari, S.B. Preparation, characterization and in vivo evaluation of antihyperglycemic activity of microwave generated repaglinide solid dispersion. *Chem Pharm Bull (Tokyo)* **60**, 482-487 (2012).

56. Varshosaz, J., Minayian, M., Ahmadi, M. & Ghassami, E. Enhancement of solubility and antidiabetic effects of Repaglinide using spray drying technique in STZ-induced diabetic rats. *Pharm Dev Technol* **22**, 754-763 (2017).

57. Kavitha, R. & Sathali, A.A.H. Enhancement of solubility of repaglinide by solid dispersion technique. *Int J Chem Sci* **10**, 377-390 (2012).

58. Mitra, A. et al. Impact of polymer type on bioperformance and physical stability of hot melt extruded formulations of a poorly water soluble drug. *Int J Pharm* **505**, 107-114 (2016).

59. Yan, H.M. et al. [Compared with colloidal silica and porous silica as baicalin solid dispersion carrier]. *Zhongguo Zhong Yao Za Zhi* **39**, 2484-2488 (2014).

60. Khan, A. et al. Enhancement of dissolution rate of class II drugs (Hydrochlorothiazide); a comparative study of the two novel approaches; solid dispersion and liqui-solid techniques. *Saudi Pharm J* **23**, 650-657 (2015).

61. Balfour, J.A. & Faulds, D. Repaglinide. *Drugs Aging* **13**, 173-180 (1998).

62. Shinde, U.A., Modani, S.H. & Singh, K.H. Design and Development of Repaglinide Microemulsion Gel for Transdermal Delivery. *AAPS PharmSciTech* **19**, 315-325 (2018).

63. Gadadare, R., Mandpe, L. & Pokharkar, V. Ultra rapidly dissolving repaglinide nanosized crystals prepared via bottom-up and top-down approach: influence of food on pharmacokinetics behavior. *AAPS PharmSciTech* **16**, 787-799 (2015).

64. Yin, L.F. et al. In vitro and in vivo studies on a novel solid dispersion of repaglinide using polyvinylpyrrolidone as the carrier. *Drug Dev Ind Pharm* **38**, 1371-1380 (2012).

65. Hatorp, V., Oliver, S. & Su, C.A. Bioavailability of repaglinide, a novel antidiabetic agent, administered orally in tablet or solution form or intravenously in healthy male volunteers. *Int J Clin Pharmacol Ther* **36**, 636-641 (1998).

66. Mandic, Z. & Gabelica, V. Ionization, lipophilicity and solubility properties of repaglinide. *J Pharm Biomed Anal* **41**, 866-871 (2006).

67. Purvis, T., Mattucci, M.E., Crisp, M.T., Johnston, K.P. & Williams, R.O., 3rd Rapidly dissolving repaglinide powders produced by the ultra-rapid freezing process. *AAPS PharmSciTech* **8**, E58 (2007).

68. Grell, W. et al. Repaglinide and related hypoglycemic benzoic acid derivatives. *J Med Chem* **41**, 5219-5246 (1998).

69. Patel, V.I. & Dave, R.H. Evaluation of colloidal solid dispersions: physiochemical considerations and in vitro release profile. *AAPS PharmSciTech* **14**, 620-628 (2013).

70. Wang, L., Cui, F.D. & Sunada, H. Preparation and evaluation of solid dispersions of nitrendipine prepared with fine silica particles using the melt-mixing method. *Chem Pharm Bull (Tokyo)* **54**, 37-43 (2006).

71. Kim, K.H., Frank, M.J. & Henderson, N.L. Application of differential scanning calorimetry to the study of solid drug dispersions. *J Pharm Sci* **74**, 283-289 (1985).

72. Takeuchi, H., Nagira, S., Yamamoto, H. & Kawashima, Y. Solid dispersion particles of amorphous indomethacin with fine porous silica particles by using spray-drying method. *Int J Pharm* **293**, 155-164 (2005).

73. Guerette, M., Ackerson, M.R., Thomas, J., Watson, E.B. & Huang, L. Thermally induced amorphous to amorphous transition in hot-compressed silica glass. *J Chem Phys* **148**, 194501 (2018).

74. Martin, K.R. The chemistry of silica and its potential health benefits. *J Nutr Health Aging* **11**, 94-97 (2007).

75. Tahir, H. et al. Impact of processing methods on the dissolution of artemether from two non-ordered mesoporous silicas. *Eur J Pharm Sci* **112**, 139-145 (2018).

76. Pardhi, V. et al. Preparation, characterization, and cytotoxicity studies of niclosamide loaded mesoporous drug delivery systems. *Int J Pharm* **528**, 202-214 (2017).

77. De Figueiredo, L.P. & Ferreira, F.F. The Rietveld method as a tool to quantify the amorphous amount of microcrystalline cellulose. *J Pharm Sci* **103**, 1394-1399 (2014).

78. Sharma, V. & Pathak, K. Effect of hydrogen bond formation/replacement on solubility characteristics, gastric permeation and pharmacokinetics of curcumin by application of powder solution technology. *Acta Pharm Sin B* **6**, 600-613 (2016).

79. Miller, D.A., McConville, J.T., Yang, W., Williams, R.O., 3rd & McGinity, J.W. Hot-melt extrusion for enhanced delivery of drug particles. *J Pharm Sci* **96**, 361-376 (2007).

80. Taylor, L.S. & Zografi, G. Spectroscopic characterization of interactions between PVP and indomethacin in amorphous molecular dispersions. *Pharm Res* **14**, 1691-1698 (1997).

81. Rogers, T.L., Johnston, K.P. & Williams, R.O., 3rd Solution-based particle formation of pharmaceutical powders by supercritical or compressed fluid CO2 and cryogenic spray-freezing technologies. *Drug Dev Ind Pharm* **27**, 1003-1015 (2001).

82. Andrews, G.P. & Jones, D.S. Hot melt extrusion - processing solid solutions? *J Pharm Pharmacol* **66**, 145-147 (2014).

83. Breitenbach, J. Melt extrusion: from process to drug delivery technology. *Eur J Pharm Biopharm* **54**, 107-117 (2002).

84. Keen, J.M. et al. Investigation of process temperature and screw speed on properties of a pharmaceutical solid dispersion using corotating and counter-rotating twin-screw extruders. *J Pharm Pharmacol* **66**, 204-217 (2014).

85. Djuris, J. et al. Selection of the suitable polymer for supercritical fluid assisted preparation of carvedilol solid dispersions. *Int J Pharm* **554**, 190-200 (2019).

86. Mahmah, O., Tabbakh, R., Kelly, A. & Paradkar, A. A comparative study of the effect of spray drying and hot-melt extrusion on the properties of amorphous solid dispersions containing felodipine. *J Pharm Pharmacol* **66**, 275-284 (2014).

87. Mondal, R., Das, A., Sen, D., Satapathy, D.K. & Basavaraj, M.G. Spray drying of colloidal dispersions containing ellipsoids. *J Colloid Interface Sci* **551**, 242-250 (2019).

88. Iskandar, F., Gradon, L. & Okuyama, K. Control of the morphology of nanostructured particles prepared by the spray drying of a nanoparticle sol. *J Colloid Interface Sci* **265**, 296-303 (2003).

89. Cal, K. & Sollohub, K. Spray drying technique. I: Hardware and process parameters. *J Pharm Sci* **99**, 575-586 (2010).

90. Kralchevsky, P.A. & Nagayama, K. Capillary interactions between particles bound to interfaces, liquid films and biomembranes. *Adv Colloid Interface Sci* **85**, 145-192 (2000).

91. Sollohub, K. & Cal, K. Spray drying technique: II. Current applications in pharmaceutical technology. *J Pharm Sci* **99**, 587-597 (2010).

92. Beck, R.C., Ourique, A.F., Guterres, S.S. & Pohlmann, A.R. Spray-dried polymeric nanoparticles for pharmaceutics: a review of patents. *Recent Pat Drug Deliv Formul* **6**, 195-208 (2012).

93. Woods, B.P. & Hoye, T.R. Differential scanning calorimetry (DSC) as a tool for probing the reactivity of polyynes relevant to hexadehydro-Diels-Alder (HDDA) cascades. *Org Lett* **16**, 6370-6373 (2014).

94. Verdonck, E., Schaap, K. & Thomas, L.C. A discussion of the principles and applications of Modulated Temperature DSC (MTDSC). *Int J Pharm* **192**, 3-20 (1999).

95. Humphreys, C.J. The significance of Bragg's law in electron diffraction and microscopy, and Bragg's second law. *Acta Crystallogr A* **69**, 45-50 (2013).

96. Garbacz, P. & Wesolowski, M. DSC, FTIR and Raman Spectroscopy Coupled with Multivariate Analysis in a Study of Co-Crystals of Pharmaceutical Interest. *Molecules* **23** (2018).

97. Kane, S.R., Ashby, P.D. & Pruitt, L.A. ATR-FTIR as a thickness measurement technique for hydrated polymer-on-polymer coatings. *J Biomed Mater Res B Appl Biomater* **91**, 613-620 (2009).

98. McCool, B., Murphy, L. & Tripp, C.P. A simple FTIR technique for estimating the surface area of silica powders and films. *J Colloid Interface Sci* **295**, 294-298 (2006).

99. Shamblin, S.L. & Zografi, G. Enthalpy relaxation in binary amorphous mixtures containing sucrose. *Pharm Res* **15**, 1828-1834 (1998).

100. Xiong, J., Li, Q., Shi, Z. & Ye, J. Interactions between wheat starch and cellulose derivatives in short-term retrogradation: Rheology and FTIR study. *Food Res Int* **100**, 858-863 (2017).

101. Rasheed, M., Jawaid, M., Karim, Z. & Abdullah, L.C. Morphological, Physiochemical and Thermal Properties of Microcrystalline Cellulose (MCC) Extracted from Bamboo Fiber. *Molecules* **25** (2020).

102. Tong, H., Sengupta, S. & Tanaka, H. Emergent solidity of amorphous materials as a consequence of mechanical self-organisation. *Nat Commun* **11**, 4863 (2020).

103. Yoshioka, M., Hancock, B.C. & Zografi, G. Crystallization of indomethacin from the amorphous state below and above its glass transition temperature. *J Pharm Sci* **83**, 1700-1705 (1994).

104. Andronis, V., Yoshioka, M. & Zografi, G. Effects of sorbed water on the crystallization of indomethacin from the amorphous state. *J Pharm Sci* **86**, 346-351 (1997).

105. Chadha, R., Bhandari, S., Arora, P. & Chhikara, R. Characterization, quantification and stability of differently prepared amorphous forms of some oral hypoglycaemic agents. *Pharm Dev Technol* **18**, 504-514 (2013).

106. Gao, Y., Liao, J., Qi, X. & Zhang, J. Coamorphous repaglinide-saccharin with enhanced dissolution. *Int J Pharm* **450**, 290-295 (2013).

107. Kothari, K., Ragoonanan, V. & Suryanarayanan, R. The role of polymer concentration on the molecular mobility and physical stability of nifedipine solid dispersions. *Mol Pharm* **12**, 1477-1484 (2015).

108. Brouwers, J., Brewster, M.E. & Augustijns, P. Supersaturating drug delivery systems: the answer to solubility-limited oral bioavailability? *J Pharm Sci* **98**, 2549-2572 (2009).

109. Guzman, H.R. et al. Combined use of crystalline salt forms and precipitation inhibitors to improve oral absorption of celecoxib from solid oral formulations. *J Pharm Sci* **96**, 2686-2702 (2007).

110. Watanabe, T., Hasegawa, S., Wakiyama, N., Kusai, A. & Senna, M. Prediction of apparent equilibrium solubility of indomethacin compounded with silica by 13C solid state NMR. *Int J Pharm* **248**, 123-129 (2002).

111. Leuner, C. & Dressman, J. Improving drug solubility for oral delivery using solid dispersions. *Eur J Pharm Biopharm* **50**, 47-60 (2000).